ELECTROLESS DEPOSITION OF OXIDATION RESISTANT HIGH
TEMPERATURE COATINGS IN MOLTEN SALT

A THESIS SUBMITTED TO
THE GRADUATE SCHOOL OF NATURAL AND APPLIED SCIENCES
OF
MIDDLE EAST TECHNICAL UNIVERSITY

BY

İSHAK EMRE ÖMÜR

IN PARTIAL FULFILLMENT OF THE REQUIREMENTS
FOR
THE DEGREE OF MASTER OF SCIENCE
IN
METALLURGICAL AND MATERIALS ENGINEERING

SEPTEMBER 2021

Approval of the thesis:

ELECTROLESS DEPOSITION OF OXIDATION RESISTANT HIGH TEMPERATURE COATINGS IN MOLTEN SALT

submitted by **İSHAK EMRE ÖMÜR** in partial fulfillment of the requirements for the degree of **Master of Science** in **Metallurgical and Materials Engineering, Middle East Technical University** by,

Prof. Dr. Halil Kalıpçılar
Dean, Graduate School of **Natural and Applied Sciences**   _____

Prof. Dr. Cemil Hakan Gür
Head of the Department, **Metallurgical and Materials Engineering**   _____

Prof. Dr. İshak Karakaya
Supervisor, **Metallurgical and Materials Eng. Dept., METU**   _____

Assoc. Prof. Dr. Metehan Erdoğan
Co-Supervisor, **Metallurgical and Materials Eng. Dept., AYBU**   _____

Examining Committee Members:

Assoc. Prof. Dr. Batur Ercan
Metallurgical and Materials Eng., METU   _____

Prof. Dr. İshak Karakaya
Metallurgical and Materials Eng., METU   _____

Assist. Prof. Dr. Yusuf Keleştemur
Metallurgical and Materials Eng., METU   _____

Assoc. Prof. Dr. Metehan Erdoğan
Metallurgical and Materials Eng., AYBU   _____

Assist. Prof. Dr. Erkan Konca
Metallurgical and Materials Eng., Atılım U.   _____

Date: 10.09.2021

I hereby declare that all information in this document has been obtained and presented in accordance with academic rules and ethical conduct. I also declare that, as required by these rules and conduct, I have fully cited and referenced all material and results that are not original to this work.

Name Last name : İshak Emre Ömür

Signature :

ABSTRACT

ELECTROLESS DEPOSITION OF OXIDATION RESISTANT HIGH TEMPERATURE COATINGS IN MOLTEN SALT

Ömür, İshak Emre
Master of Science, Metallurgical and Materials Engineering
Supervisor : Prof. Dr. İshak KARAKAYA
Co-Supervisor: Assoc. Prof. Dr. Metehan ERDOĞAN

September 2021, 90 pages

Molybdenum and molybdenum alloy (TZM) can be protected against oxygen in high-temperature environment by developing silicide coating on their surface without damaging their mechanical properties. In this study, molybdenum di-silicide was coated on pure molybdenum and its alloy (TZM) surfaces using a molten salt method. NaCl-KCl-NaF eutectic composition was used as salt mixture, and Na_2SiF_6 and silicon powder were added to the system as silicon source. X-ray diffraction (XRD), Inductively Coupled Plasma – Mass Spectrometer (ICP-MS) and scanning electron microscope (SEM) were used for characterization of the silicide coatings. Effects of operating temperature and time on coating thickness for both pure molybdenum and TZM alloy were studied. Also, effect of silicon sources; Na_2SiF_6 and silicon powder, on thickness of silicide layer was investigated. While higher operating temperature had limited effect on coating thickness for pure molybdenum samples, thicker coatings were obtained at lower temperatures for TZM alloy samples. Also, longer operating time slightly increased coating thickness for pure molybdenum substrates, however; it had a significant effect for TZM alloy samples for 4 hours of processing time. Although amount of silicon sources in salt mixture had no effect on coating thickness for pure molybdenum samples, amount of silicon in salt mixture had an enormous effect for TZM alloy samples. Also, molybdenum di-silicide coated TZM alloy samples were tested at high-temperature oxygen environment, and it was proved that silicide coating is protective against oxidation by forming silica.

Keywords: Molten salt, high-temperature coatings, molybdenum di-silicide coatings, oxidation, crystallography

ÖZ

OKSİDASYONA DAYANIKLI YÜKSEK SICAKLIK KAPLAMALARININ AKIMSIZ OLARAK ERİYİK TUZ İÇERİSİNDE BİRİKTİRİLMESİ

Ömür, İshak Emre
Yüksek Lisans, Metalurji ve Malzeme Mühendisliği
Tez Yöneticisi: Prof. Dr. İshak KARAKAYA
Ortak Tez Yöneticisi: Doç. Dr. Metehan ERDOĞAN

Eylül 2021, 90 sayfa

Molibden ve molibden alaşımı (TZM), mekanik özelliklerine zarar vermeden yüzeylerinde silisit kaplama geliştirerek yüksek sıcaklık oksijen ortamlarında korunabilir. Bu çalışmada, molibden di-silisit saf molibden ve molibden alaşımı (TZM) yüzeylerine eriyik tuz yöntemi kullanılarak kaplanmıştır. NaCl-KCl-NaF ötetik kompozisyonu tuz karışımı olarak kullanılmış, Na_2SiF_6 ve saf silisyum tozu silisyum kaynağı olarak sisteme eklenmiştir. X-ışını kırınımı (XRD), indüktif eşleşmiş plazma – kütle spektroskopisi (ICP-MS) ve taramalı elektron mikroskobu silisit kaplamaların karakterizasyonu için kullanılmıştır. İşlem süresi ve sıcaklığının kaplama kalınlığı üzerindeki etkisi saf molibden ve molibden alaşımı (TZM) numuneleri için çalışılmıştır. Ayrıca, sistemin silikon kaynağı olan Na_2SiF_6 ve silisyum tozunun kaplama kalınlığı üzerindeki etkisi araştırılmıştır. Saf molibden numuneleri için yüksek işlem sıcaklığının kaplama kalınlığına etkisi sınırlı olsa da molibden alaşımı numunelerinde düşük sıcaklıkta daha kalın kaplamalar elde edilmiştir. Bununla birlikte, uzun işlem süresi molibden alaşımı numuneleri için bir süreye kadar önemli etki göstermiş olup, saf molibden numunelerinde saf molibden numuneleri için bu etki sınırlı kalmıştır. Silikon kaynaklarının kaplama kalınlığı üzerindeki etkisi saf molibden üzerinde görülmemiş olup, tuz karışımı içindeki silikon miktarının molibden alaşımı numunelerinin kalınlık değerlerinde önemli bir etkisi gözlenmiştir. Silisit kaplanmış olan molibden alaşımı numuneleri yüksek sıcaklıkta oksitlenme testlerine

tabi tutulmuş olup, elde edilen kaplamaların yüzeylerinde camsı silika oluşturarak oksitlenmeye karşı koruyucu olduğu tespit edilmiştir.

Anahtar Kelimeler: Eriyik tuz, yüksek sıcaklık kaplamaları, molibden di-silisit kaplamaları, oksitlenme, kristalografi

To my family..

ACKNOWLEDGEMENTS

TABLE OF CONTENT

LIST OF TABLES

TABLES

LIST OF FIGURES

FIGURES

xv

CHAPTER 1

INTRODUCTION

Different materials are of different strengths and weaknesses, and some are better for varied purposes. Materials are divided into three main groups based on the atomic bonding forces of a material, namely metals, polymers, and ceramics. As a subgroup of metal, the term 'refractory metal' is described as a group of metallic elements with high resistance to heat, wear, corrosion and deformation. However, the definition of refractory metals varies. According to most of the definitions, a crucial requirement is the high melting point of metals. When one definition describes the limit of the melting point to qualify refractory metals as above 2200°C, the other definition identifies the melting point limit for qualification to the refractory metal group comprising chromium's melting point, which is 1903°C. Also, a comprehensive definition that takes the metals into the refractory metal group describes the melting point above 1850°C. However, in all definitions, molybdenum, niobium, rhenium, tantalum, and tungsten are classified in the refractory metal group.

Molybdenum which is a transition metal, is an exceptional material due to its attractive properties. These properties are high melting point (around 2620°C), high resistance to heat and wear, good thermal conductivity (138W/m.K), low coefficient of thermal expansion ($5.35 \times 10^{-6} \, °C^{-1}$ at 20°C), high modulus of elasticity (330 GPa) and high strength at elevated temperatures[1]–[5]. Due to the combination of these attractive properties of molybdenum and its alloys, they are extensively used in the aerospace, automotive, electronics, metallurgy, nuclear, and oil and gas industry [1], [2]. However, one deficiency for high-temperature applications of molybdenum and its alloys is that molybdenum and its alloys cannot be used at elevated temperatures for a long time because of their poor oxidation resistance above 600°C [6]–[8]. It was thought that the pest oxidation that occurs at elevated temperatures is due to the formation of volatile oxides ($MoO_3(g)$, $(MoO_3)_3(g)$, $MoO_2(g)$, etc.) [9].

In order to protect molybdenum and its alloys from oxidation at high temperatures, alloying and surface modification coating are two feasible methods that can improve oxidation resistance. With alloying, the base metal is alloyed with another metal resistant to oxidation. It is expected to form a thin passive layer of oxide that prevents the base metal from oxidation. However, this type of oxide layer cannot resist oxygen at elevated temperatures [10]. Besides, alloying degree of molybdenum is low and alloying elements may damage its mechanical properties for high-temperature applications while increasing oxidation resistance [2]. Surface modification coating is the way to improve the oxidation resistance of molybdenum and its alloys without damaging mechanical properties. Therefore, developing a protective coating against oxygen is more convenient and promising for high-temperature applications of molybdenum and its alloys in the current situation.

Within the last few decades, considerable effort has been made on developing protective coatings against oxidation for structural materials. It was noticed that there would be no coatings that will protect all materials, metals-refractory metals, against all environmental conditions or any other encountered problems. Thus, coatings have to be chosen depending on the substrate that will be coated and the environment in which it will be used for desired purposes. To prevent high temperature oxidation, the coating should possess certain characteristics [11];

1. A low growth rate of the protective oxide layer
2. Resistance to cracking
3. Low evaporation rates of the protective oxide
4. Low rates of coating-substrate reaction
5. Self-healing ability.

Oxidation resistance coatings that have been applied to molybdenum and its alloys include heat-resistant alloy coatings, noble metal coatings, aluminide coatings, oxide coatings, and silicide coatings [2]. Also, borides, carbides, sulfides, and nitrides are applied to molybdenum and molybdenum base alloys, but they are not suitable for high-temperature applications because of poor oxidation resistance [12]. Among them, silicide coatings are the most promising alternative due to their high quality, wide

range of applicability to small, large, or complex shapes, ability to provide the broadest limit of temperature, and higher coating life. Also, silicide coatings are chosen because the diffusion rates of oxygen and metal ions in silica are slow, facilitating good oxidation resistance [12].

Molybdenum silicides are renowned for their high oxidation resistance, and they have emerged at equilibrium between molybdenum and silicon with three different forms, which are $MoSi_2$, Mo_5Si_3, and Mo_3Si. Among these silicide forms, molybdenum disilicide ($MoSi_2$) has two different lattice structures, tetragonal and hexagonal. Up to 1900°C, the tetragonal structure is governing, and after that, the tetragonal structure transforms into a hexagonal structure. Although molybdenum-rich silicide compounds, Mo_5Si_3 and Mo_3Si, are thought to be effective against oxygen by forming a diffusion layer [13], it was noticed that the tetragonal structure of the $MoSi_2$ is the most promising one for high-temperature applications owing to its attractive properties [14]. Molybdenum disilicide has high melting point (2030°C), moderate density, good mechanical properties [15], [16], high thermal conductivity (138 W/(m.K)) and low electrical resistivity (21.6 x 10^{-8} Ωm) , excellent oxidation resistance up to 1900°C, non-toxic and it is environmentally friendly [17], [18]. In the case of a high-temperature oxidizing environment, it is expected that coated surface must form a protective compound layer on the surface when it reacts with oxygen. When molybdenum-disilicide is subjected to oxygen at elevated temperature, silica (SiO_2) forms as a result of the reaction between $MoSi_2$ and oxygen. Thin layer of SiO_2 formed on the surface protects the base metal molybdenum from further oxidation since glassy SiO_2 is impermeable to oxygen [19], [20]. This phenomenon is known as the self-healing mechanism and is the reason to form silicide on the surface.

Another significant issue is to coat silicide on the desired substrate. In order to develop coating, several methods has been applied to molybdenum to prepare $MoSi_2$ which are pack cementation, [20]–[25] , chemical vapor deposition [26], [27], plasma spraying [28], magnetron sputtering [9], pulsed laser ablation deposition (PLA) [29], vacuum plasma [30], [31] and molten salt methods [32]–[34]. Among these techniques, molten salt is extensively used to coat silicide on different metals such as Mo, Nb, Fe, Ni, etc. [34]–[37]. The molten salt technique offers numerous advantages like low cost, easy set-up, low operation temperature, applicability to complex shapes, and short duration

to coat. Besides, the molten salt technique is a diffusional type and minimizes the adhesion problem between substrate and coating, which results in a coherent silicide layer. Also, lower operating temperature compared to other processes changing between 700-900°C, eliminates the possibility of substrate's oxidation during the process and lowers the cost of the process. In this sense, molybdenum di-silicide is a protective layer against oxidizing environment in terms of forming silica layer by self-healing mechanism at elevated temperatures. The molten salt method is a suitable way to prepare the coating due to providing better adherence of coating to substrate, easy setup and economic considerations.

Therefore, this study aims to develop an oxidation-resistant coating with the aid of a single metal silicide layer on molybdenum and molybdenum alloy (TZM) surfaces using molten salt media. Briefly, the effects of operation temperature, immersion time, electrolyte composition, and substrate type were investigated. As the substrate, pure molybdenum and molybdenum alloy TZM (Ti-Zr-Mo) were used. These samples were coated at temperatures 700, 800, and 900°C for 1 to 10 hours. Electrolyte composition was also studied, and the effects of the amount of pure silicon powder and Na_2SiF_6 in the electrolyte were investigated. Encountered phases, coating thickness, surface roughness, and weight gain were considered and evaluated. In the end, selected samples were tested in an oxidizing environment at elevated temperatures to investigate oxidation behavior in terms of phases formed and mass change.

CHAPTER 2

LITERATURE REVIEW

2.1 Background of the Problem

Refractory metals have different physical properties and crystal structures, as shown in Table 1. However, one common property of them is high-temperature strength. Therefore, refractory metals have been studied for utilizing them in high-temperature applications such as jet turbine engines, rocket, and missile engine components, etc. High temperature is needed for many applications to provide high efficiency since it increases as the temperature increases. Thus, for most of the processes, high temperature is preferred because of high efficiency.

Table 1 Properties of some refractory metals [12].

Metal	Melting Point (°C)	Boiling Point(°C)	Crystal Structure	Density at R.T. (g/cm^3)	C.T.E. (10^{-6} per °C)
Tungsten	3422	5555	BCC	19.30	4.5
Rhenium	3185	5597	HCP	21.02	6.7
Osmium	3033	5027	HCP	22.57	6.6
Tantalum	3017	5457	BCC	16.65	6.6
Molybdenum	2623	4639	BCC	10.20	5.4
Niobium	2477	4927	BCC	8.57	7.1
Iridium	2466	4130	FCC	22.65	6.5
Titanium	1668	3287	HCP	4.50	7.1

Refractory metals offer several advantages like high resistance to heat and wear but also come up with some problems. One of the severe issues with refractory metals is low oxidation resistance at an elevated temperature at which strength is needed. While some of the refractory metals are oxidation-resistant, like rhodium and chromium, the rest do not have adequate oxidation resistance at high temperatures. When they are exposed to oxygen at elevated temperatures, their surface is easily oxidized, which makes them vulnerable to chemical or physical attack. Also, as a result of surface oxidation, the material's structure and integrity break down. Among the refractory metals, tungsten, tantalum, molybdenum, and rhenium are the least oxidation resistant [12]. One of the group elements, molybdenum, is oxidized even at 600°C and which makes it useless, although its mechanical properties are excellent. That is why it has to be protected to ensure its usage in a high-temperature oxygen atmosphere.

To control the surface oxidation problem, alloying and surface modification coatings are two possible ways. However, alloying has some limitations, which are molybdenum's alloying degree is respectively low, and alloying elements may harm molybdenum's mechanical properties. Therefore, surface modification coatings are a promising alternative to protect molybdenum and molybdenum base alloys from surface oxidation without damaging their mechanical properties. The coating protects the surface from further oxidation by serving as a barrier against oxygen.

2.2 Oxidation

Metals used in high-temperature applications are being in media with gaseous species such as oxygen, nitrogen, and water vapor. Due to the high reactivity of oxygen and also the high temperature that is a powerful driving force, metals react with oxygen. Depending on chemical equilibria between gaseous species and metals, different phases form as a result of reactions. When a metal is in contact with oxygen at high temperature, there usually exists a metal-oxide phase which is more stable than metal. Most of the time formed metal-oxide phase as a result of oxidation is weak in terms of mechanical property and is not protective against oxidation. Also, the formation of this oxide phase leads to a drop in other properties such as; electrical and thermal properties

of the materials. Therefore, oxidation that could cause catastrophic results has to be prevented, particularly at high-temperature applications.

2.2.1 Mechanism of Oxidation

The oxidation reaction starts at the interface between metal and oxygen by adsorption of oxygen atoms on the metal surface. Then, oxygen atoms dissolve and diffuse through the metal. Metal atoms are chemically bonded with oxygen atoms due to the reaction, and a thin metal-oxide layer forms on the metal surface. The thin layer on the surface is known as a chemisorbed layer which shows metal and oxygen have been bound chemically. Later, the thin layer grows as time passes and forms a continuous oxide layer as the reaction proceeds. In particular, higher temperature increases the growth rate of the oxidation layer. Also, oxide nucleates through favorable sites such as dislocations or impurity atoms.

Several stages of metal oxidation are illustrated and shown in Figure 1. Firstly, oxide layers exist in several regions separately on the metal surface. Later, as oxygen atoms move forward to the metal surface, the oxide layer cover the whole surface of the metal, and then solid-state diffusion takes place via metal and oxygen ions. The formed first layer of oxide may have a porous structure, which leads to build up of all oxide layers in the same way through these pores and grows more oxide. In addition to pores, there exist voids and cracks that may lead to regional spallation. Since oxides already have weaknesses in terms of mechanical properties, a formed porous oxide layer allows oxygen to diffuse into metal, which causes more oxide formation and makes it non-protective.
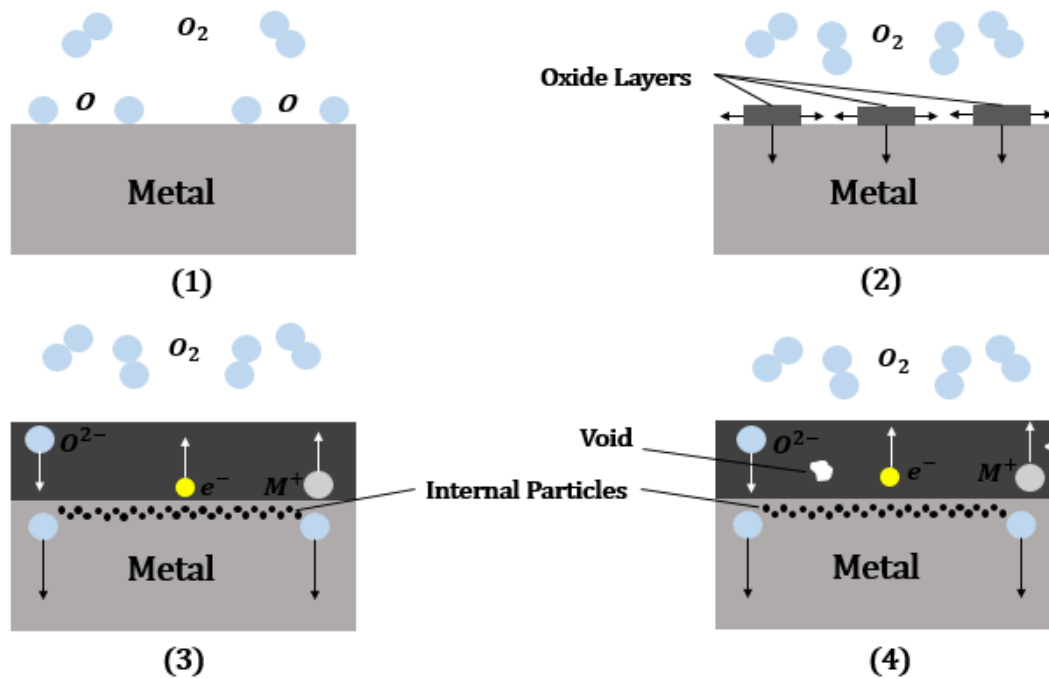
Figure 1 Schematic illustration of oxidation mechanism of metals. Reproduced from the ASM Handbook Volume 13A [38].

Some of the metals form protective oxide as they react with oxygen. The protection of oxide can be roughly predicted from a ratio known as the Pilling-Bedworth ratio, which is the ratio of oxide to metal inside the oxide scale in terms of molar volume [39]. This ratio does not precisely predict whether metal-oxide is protective or not because it does not consider some other important parameters like diffusivity, melting point, adherence, etc., while determining the ratio. P-B ratios (Pilling-Bedworth) of some metals are shown in Table 2, and they are classified as protective and non-protective depending on the P-B ratio, and which states that in general protective oxides has P-B ratios between 1-2.

Table 2 P-B ratio of protective and non-protective oxides [40].

Protective	Al	Be	Ce	Co	Cr	Cu	Mn	Ni	Si
Oxides	1.28	1.59	1.16	1.99	1.99	1.68	1.79	1.52	2.27
Non-Protective	Ag	Cb	Fe	Mo	Ti	Ta	U	V	W
Oxides	1.59	2.61	2.26	3.40	1.95	2.33	3.05	3.18	3.40

2.2.2 Thermodynamics of Oxidation

Thermodynamics is an essential instrument in either oxidation or other chemical reaction to precise the boundaries of reaction in terms of temperature and pressure constraints. Particularly for oxidation reaction, it can be determined that metals or alloys oxidize at which temperature or oxygen pressure by evaluating thermodynamic data. It states that oxygen partial pressure is lower or higher than the critical data to oxidize or not when the equilibrium is reached. General oxidation reaction can be expressed as follows:

$$x\, M(s) + \frac{y}{2}\, O_2(g) \rightarrow M_x O_y(s) \tag{2.1}$$
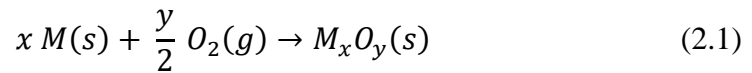
The change in Gibbs Energy of reaction can be stated as:

$$\Delta G_{reaction} = \sum \mu_{products} - \sum \mu_{reactants} \tag{2.2}$$

where $\mu_{products}$ and $\mu_{reactants}$ are the chemical potentials of the oxidation product, $M_x O_y$, and oxidation reactants, metal (M), and oxygen.

Also, the chemical potential of the products and reactants can be detailed, and change in Gibbs Energy of the reaction can be written as follows:

$$\Delta G_{reaction} = \left[\mu^{\circ}_{M_xO_y} + RT \ln\left(a_{M_xO_y} \right) \right]$$
$$- \left[(x\mu^{\circ}_{M_x} + RT \ln(a_M)^x) \right] - \left[\left(\frac{y}{2} \mu^{\circ}_{O_2} \right. \right. \tag{2.3}$$
$$\left. \left. + RT \ln\left(\frac{P_{O_2}}{p^0} \right) \right) \right]$$

Assuming that metal and metal-oxide are pure, so that a_M and $a_{M_xO_y}$ are equal to 1, and also assuming p^0 is 1 atm. The equation will be as follows:

$$\Delta G_{reaction} = \left(\mu^{\circ}_{M_xO_y} - x\,\mu^{\circ}_M - \frac{y}{2}\mu^{\circ}_{O_2} \right) - RT\ln P_{O_2} \tag{2.4}$$

Gibbs Energy change of the oxidation reaction can be generally stated as:

$$\Delta G_{reaction} = \Delta G^{\circ}_r + RT \ln \frac{1}{P_{O_2}} \tag{2.5}$$

where $\Delta G^{\circ}_r = \left(\mu^{\circ}_{M_xO_y} - x\,\mu^{\circ}_M - \frac{y}{2}\mu^{\circ}_{O_2} \right)$. When equilibrium is reached, $\Delta G_{reaction}$ is equal to zero. Then,

$$\Delta G^{\circ}_r = RT \ln P_{O_2} \tag{2.6}$$

This equation gives the equilibrium oxygen partial pressure. If the partial pressure of oxygen exceeds the critical value calculated from the equilibrium condition, this may result in oxidation of metal or alloy. On the contrary, if the partial pressure of oxygen is below the critical value, metal or alloy cannot be oxidized.

2.2.3 Kinetics of Oxidation

To understand the reaction mechanism and rate of the reaction during the oxidation process, kinetics of the process must be known to evaluate all aspects of the oxidation reaction. Temperature, pressure, and time are the most critical factors to identify a reaction and its rate.

The oxidation rate is investigated by observing consumed metal, i.e., by monitoring the weight change of metal or measuring the thickness of the oxide layer. Also, the oxidation rate is evaluated as a function of time since oxidation proceeds as time passes and depends on some variables such as type of metal or alloy, temperature range, etc. Therefore, the oxidation rate has been represented by three different rate laws that are linear, parabolic, and logarithmic as a function of time for pure metals and alloys [41], as shown in Figure 2.
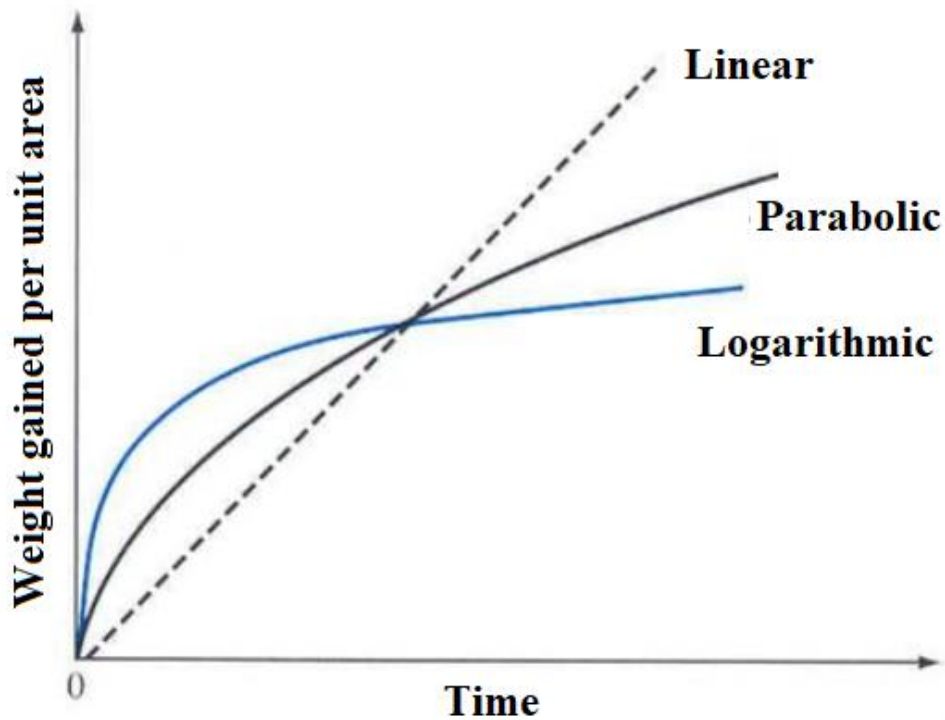
Figure 2 Illustration of linear, parabolic, and logarithmic rate laws of metals in terms of weight gain vs. time.

The linear rate law implies that oxygen diffuses through metal at a constant rate and does not depend on weight gain or consumed gas. Thus, oxide grows at the metal interface by following a linear path, and it is expected that the oxide layer is porous

11

and will not be protective for further oxidation. The equation for linear oxidation is as follows:

$$W = k_L t \qquad (2.7)$$

where W is mass gain due to oxidation or thickness of oxide layer, k_L is the linear rate constant and t is the time.

The parabolic rate law is derived from Fick's first law. Most of the metals obeys a parabolic path during high-temperature oxidation. It is assumed that the concentration of diffusing oxygen at the interface is constant. The initially formed oxide layer on the surface is getting thicker as metal ions continue to diffuse through the surface. After a while, diffusion distance increases, and the oxidation rate decreases. Parabolic kinetics of oxidation equation is as follows:

$$W^2 = k_P t + W_0 \qquad (2.8)$$

where W is mass gain due to oxidation or thickness of oxide layer, k_P is the parabolic rate constant, t is the time, and W_0 is constant which may be obtained from the parabolic fit of rate data.

The logarithmic kinetics is observed during low-temperature oxidation. Also, it generally occurs at thin oxide layers. Thus, the oxidation rate is very high initially, then drops to lower values. The rate equation is as follows:

$$W = k_{log} \, log(ct + b) \qquad (2.9)$$

where W is mass gain due to oxidation or thickness of oxide layer, k_{log} is the logarithmic rate constant, t is the time, and c and b are constants which may be obtained from the logarithmic fit of rate data.

Oxidation behavior of metals may change as the temperature changes. To fully understand mechanisms at different time intervals, some other equations such as cubic and power-law were derived. These equations are a combination of ideal rate laws or

deviations of them. The reason for deviation may be related to a change in grain size, cracking, or high reactivity of elements at elevated temperatures [42]. To sum up, when metal or alloy has poor oxidation resistance, it obeys linear rate law; however, if they are protective at high-temperature oxidation, the rate follows a parabolic path [43].

2.2.4   Oxidation of Molybdenum

Molybdenum reacts with oxygen under the conditions of water vapor and a high-temperature environment, and molybdenum oxides MoO_2 and/or MoO_3 form as a result of reactions. Since MoO_3 is quite volatile, in addition to weight change, consumed oxygen has to be calculated to follow reactions taking place.

Oxidation process of molybdenum has several stages in terms of the temperature range. Studies related to molybdenum's oxidation behavior at low temperatures show that oxidation obeys parabolic rate law between 250°C and 400°C [44]. Besides, it is found that the formation of the passivating adherent oxide layer is observed below 400°C [45]. However, deviations from parabolic rate law were observed above 400°C and data fitted to linear rate law.

Molybdenum trioxide begins to volatilize at 450°C under a vacuum atmosphere. Volatilization of MoO_3 may lead to govern all systems depending on the amount of oxygen present in the system since its vapor pressure increases with increasing temperature [45]. Gulbransen et al. calculated the vapor pressure of molybdenum trioxide as 6.08 x 10^{-6} atm at 600°C and 4.69 x 10^{-4} atm at 700°C [46]. Melting and boiling points of MoO_3 are around 800 and 1150°C, respectively. An increase in vapor pressure will continue until the oxide melts, which affects the possible oxidation rate. Therefore, it is supposed that catastrophic oxidation starts at around 725°C [47]. Spretnak et al. [48] oxidized molybdenum in air between 800-980°C and reported that the rate of volatilized molybdenum trioxide is approximately equal to the rate of formed oxide. Also, it is found that above 795°C, the oxidation rate is almost constant [49].

Nelson et al. [45] approached the oxidation phenomenon of molybdenum by dividing it into two distinct regions; weight gain and weight loss. It is supposed that weight gain

is observed simply below 600°C that fitted into parabolic rate law, and weight loss is detected above 700°C because molybdenum trioxide volatilizes with increasing temperature and the rate of mass loss increases with increasing temperature. The situation is summarized by Barlett who reported that the availability of oxygen on the molybdenum's surface above 800°C directly affects weight loss increment, which shows the oxidation rate is proportional to the amount of oxygen present at molybdenum surface [49]. Therefore, molybdenum has to be protected during its high-temperature usage since molybdenum does not form protective oxide film when oxidized and does not form a barrier to oxygen due to volatile oxide MoO_3.

2.2.5 Coating

In many cases, metal's high susceptibility to oxygen has been solved by alloying and expected that the addition of resistant metal acts as a barrier to oxygen invasion. However, suitable alloy development has not been reached success at the desired level due to the low alloying degree of molybdenum and not adequate oxidation resistance at elevated temperatures. While increasing resistance against oxygen, there may be loss in high-temperature strength, workability, and weldability [50]. Therefore, coating is a solution to overcome pest oxidation without damaging mechanical properties.

Coatings are applied to the surface or interface to provide either protection or enhance performance against the conditions at which materials cannot withstand. The type of coating depends on the application for which materials are used. There is no single perfect coating that protects all materials against all conditions. However, specifically, the suitable coating could be designed for each metal or alloy with desired properties. Since molybdenum is used at a temperatures higher than 1800°C for a short period of time or several hours above 1000°C and oxidizes at intermediate temperature (600-800°C), the coating must be suitable for use under these conditions. Also, molybdenum's low thermal expansion coefficient may lead to a matching problem between coating and base metal molybdenum. Therefore, creating coating by diffusional synthesis will be a more effective way to provide good adherence [50].

Oxides, carbides, aluminides, borides, and nitrides have been applied, and they showed relatively poor oxidation resistance considering some exceptions [51]. Aluminide coating can be applied to the surface directly or combining with other elements.

Although aluminide coating forms protective alumina oxide when exposed to oxygen, its lifetime is limited due to inter-diffusion between the base metal and aluminum, resulting in loss of aluminum [52]. Nitride coatings that are excessively used to improve hardness and wear resistance are also effective against oxidation; however, the operation temperature that nitride coatings can be safely used is between 500-900°C despite most of the nitrides are stable even at 2000°C [52]. Another approach to improve the oxidation resistance of metals at high temperatures is to have boride coating that has been widely used to harden the surface, but there may be loss in mechanical properties, particularly weak binding between the base metal and the coating [53].

Silicide coatings are considered the most suitable way for oxidation protection systems at elevated temperatures, particularly for refractory metals. Initially, silicide coatings were applied to niobium and tantalum surfaces to enhance their oxidation resistance by forming SiO_2 at elevated temperatures. However, they form metal oxide in addition to silica when they are oxidized and produce a physical mixture of them which has high oxygen diffusivity and higher growth rate than silica formation on molybdenum and tungsten [52]. Although silicide coating on niobium and tantalum provides protection up to a certain point, it is reported that there may be cracking and a problem with adhesion to substrate due to the formation of mixed oxide [54].

2.2.6 Molybdenum Silicides and Self-Healing Mechanism

Silicides are well known for their excellent oxidation resistance. There are three silicide compounds of molybdenum Mo_5Si_3, Mo_3Si, and $MoSi_2$, which are formed at the equilibrium between molybdenum and silicon. Although $MoSi_2$ has been regarded as the most protective silicide among them because of forming diffusion barrier, lower silicides; Mo_5Si_3 and Mo_3Si, are sufficient to form the diffusion layer [13].

Furthermore, $MoSi_2$ is considered the most promising intermetallic layer against oxidation due to high-temperature stability without degradation of any properties and, most importantly, the formation of the silica passivation layer that grows on silicide [55]. This silica layer protects the surface from further oxidation. However, the formation of silica layer as a result of oxidation of molybdenum di-silicide is somehow

conflicted so that it cannot be explained by just simple mechanisms since reactions taking place at high temperatures are quite different than at intermediate temperatures. Even though high-temperature oxidation is a significant interest in literature, a low-temperature mechanism must be explained to get the mechanism of what it is beyond. As it is known from oxidation behaviour of molybdenum, the most stable oxide, MoO_3, is the product from intermediate oxidation, which is also the end product of disilicide oxidation along with SiO_2 simultaneously [56]. Birchenall suggests that there is a linear vaporization of MoO_3 while solid MoO_3 and SiO_2 grow following the parabolic route below 750°C [57]. Therefore, the reaction taking place is summarized in the following equation;

$$7MoSi_{2(s)} + 7O_{2(g)} \rightarrow 2MoO_{3(g)} + 4SiO_{2(s)} \qquad (2.10)$$
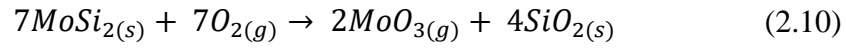
As the temperature is raised above 750°C, MoO_3 becomes a less critical compound for the oxidation of $MoSi_2$ since formation and volatilization of MoO_3 are practically low, so that reaction becomes as the following equation;

$$5MoSi_{2(s)} + 7O_{2(g)} \rightarrow Mo_5Si_{3(s)} + 7SiO_{2(s)} \qquad (2.11)$$
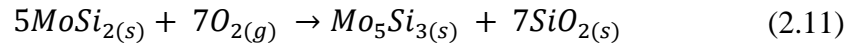
The formation of molybdenum-rich compound Mo_5Si_3 rather than MoO_3 is identified from X-Ray patterns of high-temperature oxidation of $MoSi_2$ [56]. Furthermore, if oxygen activity is low during the oxidation reaction, formation of Mo_5Si_3 and SiO_2 is thermodynamically more favorable than MoO_3 and SiO_2 [58]. Besides, the development of Mo_5Si_3 on the surface has been observed at a high-temperature vacuum atmosphere [59]. Silicon in $MoSi_2$ diffuses through the Mo-$MoSi_2$ interface because of the high mobility of silicon, and the rate of diffusion is higher than that of silicon diffusing through silica, which results in Mo_5Si_3 formation under the silica [56]. However, the formation of Mo_5Si_3 employing decomposition of $MoSi_2$ occurs after SiO_2 formation. For a long period of oxidation, oxidation will occur from Mo_5Si_3 surface instead of $MoSi_2$ by the following reaction;

$$2Mo_5Si_{3(s)} + 21O_{2(g)} \rightarrow 10MoO_{3(g)} + 6SiO_{2(s)} \qquad (2.12)$$

Suzuki et al. [34] conducted an oxidation study for siliconized samples in an open atmosphere. It is reported that Mo_5Si_3 was not found between $MoSi_2$ and Mo substrate [34]. However, it is believed that Mo_5Si_3 initially forms at the oxidation front beneath glassy silica, then it ultimately turns out to silica as oxidation proceeds [34]. Simultaneously, molybdenum di-silicide decomposes to Mo_5Si_3 by mutual diffusion and forms between $MoSi_2$ and Mo substrate. As illustrated in Figure 3, when $MoSi_2$ is exposed to oxygen at elevated temperatures, oxide volatilizes, and glassy silica forms. The formation of a protective silica layer on $MoSi_2$ is known as self-healing mechanism or selective oxidation. Lavendel and Elliot [60] reported that the formation of silica layer, in other words, selective oxidation, occurs because the thermodynamic stability of silica is immensely higher than that of molybdenum oxides (MoO_2 and MoO_3) at 1500 K.
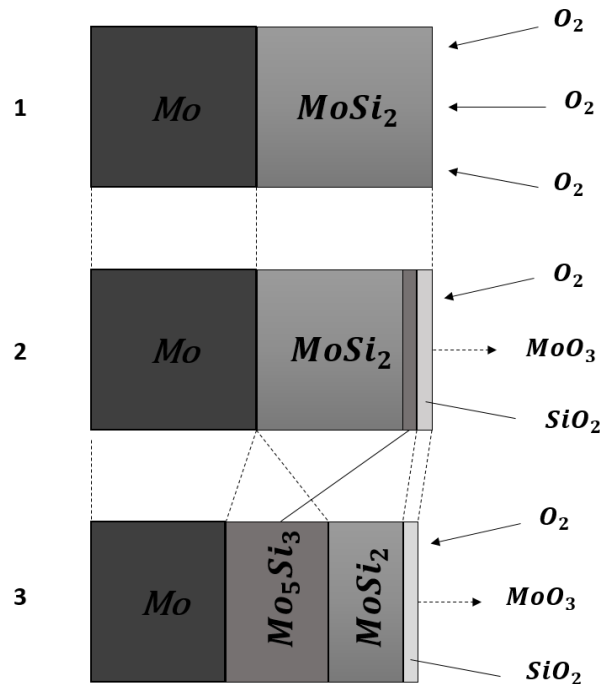
Figure 3 Oxidation mechanism of molybdenum di-silicide layer at elevated temperature and formation of silica layer and molybdenum rich phases. Reproduced from reference [34].

17

2.3   Electroless Deposition

Electroless metal deposition is a process of deposition of a metal from aqueous or non-aqueous solutions or fused salts in the absence of any external energy source, which results in the deposition of a uniform film on the substrate due to chemical or autocatalytic nature of process [61], [62]. This process is most often related to the deposition of metals and alloys; however, also used to deposit oxide, salts, polymers, and composites. The term "Electroless" is generally used for most of the processes based on non-current type. However, electroless plating is firstly described for a nickel coating process that deposited metal becomes a catalyst to proceed coating [63], [64]. Afterward, the term "electroless" is broadened to define some other processes that deposit metal without current. Even though electroless deposition processes have many similarities in terms of kinetics and mechanisms, there are also several points that differ from each other. Similar to the electrolytic deposition process, electroless deposition includes oxidation and reduction reactions due to its chemical nature. Also, it can be stated that electroless deposition is a spontaneous reaction from the thermodynamic point of view. The final reaction taking place can be stated as follows;

$$X + Y \rightarrow XY \tag{2.13}$$

Since there is no external energy source and reaction is considered as spontaneous, Gibbs Energy change will be stated as;

$$\Delta G < 0 \tag{2.14}$$

Besides, there is no energy source in the electroless deposition, and energy is produced by the reaction, as Eq. 2.14. Since there are differences between electroless deposition processes in terms of mechanisms and kinetics, it is divided into three main groups; autocatalytic, contact, and displacement deposition.

2.3.1 Autocatalytic Deposition

The autocatalytic deposition has been described as controlled chemical reactions that metals and alloys involved as a catalyst for further deposition, which results in deposition of a metallic layer [65], [66]. It is the most common type of depositing a metal from an aqueous solution. The metallic layer on the surface is deposited by the reaction of metal ions from a solution that contains a reducing agent [67]. There are several reducing agents reported in the literature, e.g., formaldehyde, hypophosphite, hydrogen, ascorbic acid, etc. The reduction reaction can be simply shown by the following reaction:

$$M^{X+} + R^{y-} \rightarrow M + R^{x-y} \tag{2.15}$$
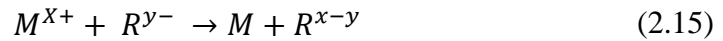
As shown in the reduction reaction, metal ions M^{x+} are reduced to M while reducing agent R^{y-} ions are oxidized to R^{x-y}. This reduction reaction occurs on the surface of the deposited metal as the process proceeds. Besides, deposited metal will be a catalyst to proceed deposition. Also, it is reported that the type of reducing agent would have been an effect on not only the kinetics of deposition but also surface morphology and physicochemical properties [68].

2.3.2 Contact Deposition

Contact deposition is another electroless deposition that is a relatively small part of industrial applications; however, it is generally used to initiate autocatalytic deposition. Current is not supplied to the system by energy source, and it is produced as a result of a chemical reaction. Metal that will be deposited acts as a cathode, and auxiliary metal in aqueous or non-aqueous solution dissolves and simply becomes the anode, resulting in deposition onto the surface of metal acting as a cathode [67].

2.3.3 Displacement Deposition

The displacement deposition process is also known as immersion plating. The reason why it is called immersion plating is that less noble metal is immersed into a solution containing more noble metal. The reduction reaction of more noble metal occurs while

less noble metal dissolves and powder or layer of more noble metal is formed on the surface of less noble metal. For instance, when copper plate is immersed in a solution contains silver ions (Ag+), copper begins to give electrons, and dissolves while silver ions take electrons, and reduced. In this way, metallic silver layer forms on copper plate. The reaction takings place is shown in following equations.

$$Cu + Ag^+ \rightarrow Cu^+ + Ag \qquad (2.16)$$
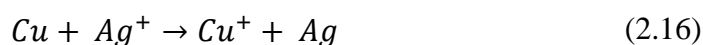
The metallic layer on less nobel metal(copper in previous example) obtained by displacement deposition is very thin due reaction is galvanic. Therefore, oxidation and reduction reactions stops when potential difference is zero. Thus, displacement plating is used to obtain very thin metallic layers.

2.4   Electroless Deposition in Molten Salts

Molten salts, which are defined as the most concentrated ionic liquids, are promising reaction media to carry ions for deposition. Furthermore, the utilization of molten salt systems is not only to deposit, however, they are used in the processing of metals, alloys, elements, extraction of metals, and energy storage in terms of nuclear energy, solar cells, batteries, fuel cells [69]. They also provide many advantages in processing and production where reduction by pyro and/or hydrometallurgy is not feasible because of the thermodynamic and kinetic limitations [70]. The reason why molten salt media is preferred over many traditional methods is simply that it removes water from the system and is applicable at higher temperatures, which enables higher reaction rates. In addition to these, molten salts are capable of dissolving organic and inorganic compounds, and it is possible to support the oxidation states of ions that cannot be obtained by traditional processing [71]. These characteristics are the results of special properties of molten salts such as high mass transfer, high thermal conductivity, low viscosity and low density.

Electroless deposition in molten salt leads to the formation of a protective metallic layer that is a significantly effective way to protect metal over a corrosive environment. The formation of intermetallic compounds or solid solutions is an underlying requirement in an electroless deposition using molten salt media like any other plating

process to ensure good bonding between the base metal and depositing layer [71]. Formation of the metallic layer, deposition of metal on the substrate, is based on diffusion employing saturation of surface with silicon, boron and/or carbon. In literature, refractory metals have been deposited in molten salt media, and particularly molybdenum has been coated with silicon and boron using current and non-current type depositions [72]. However, carbide could be formed on molybdenum only using electrolytic deposition [73]. In another study, Ueda et al. [74] reported that deposition was dendritic and powdery during the electrolytic deposition of silicon on iron using molten salts of LiCl-KCl-LiF-K_2SiF_6 at 500°C.

There are specific parameters affecting deposition in molten salt, which are temperature, immersion time, salt composition, and also the base metal. Parameters should be enhancing the diffusion rate since electroless deposition is diffusional. Therefore, in literature, operation temperature and immersion time were studied and their effects on coating thickness and surface quality were investigated. Although most of the time, a eutectic salt mixture was used to provide a lower melting point, some other chemicals and mixtures have also been studied. Furthermore, these variables were tested on different metals for different purposes. As expected, different materials do not behave the same way, and their response under different conditions will be separating them from each other.

2.4.1 Effect of Salt Composition

Molten salt media that is used to carry and transfer ions is an essential parameter for the deposition. Generally, eutectic mixtures are used as media due to the lower melting point of mixture. However, there are various classes of binary and ternary molten salts, which include fluorides, chlorides and/or nitrates because of their unique thermodynamic and thermoelectrolytic properties [75]. Saltarella et al. [76] stated that ideal working fluid should have some characteristics, which are;

1. Low vapor pressure

2. High melting point

3. High thermal conductivity

4.	High density at low pressure

5.	High specific heat.

Therefore, fluoride systems are generally used since their salts possess low vapor pressure, as fluoride salts have the highest melting point among alkaline salts, as shown in Table 3. Also, molten salt systems consist of eutectic alkaline halide mixtures. The ternary eutectic of the LiF-NaF-KF salt mixture has been commonly used in the deposition of refractory metals due to a lower melting point of 453°C [77]. However, Senderoff and Mellors deposited refractory metals using this salt mixture, and they reported that refractory metals could not be deposited at this temperature, and it is needed to raise the temperature above 700°C [78]. Also, Stern produced carbide on refractory metals of Ti, V, Cr, Ta, W, Mo, Nb, Zr by using electrolytic plating and stated that temperature has to be at least 750°C to ensure a totally molten salt mixture [79].

On the other hand, the fluoride-based salt mixture comes with corrosion problems against the reaction tube, particularly at elevated temperatures due to fluoride's higher electronegativity and reactivity. Thus, chloride salt mixtures have seen intense interest in depositing refractory metals instead of fluorides. Nevertheless, most of the refractory metal chloride vaporize below 320°C, and it will be difficult to deposit due to the vaporization of substances [77].

Table 3 The melting point of alkaline salts.

Melting Point(°C)	F⁻	Cl⁻	Br⁻	I⁻
Li⁺	848	610	550	469
Na⁺	995	800	747	660
K⁺	857	770	734	681
Rb⁺	795	722	692	647
Cs⁺	703	645	636	626

Therefore, to balance fluoride's reactivity and chloride's vaporization problem, fluorides and chlorides have been used together. Most of the mixtures consisted of NaCl-KCl at eutectic composition. Furthermore, some other molten salts include the mixture of NaCl-KCl-NaF salts whose liquidus temperature is around 650°C [80]. Also, Na_2SiF_6 and Si are added to the salt mixture as supporting materials. The amount of salts and supporting materials found in the literature survey is shown in Table 4. Instead of supporting materials Na_2SiF_6 and Si; SiO_2 is also used; however, it was found that its solubility is pretty much lower in chloride melts than fluorides [81].

Table 4 Amount of used salts and supporting materials found in the literature survey.

	Salt Composition in mole fraction %					
	NaCl	KCl	NaF	Na_2SiF_6	Sub Total	Si powder
Hasokawa [82]	50	50	-	-	100	100
Gay and Quakemaat [36]	40.88	32.05	22.13	4.94	100	23.63
Oki and Tanikawa [83]	40.98	32.12	22.00	4.90	100	22.05
Suzuki et al. [35]	36.58	36.58	21.95	4.89	100	21.85

As for the effect of salts, Tyagi et al. [84] conducted three sets of experiments with three different salt mixtures to identify diffusing species from Si and Na_2SiF_6. In addition to the NaCl-KCl-NaF mixture, only Na_2SiF_6 for the first case, only Si for the second case, and both were used for the latter case. There was no coating for the first case. In contrast, the latter two cases had a di-silicide layer, which indicates that Na_2SiF_6 supplies to medium only Si^{4+} ions whereas Na_2SiF_6 and pure Si supply to medium Si^0 and Si^{4+} states that makes Si^{2+} to develop coating. Furthermore, in the case of only Na_2SiF_6 addition, mass loss was observed; in contrast, others gained mass. It is believed that the reason for the mass loss was associated with the etching effect of F^- ions [84]. Also, Suzuki et al. reported that SiF_4 evaporation might lead to a decrease in the rate of siliconizing when the only silicon source was Na_2SiF_6 [35]. As compared to only Si addition and addition of both, Na_2SiF_6 and Si make a thicker di-silicide layer and have better surface quality in terms of smaller and lesser pits.

2.4.2 Effect of Base Metal

Another important point that affects layer thickness is the base metal that will be coated. Most of the research efforts have been directed to coat refractory metals to

enhance their oxidation resistance at high temperatures. Besides, some other metals such as iron and nickel have been used as a substrate to develop silicide coating. Suzuki et al. [32] conducted a set of experiments using pure iron and low carbon steel in molten salt medium to develop corrosion resistant silicide coating and obtained a Fe_3Si layer whose thickness varied between 50 and 300 microns [35]. In the same way, Gay and Quakernaat applied the same process to nickel for the same purpose and obtained the Ni_3Si layer with a thickness of 20-200 microns [36]. The silicide layer thickness was higher than that of molybdenum di-silicide and niobium di-silicide; because they formed lower silicides like Fe_3Si and Ni_3Si.

Tatemoto et al. carried out electroless silicide coating experiments in molten salt media by using both refractory and non-refractory metals to differentiate mechanism and observe the effects of substrate on layer thickness [32]. As refractory metal substrate molybdenum, niobium, and chromium, as non-refractory metal substrate, iron, cobalt, and nickel were used. According to results, silicides that had been coated on refractory metals formed higher silicides (MSi_2) and lower silicides (MSi_n, n<2) were formed on non-refractory metals. It was reported that higher silicides formed in non-refractory metal group at the very beginning of the deposition, then dissociated and formed lower silicides [32]. Lower silicide reacted with base metal and grew while higher silicides remained faint amount at outer layer as shown in Figure 4. This situation that lower and higher silicides being together was observed for Fe, Co, and Ni.
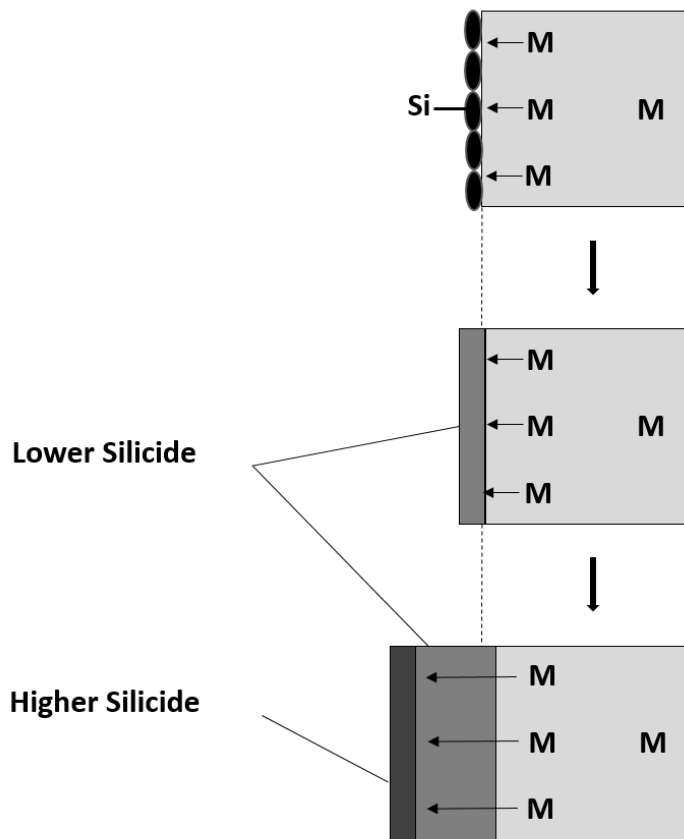
Figure 4 Mechanism of lower and higher silicide formation on non-refractory metals. Reproduced from reference [32].

On the other hand, lower silicide formation was not observed for refractory metals; Mo, Nb, and Cr. As shown in Figure 5, a higher silicide phase exists on the metal substrate and grows. Even though a lower silicide phase could not be found between higher silicide and substrate experimentally, it is believed that lower silicides must form between the base metal and higher silicide phase just after higher silicides cannot diffuse anymore[33]. However, there is no evidence reported by the researchers supporting this claim [33].
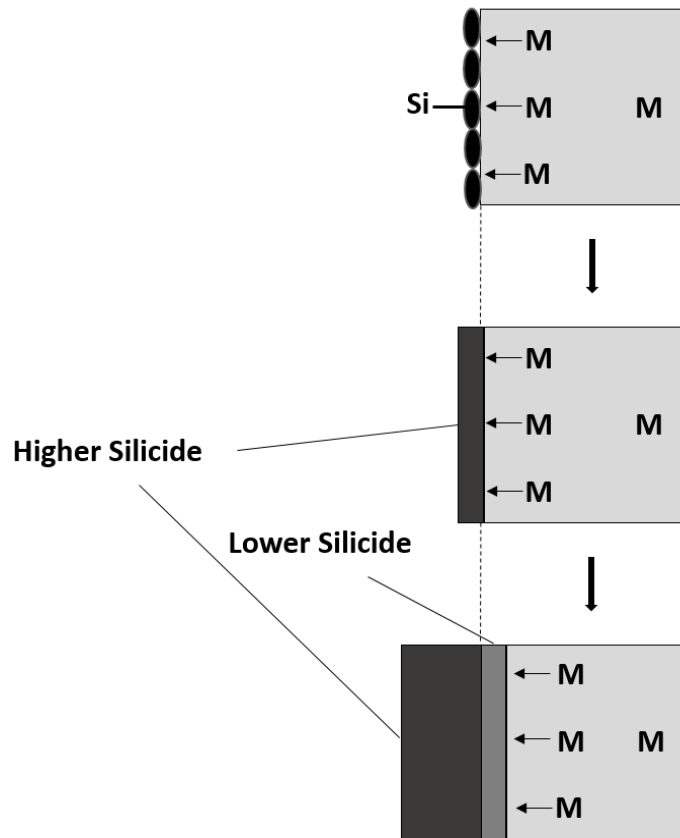
Figure 5 Mechanism of lower and higher silicide formation on refractory metals. Reproduced from reference [32].

Another research [85] on diffusion rates of silicides in metals with diffusion couples shows that lower silicide formation in refractory metals is detected for chromium, niobium, and molybdenum after annealing. In particular for molybdenum, lower silicide phases such as Mo_3Si and Mo_5Si_3 exist in the inter-diffusion zone. However, presence of Mo_3Si was negligible and not even detected by SEM.

Tortorici et al. [86] also reported that the Mo_3Si phase formed after the consumption of $MoSi_2$ totally. The growth mechanism of the molybdenum phases was explained by the physicochemical approach using diffusion couples. As shown in Figure 6, molybdenum dissociates at interface 1. It diffuses towards Mo_3Si to react with Mo_5Si_3 at interface 2, and at the same time, Mo_5Si_3 dissociates at interface 3 to produce molybdenum di-silicide. In contrast, the other side of molybdenum reacts with silicon

to form the same molybdenum phase [85]. Therefore, all phases grow in two directions. However, Mo_3Si is not a detectable amount, and molybdenum has quite a low diffusion rate in $MoSi_2$ since the Kirkendall marker plane was found in the $MoSi_2$-Si interface [86].
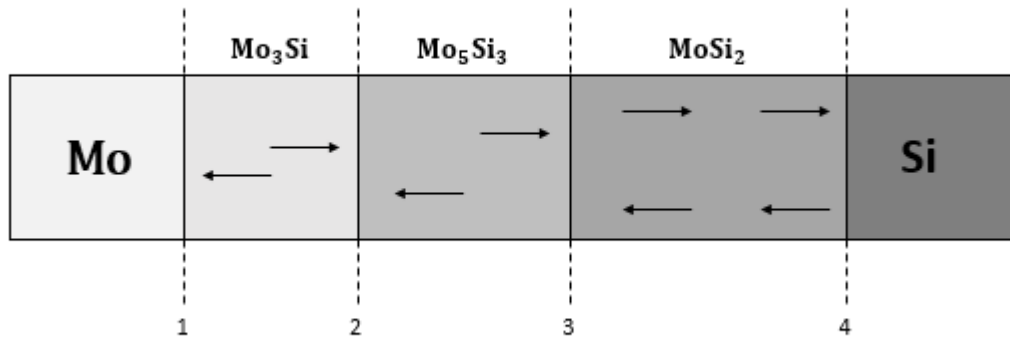
Figure 6 Schematic illustration of diffusion process in Mo-Si diffusion couple. Reproduced from reference [87]

2.4.3 Effect of Temperature and Immersion Time

Electroless deposition in the molten salt is one of the diffusional type coating processes. Of the parameters that affect diffusion, the temperature is vital to increase the diffusion rate by increasing the movement of atoms due to increasing energy. Also, deposited atoms act as a catalyst to develop further coating, and time is needed to enhance coated layer. Therefore, layer thickness or mass gain per unit area could be increased by varying temperature and duration of the process. However, the layer thickness cannot be adjusted precisely due to some process or material constraints such as the dissolution of coated di-silicide in molten salt and/or low diffusion rate of silicon in the substrate, but it can be predicted whether the layer grows parabolic or linear by studying different time and temperature intervals.

In the literature survey, the effect of process temperature and immersion time on layer thickness were studied using molten salt media. Process temperatures were changed between 700°C and 1000°C for the duration of 1-10 hours. Gay and Quakernaat

siliconized nickel using electroless deposition at 700°C, 800°C, and 900°C for 2, 4, and 6 hours [36]. The slope of the layer thickness line increased with an increasing duration for 800°C and 900°C. At 700°C, the deposited layer thickness was almost constant while its mass gain slightly increased with time. This may be due to formation of Ni_5Si_2 at the outer layer instead of Ni_3Si.

In comparison between 800°C and 900°C, the siliconized layer thickness at 900°C is influenced significantly higher than that of 800°C, and also the effect of immersion time can be seen as much more effective at a higher temperature. Suzuki et al. deposited di-silicide onto niobium using electroless deposition at 700°C, 800°C, and 900°C for 0.5, 1, and 2 hours [37]. It was stated that mass gain was a faint amount at 700°C and the deposited layer was not homogenous for 700°C, and 800°C [37]. Then the temperature was increased to 900°C, the mass gain was more evident, and an increase in immersing time resulted in a rise of mass gain. When the coating was applied to molybdenum substrate under the same conditions, it was found that there is a nearly linear correlation between immersing time and layer thickness at 700°C. Also, growth rate of coated layers and immersion time, 0.5 and 1 hour, was proportional for all temperatures [34]. As the processing time was extended, the linear correlation was lost, and the reason for deviation from linearity was associated with non-homogenous deposition at the edges of samples [34]. It was stated that the edges of samples could be fully coated at 800°C, and it came up with a porous structure. Tyagi et al. faced with pores during coating of Nb alloy using the molten salt method and obtained porous $NbSi_2$ was heat treated at 1200°C, 1350°C, and 1400°C for times changing between 2 and 10 hours, which resulted in Nb_5Si phase with two different regions; porous and non-porous [88]. Then, porous samples were re-coated at their production temperature, and three different layers were obtained. The inner layer was Nb_5Si_3 and $NbSi_2$ consisted of a non-porous and porous layer, but the porous layer remained a faint amount. It was reported that re-coated samples had much better oxidation resistance in comparison to heat-treated and coated samples [88].

CHAPTER 3

EXPERIMENTAL

Molybdenum and TZM alloy samples were coated by silicide using electroless deposition in a molten salt solution to enhance their oxidation resistance at elevated temperatures in this study. Parameters that affect coating thickness are designated as operation temperature, immersion time and salt composition for both Mo and TZM samples. The selected parameters with their levels are shown in Table 5. NaCl-KCl-NaF-Na_2SiF_6-Si salt mixture was used in the experiments. E1, E2 and E3 salt mixtures were used to investigate the effect of silicon sources which are Na_2SiF_6 and Si powder on coating thickness. Lindberg LCC114PC high-temperature furnace, as shown in Figure 7, was used in the studies.

Table 5 Parameters and levels designated for this study.

	PARAMETERS		
Substrate	Temperature(°C)	Time(hour)	Salt Composition
Pure Molybdenum	700	3	E1
TZM	700	3	E1
Pure Molybdenum	800	3	E1
Pure Molybdenum	800	3	E2
TZM Alloy	800	1	E1
TZM Alloy	800	3	E1
TZM Alloy	800	3	E2
Pure Molybdenum	800	3	E3
Pure Molybdenum	800	4	E1
TZM Alloy	800	4	E1
TZM Alloy	800	4	E2
Pure Molybdenum	800	6	E1
Pure Molybdenum	800	6	E3
TZM Alloy	800	6	E1
TZM Alloy	800	6	E2
Pure Molybdenum	900	3	E1
Pure Molybdenum	900	3	E2
Pure Molybdenum	900	3	E3
TZM Alloy	900	3	E1
TZM Alloy	900	3	E2
Pure Molybdenum	900	4	E1
TZM Alloy	900	4	E1
TZM Alloy	900	4	E2
Pure Molybdenum	900	6	E1
TZM Alloy	900	6	E1
TZM Alloy	900	6	E2
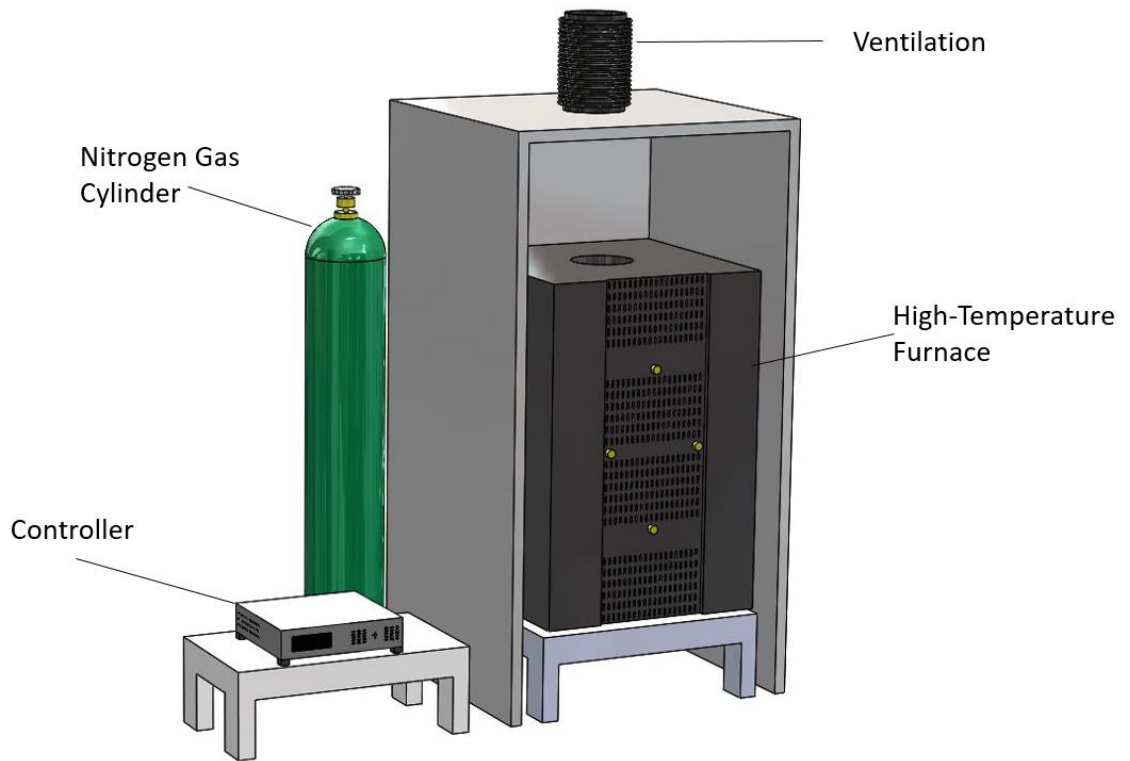
Figure 7 Schematic illustration of Lindberg LCC114PC high-temperature furnace.

3.1 Preparation of Salt Mixture

In this study, the NaCl-KCl-NaF salt mixture was chosen as the ionic media. In order to provide silicon to the system, Na_2SiF_6 and silicon powder were added to this mixture. The purity information of components contained in the salt mixture is shown in Table 6. This mixture was stirred mechanically and placed into an alumina crucible before each experiment. Then, the alumina crucible was placed into the NUVE EV 018 Vacuum furnace and heated up to 100°C to dry, in other words, to get rid of physically bound water.

Table 6 Information about the raw materials used in this study.

Chemical	Purity(mass contents in %)	Morphology	Supplier
NaCl	≥99%	Powder	Sigma-Aldrich
KCl	≥99%	Powder	Merck
NaF	≥99%	Powder	Sigma-Aldrich
Na_2SiF_6	≥99%	Powder	Sigma-Aldrich
Si	≥99%	Powder	Sigma-Aldrich

Salt composition was one of the parameters changed to observe the effects on coating thickness as mentioned in Table 5. The composition of salt mixtures, designated as E1, E2 and E3 in Table 5 are given in Table 7.

Table 7 Compositions of the electrolyte.

Ingredients	E1		E2		E3	
	mol%	wt%	mol%	wt%	mol%	wt%
NaCl	36.57	31.87	36.57	31.87	34.46	30.04
KCl	36.58	40.67	36.58	40.67	34.45	38.30
NaF	21.96	13.75	21.96	13.75	20.67	12.95
Na_2SiF_6	4.89	13.71	4.89	13.71	10.42	18.71
Si(additional)	21.83	9.14	35.81	15.00	21.83	9.14

3.2 Preparation of Samples

In this study, two different substrates; pure molybdenum and TZM alloy samples were used to deposit silicide. X-ray diffraction results of samples before experiments are shown in Figure 8 and Figure 9. Thus, it was proved that the used samples are pure molybdenum and TZM alloy.

A 3mm diameter hole was drilled on each sample to hang them by a tungsten wire. Both sides of the samples were cleaned to remove possible residues with 1000 grid sandpaper. Before placing in the experimental setup, the samples were cleaned in an

ultrasonic bath using deionized water, ethanol, and acetone respectively. Then, samples were weighed and placed into the experimental setup.
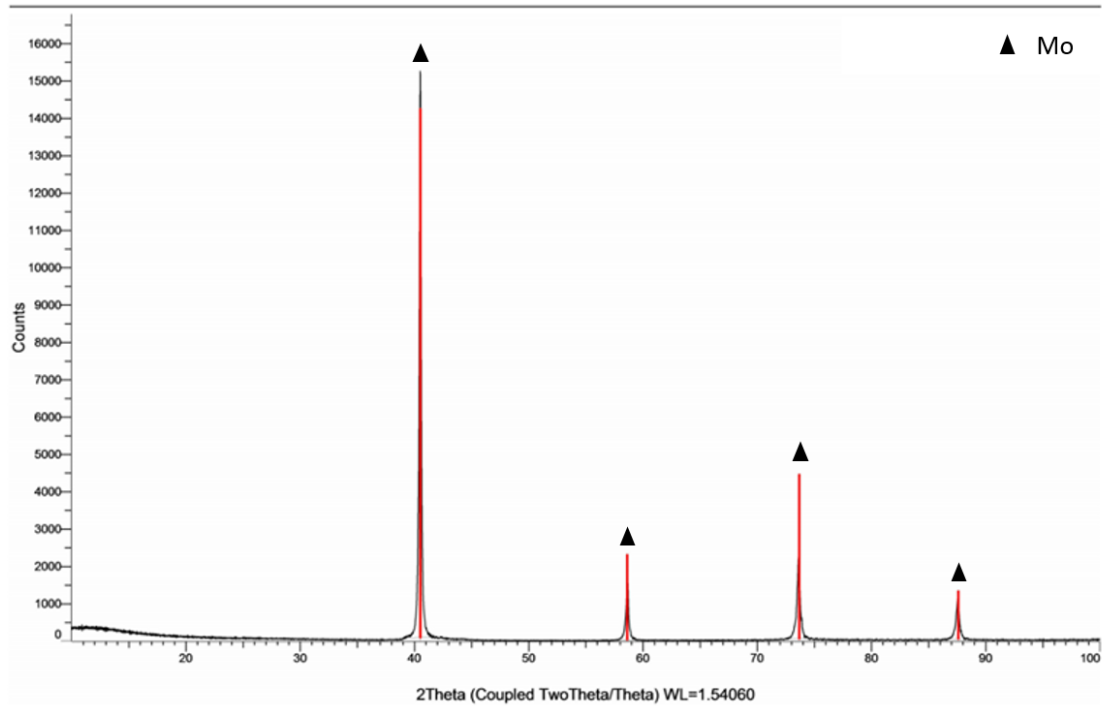
Figure 8 X-Ray Diffraction result of pure molybdenum sample before the experiment.
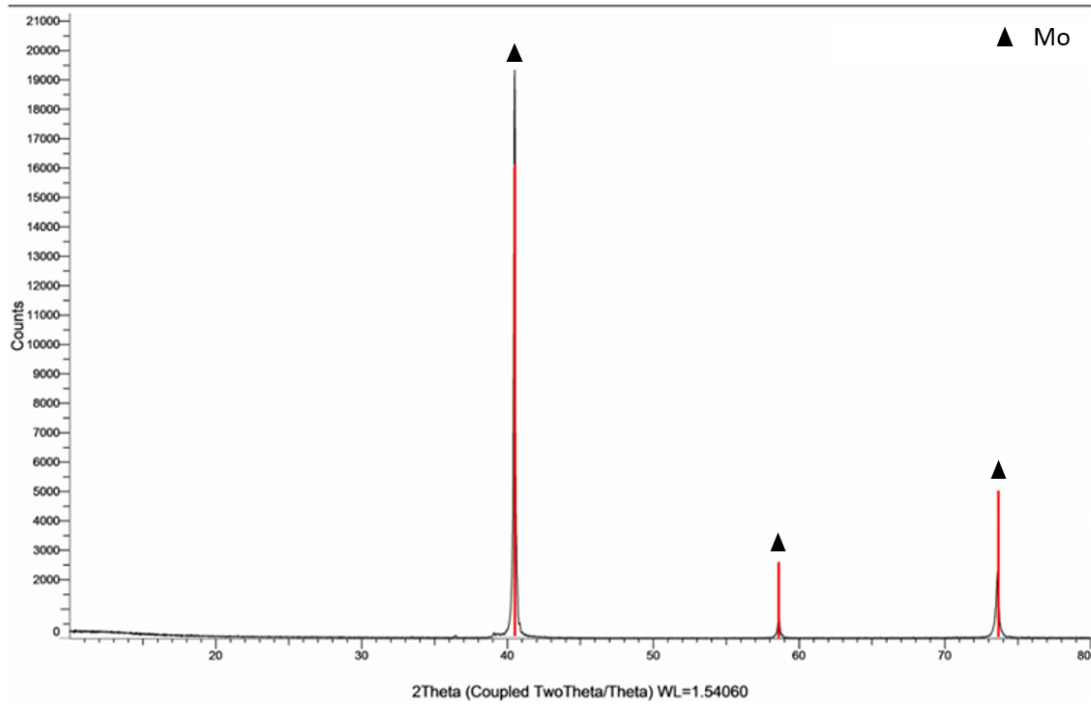
Figure 9 X-Ray Diffraction result of TZM alloy sample before the experiment.

3.3 Experimental Setup for Silicide Coating Process

The experimental setup consists of a high-temperature furnace and its controller, nitrogen gas cylinder, quartz reactor, alumina crucible, and tungsten-kanthal wire. Kanthal-tungsten wire was used to avoid kanthal-salt interaction. Therefore, tungsten wire was welded to kanthal wire above the electrolyte level. The cross-section of the reactor which was placed inside the furnace is illustrated in Figure 10. Another precaution to prevent the alumina crucible from being damaged and salt solutions from forming aqueous solutions due to moisture by the sudden temperature increase, the temperature was increased gradually to the aimed temperatures.
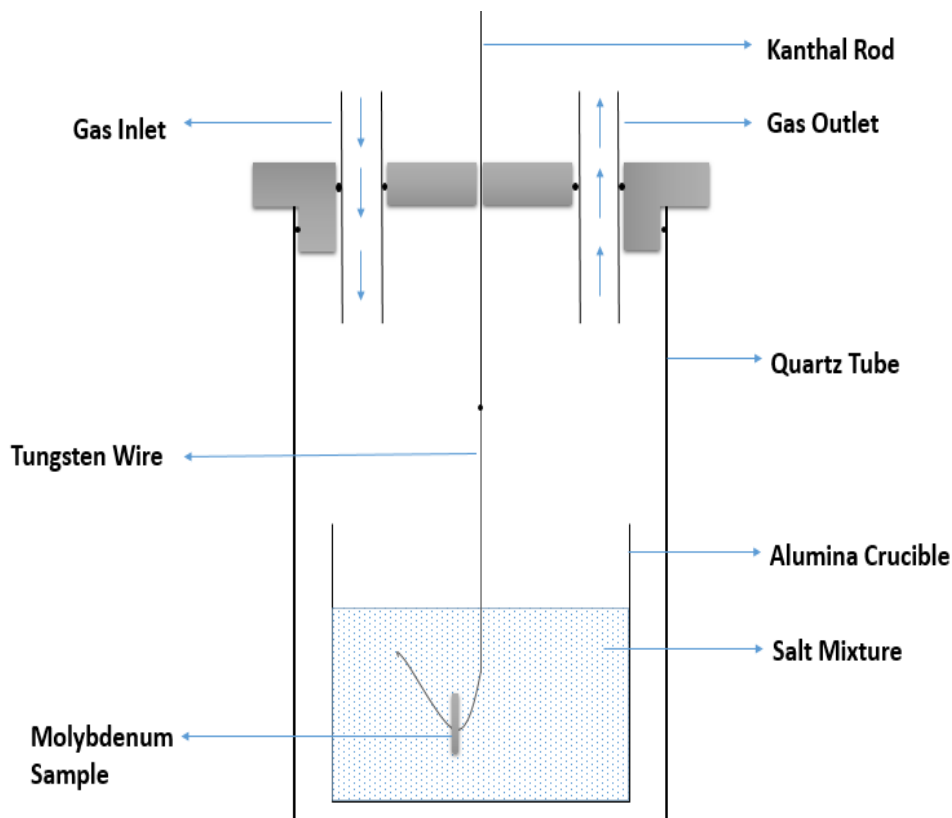
Figure 10 Schematic representation of cross-section of experimental setup.

The prepared salt mixture in the alumina crucible was placed into a quartz tube. Then, the cleaned sample was suspended by a kanthal-tungsten wire. After that, the quartz tube was closed by a Teflon lid that had three inlets on it. One of the inlets was used to deliver tungsten-kanthal wire that holds the sample, and others were used for gas inlet and outlet. The Teflon lid was clamped to the quartz tube by metal screws, and then the tube was placed into the high-temperature furnace. All these steps are shown in Figure 11, respectively.

Figure 11 The preparation steps for the experiments: (a) TZM/Mo samples, (b) suspension of the samples by the tungsten wire; (c) immersion of the sample into the alumina crucible with the help of the wire and (d) placement of the quartz tube into the furnace.

Afterward, gas inlet and outlet connections were made and the furnace was heated gradually; from room temperature to 100°C using 4°C/min, up to 300°C using 3°C/min and finally up to process temperature (800-900 °C) using 6°C/min as shown in Figure 12.
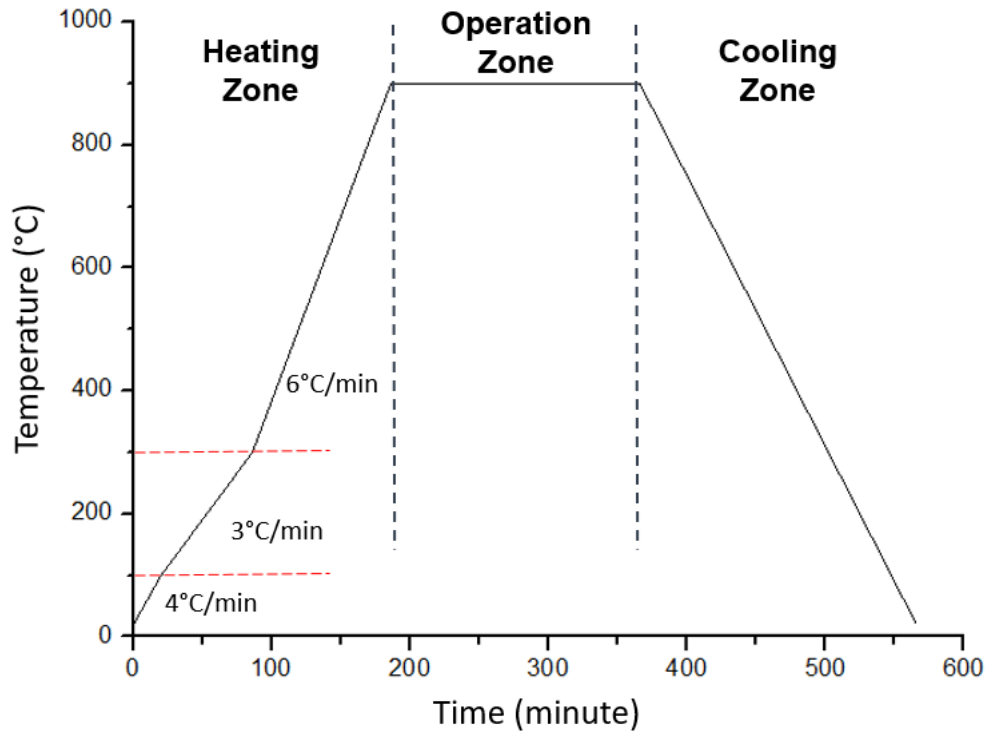
Figure 12 Temperature profile used during heating and cooling the samples.

At the end of the process, the sample was taken from the salt mixture that was cooled to room temperature in the furnace environment. The frozen salt residue accumulated on the samples after the experiment was cleaned by using deionized water in an ultrasonic cleaner. The whole test and cooling process was completed under a nitrogen gas atmosphere to create a protective environment. At the end of each experiment, the sections of the samples were examined under optical and scanning electron microscopes to evaluate the coating thickness. Besides, X-ray diffraction and EDS analyzes were performed to determine the phases that were formed.

3.4 Experimental Setup for Oxidation Tests

Molybdenum di-silicide were formed on pure molybdenum and TZM alloy surface to enhance their oxidation resistance at elevated temperatures. Therefore, silicide coated TZM alloy samples were tested in a high-temperature oxidizing environment. In order

to test coated samples, two different temperatures, 800°C and 1200°C, were selected. These temperatures were chosen by taking into account pure molybdenum's oxidation behavior. In addition to coated samples, uncoated samples were also tested under the same conditions to compare their oxidation behavior. An atmosphere-controlled furnace was designed to oxidize samples. The system consists of a furnace, its controller, dry air gas cylinder and a flowmeter. A water cooling system was installed to protect the ends of reaction chamber where metallic lids and a pressure gauge were present. Schematic illustration of the system and its apparatus are illustrated in Figure 13.
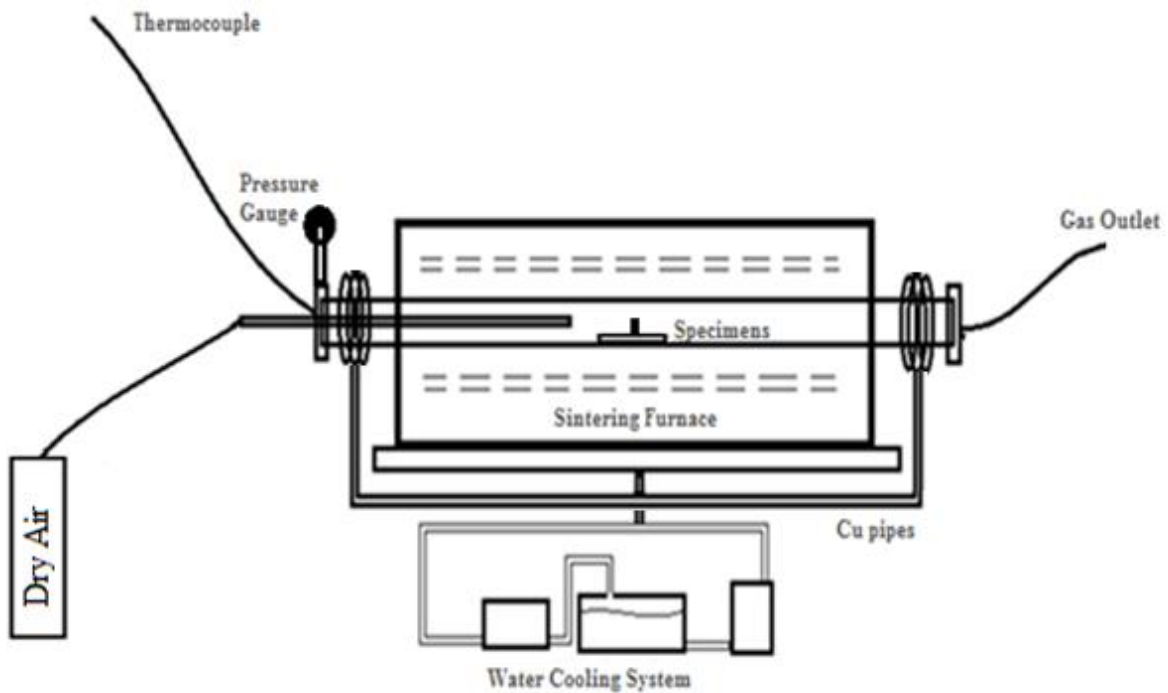
Figure 13 Schematic illustration of the system used in high temperature oxidation tests.

During an oxidation test, a coated sample was placed on an alumina plate vertically and then placed into the high-temperature furnace. The temperature was increased to 800°C and 1200°C using 6°C/min ramp rate, and after reaching the operating temperature, 30 minutes was allowed for the system to stabilize. Then, dry air was

supplied to the system for the specified period of time. In order to simulate near-realistic conditions, dry air, which is high purity and contains oxygen and nitrogen, was supplied at a flow rate of 5lt/min. With the aim of providing direct contact between the sample and dry air, air was supplied through the sample surface using a silica tube. Also, to ensure system temperature, a K-type thermocouple was placed near the silica tube which provides air through the system.

At the end of these tests, samples were cooled to room temperature in the furnace atmosphere. Then, a section of the sample was examined under optical and scanning electron microscopes to evaluate their performance under oxidizing conditions. In addition, X-ray diffraction and EDS analyzes were performed to determine the phases formed.

CHAPTER 4

RESULTS AND DISCUSSION

4.1 Pure Molybdenum Studies

4.1.1   Identification of Silicide Layer

Pure molybdenum samples were silicide coated at 800 and 900°C from 3 to 10 hours using the molten salt method. First of all, coated layers were examined using X-ray diffraction method to make sure that the molybdenum di-silicide phase formed on pure molybdenum surface. Figure 14 shows that X-Ray Diffraction pattern of the sample coated at 800°C for 10 hours is consistent with $MoSi_2$ phase.
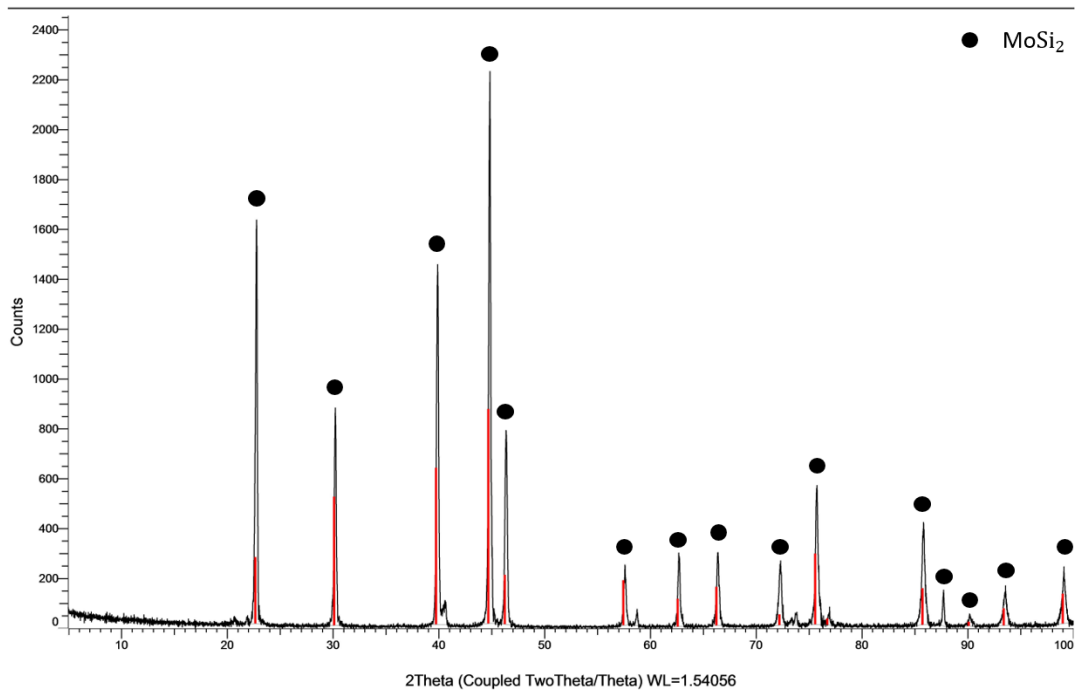
Figure 14 X-Ray Diffraction result of pure molybdenum sample coated at 800°C for 10 hours.

Furthermore, cross-section of the sample was examined by scanning electron microscope and EDS analyses. These analyses verified that formed phase on the surface was MoSi$_2$. Figure 15 shows EDS analysis of the sample coated at 800°C for 10 hours and quantitative analysis results is consistent with atomic ratio of MoSi$_2$ phase.


```
EDAX ZAF Quantification (Standardless)
Element Normalized
SEC Table : Default

Element    Wt %     At %    K-Ratio     Z        A        F
  SiK     34.28    64.05    0.2791    1.1202   0.7161   1.0150
  MoL     65.72    35.95    0.4757    0.9109   0.7946   1.0000
 Total   100.00   100.00

Element   Net Inte.     Bkgd Inte.    Inte. Error      P/B
  SiK     903.20         37.48          0.54         24.10
  MoL     590.31         30.09          0.67         19.62
```
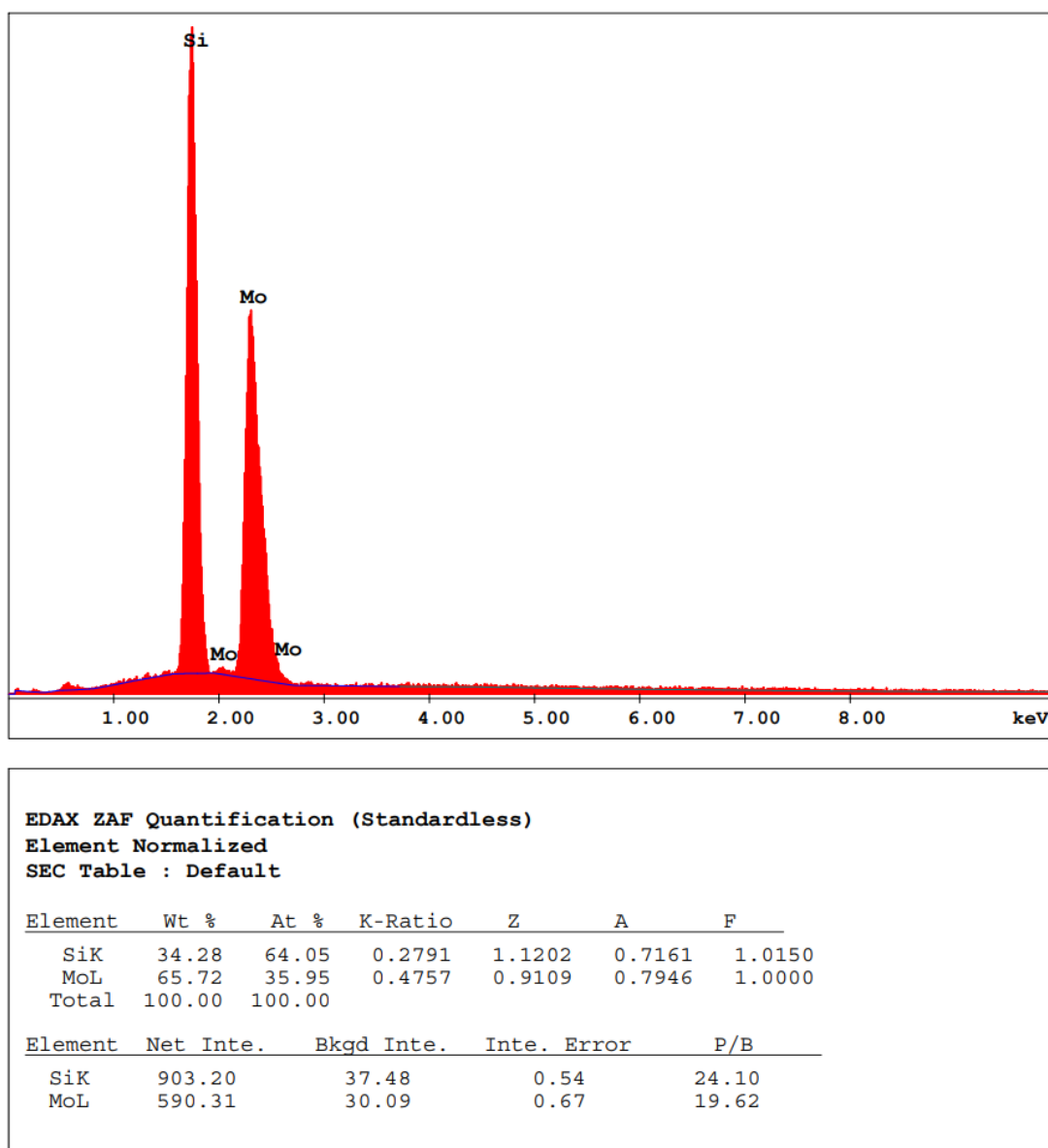
Figure 15 EDS analysis of the silicide layer of pure molybdenum sample coated at 800°C for 10 hours.

Besides, molybdenum and silicon atoms were traced throughout the line that lies from molybdenum di-silicide to pure molybdenum substrate using EDS line analysis as

shown in Figure 16. The result of the EDS analysis given along the line with the red arrow in Figure 16 is shown in Figure 17. As seen in Figure 17, it was determined that the distributions of silicon and molybdenum atoms were homogeneous in the coating section and the composition was constant in the scanning from the coating surface to the base. The fixed composition was determined to be $MoSi_2$ as previously determined by X-ray diffraction (Figure 14) and EDS (Figure 15) analyses.
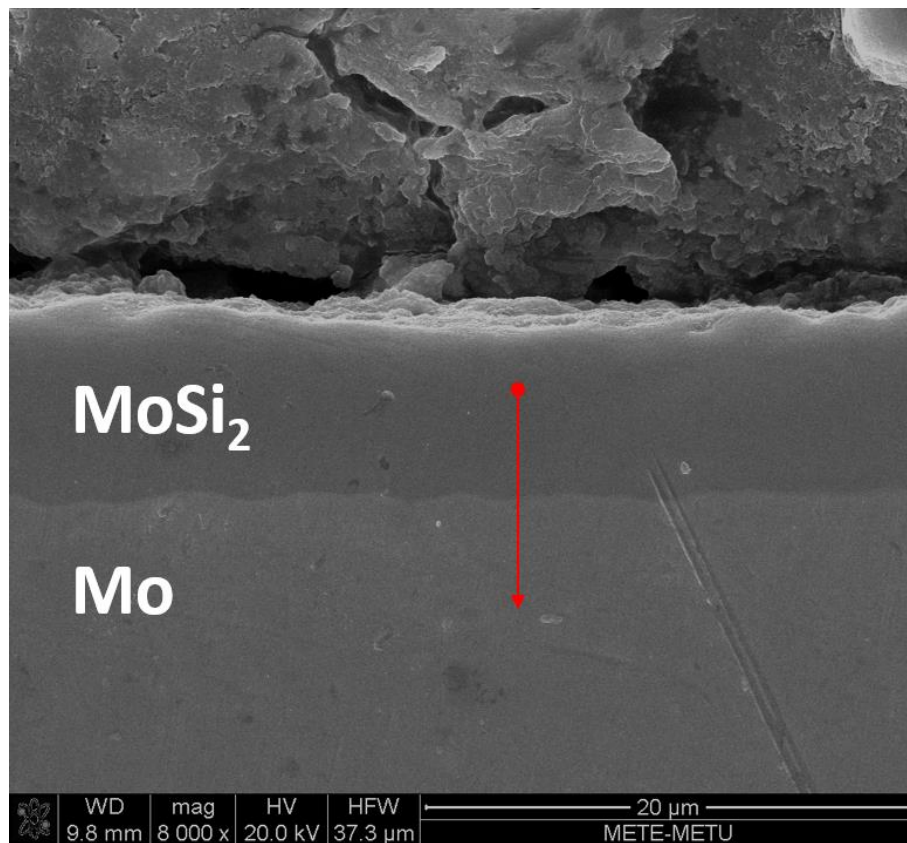
Figure 16 SEM image of the section of silicide coated pure molybdenum sample at 800°C for 10 hours and line on which EDS line analysis was done.
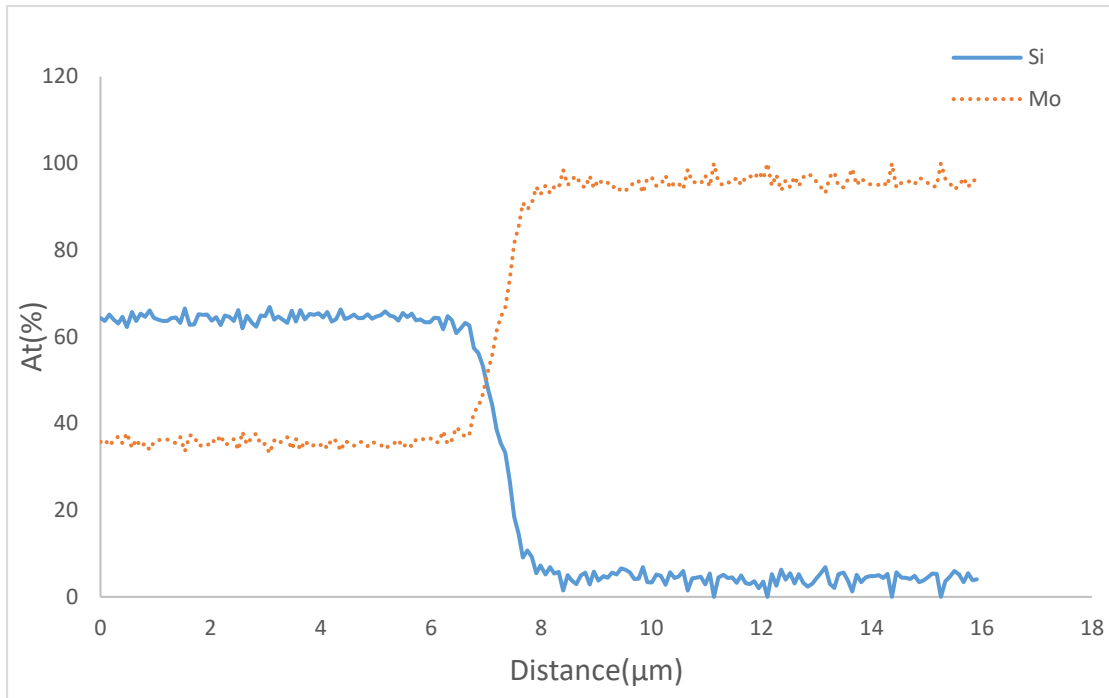
Figure 17 Silicon and molybdenum dispersion results obtained by line analysis in scanning electron microscope.

4.1.2 Coating Thickness

Figure 18 shows low magnification SEM image of the silicide coated sample. In addition to the absence of cracks or pinholes in di-silicide layer, coating is homogenous all around the sample and consistent with base metal even at sample edges. It was observed that the coating was compatible with the base metal and there was no adhesion problem between silicide layer and base metal, which was deduced from the regional scanning made on the edges of the section sample at higher magnifications by scanning electron microscopy. Also, there was no obvious cracks or voids in the coating layer in any of the scanned areas.
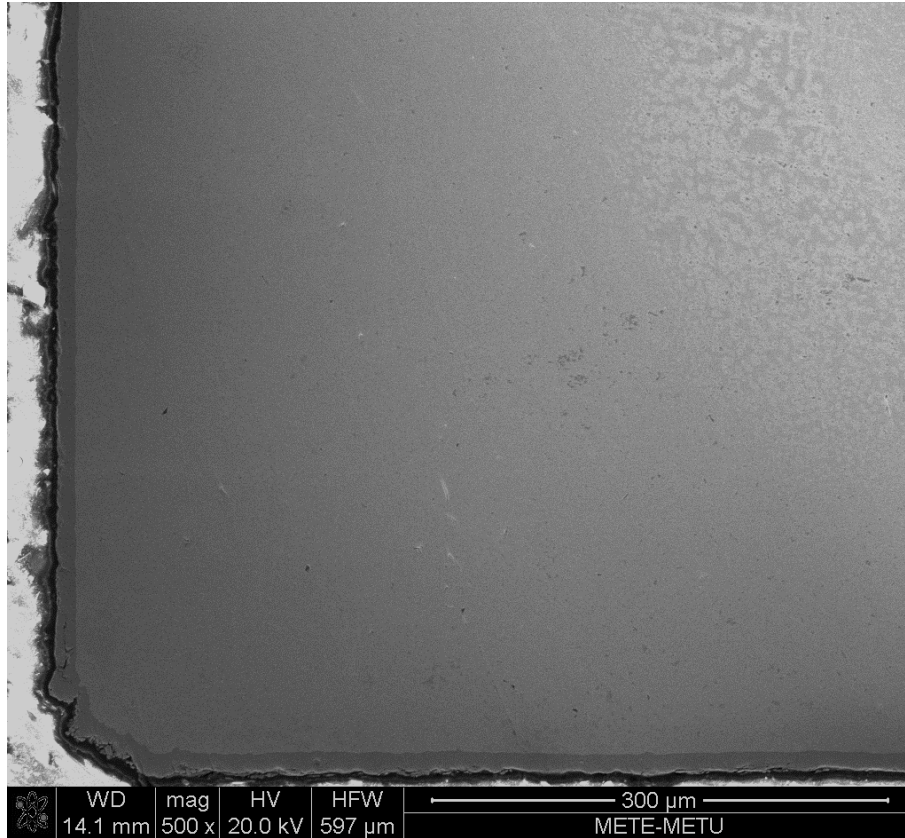
Figure 18 SEM image of the section of silicide coated pure molybdenum sample at 900°C for 4 hours.

The cross-sections of coated samples were examined under scanning electron microscope and thicknesses of molybdenum di-silicide layers were measured. The thicknesses were obtained by measuring the coating thickness from four different points in the cross-section SEM image. Figure 19 shows the change in thickness of silicide coating on pure molybdenum substrate with time from 3 to 10 hours at 800°C and 900°C. When all the results obtained were considered, it was found that the coating thicknesses ranged from 10 to 22 microns. While the coatings thicknesses obtained at 800°C were not affected by immersion time and remained nearly constant as the immersion time increased, coating thicknesses slightly increased as temperature increased to 900°C. The reason in coating thickness at 900°C may be related to faster diffusion of silicon atoms. By this way, more reaction that yields in formation of silicide on molybdenum surface might have taken place.

47
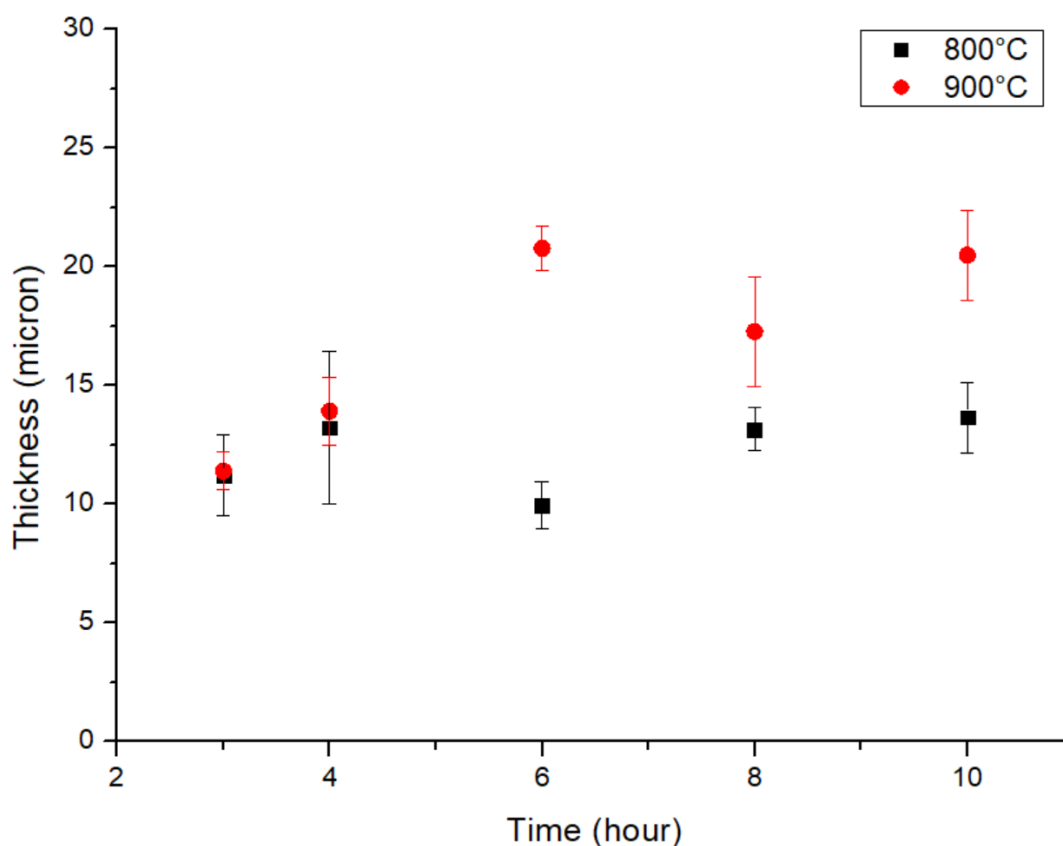
Figure 19 Time-dependent thickness changes of coatings on pure molybdenum substrates at 800°C and 900° C.

In this system, there are two silicon sources that supply silicon to the surface, which are Na_2SiF_6 and silicon powder. As seen in Figure 19, resulting coating thicknesses of silicide layers for 3 hours of siliciding are very close to each other at two different temperatures. It was thought that silicon amount in the system may be insufficient to cover all over the surface and form di-silicide layer. Therefore, the amount of silicon, one of the silicon sources of the system, was increased and salt mixture E2 was used at 800°C and 900°C for 3 hours of operation to enhance the coating thickness. While coating thickness remained constant at 800°C, it slightly increased to 15 microns at 900°C. It was assumed that increasing the amount of silicon alone in mixture is not enough, also temperature has to be increased to 900°C to obtain thicker di-silicide layer for the studies that lasted 3 hours.

To estimate the siliconizing limit of the molybdenum surface, the amount of silicon in the salt mixture was increased again. An additional 5% silicon was added to E2, which

already contained 15% silicon to make it 20%. Under the same conditions, 900°C and 3 hours, obtained coating thickness remained constant by using salt mixture containing 20 wt% pure silicon powder although the di-silicide layer homogeneous and pore-free. Therefore, it was concluded that composition in E2 affects the coating thickness slightly, changing silicon composition to 20% has no important effect on coating thickness, and initial composition, E1, supplies enough silicon to pure molybdenum to cover the surface with silicide.

Changing the amount of the other silicon source, Na_2SiF_6, was another parameter studied to increase the coating thickness. The reason behind this change is evaporation. It was known that salt mixture contains species which evaporate with increasing temperature and some residue was observed on the walls of the tube at the end of experiments. Also, in literature, evaporation of silicon as SiF_4 was reported [35]. Therefore, some of the silicon may leave system as SiF_4 and the reduced amount of silicon in the system may affect the coating process. For this purpose, E3 salt composition was used as media at 800 and 900°C for 3 hours of operating time. Resulting coating was almost the same in terms of thickness and homogeneity. Even if silicon evaporated as SiF_4, no effect was observed on coating thickness.

One final attempt to enhance coating thickness was increasing immersion time at 800°C. As the time passes, fluoride ions in the system decreases due to evaporation F^- ions as SiF_4. The decrease in the amount of fluoride ions in the system may lead to a reduction in silicon ions moving through the molybdenum surface since fluoride ions carry silicon ions to react with the substrate. Therefore, it was thought that increasing the amount of fluoride ions in the system by using E3 mixture could keep F^- ions at sufficient levels for longer operating time. Therefore, the experiment was conducted at 800°C for 6 hours using E3 mixture. However, obtained coating results were almost the same as previously obtained results using E1 mixture. Thus, it was concluded that E3 mixture had no effect on coating thickness at both temperatures and durations.

As a result, thickness of di-silicide layer coated at 900°C increased gradually over time while it remained constant for studies performed at 800°C for pure molybdenum. Also, addition of silicon using E2 mixture had partial effect on coating thickness. On the other hand, any effect of addition of Na_2SiF_6 using E3 mixture was not observed.

4.1.3 Mass Change

Mass change of the samples after experiments is an important indicator to observe correlation with layer thickness. Mass change of pure molybdenum samples with coating thicknesses at 800 and 900°C is shown in Figure 20 and Figure 21. As shown in these figures, there is a correlation between thickness and mass change up to 6 hours of immersion time for both 800 and 900°C. However, for long hours of siliciding i.e. 10 hours, correlation was lost since there is a decrease in mass change while coating thickness increased for both temperatures.
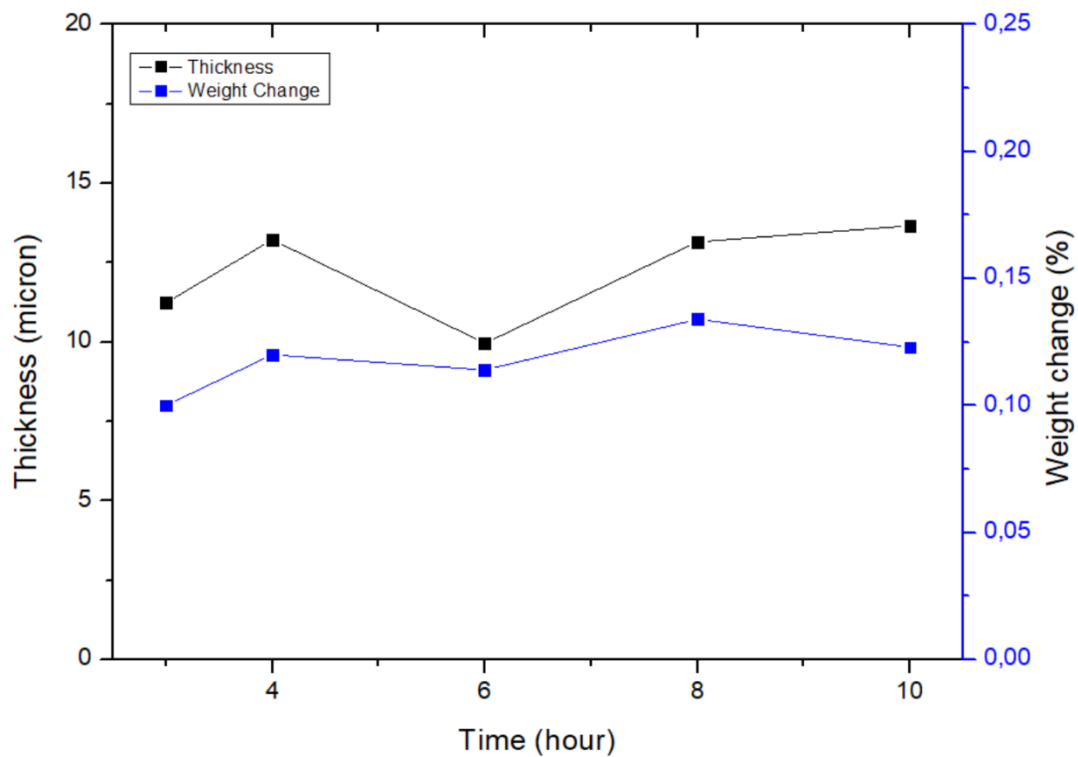
Figure 20 The relationship between mass change and coating thickness over time for the coated pure molybdenum samples at 800°C.
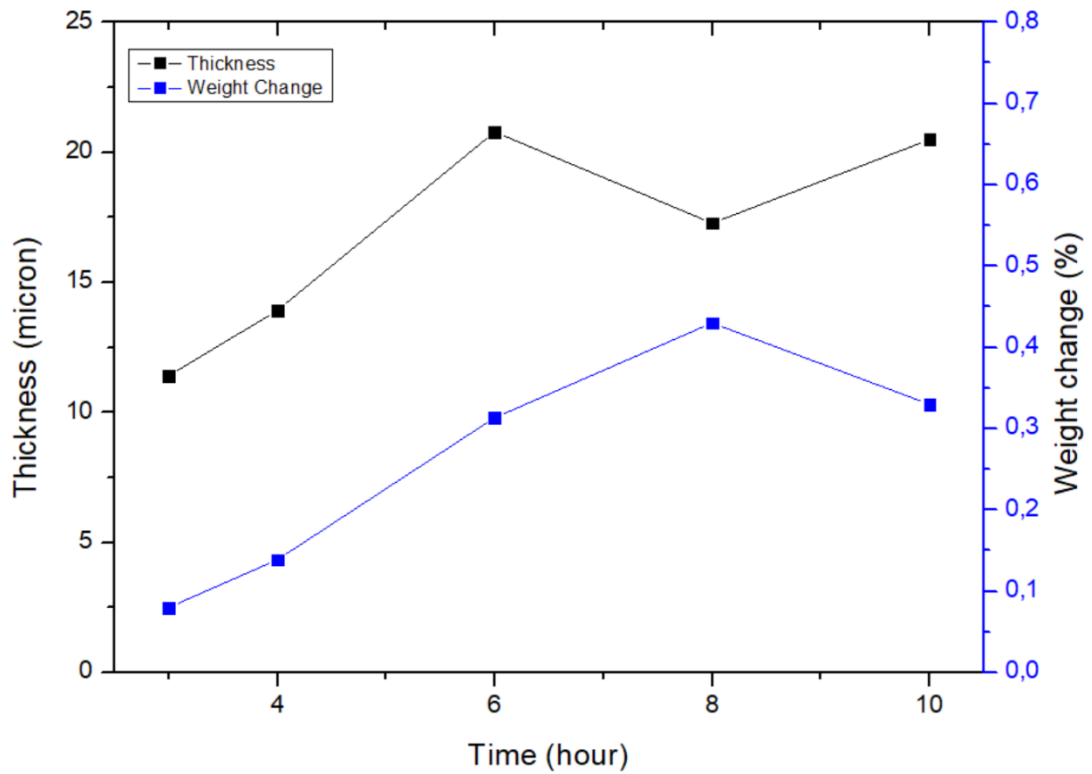
Figure 21 The relationship between mass change and coating thickness over time for the coated pure molybdenum samples at 900°C.

In literature, loss of correlation was associated with inhomogeneous deposition at sample edges, in other words, coating at sample edges was lost for longer time and higher temperatures [32], [34], [35], [37]. However, in this study, interval of immersion time has a wider range than ever done, and there is a correlation when results compared to literature survey. As seen in Figure 21, thicknesses of samples siliconized for 6 and 10 hours are same, and also weight change is nearly slight for both. However, sample siliconized for 8 hours has lower thickness and higher weight change. This may be due to inhomogeneous deposition at sample edges, but lost at sample edges was not observed. On the other hand, all implies that there is a correlation between thickness and weight change for both temperatures until 6 hours of immersion time than correlation gave way to stability for longer hours at 900°C.

4.1.4 Surface Roughness

Surface roughness measurements were done to observe changes of surface morphology of after coating process. Surface roughness values were obtained by measuring 3 mm along 6 different lines for the front and back of the samples. Figure 22 shows the change of surface roughness of coated samples in E1 at 800°C and 900°C.

As seen in Figure 22, surface roughness of coated samples increased for both temperatures. Also, measured roughness values were very close to each other. For the samples coated at 800°C, rougher surface was obtained as the operating time increased except for 10 hours. Likewise, at 900°C, surface roughness increased as the operating time increased.
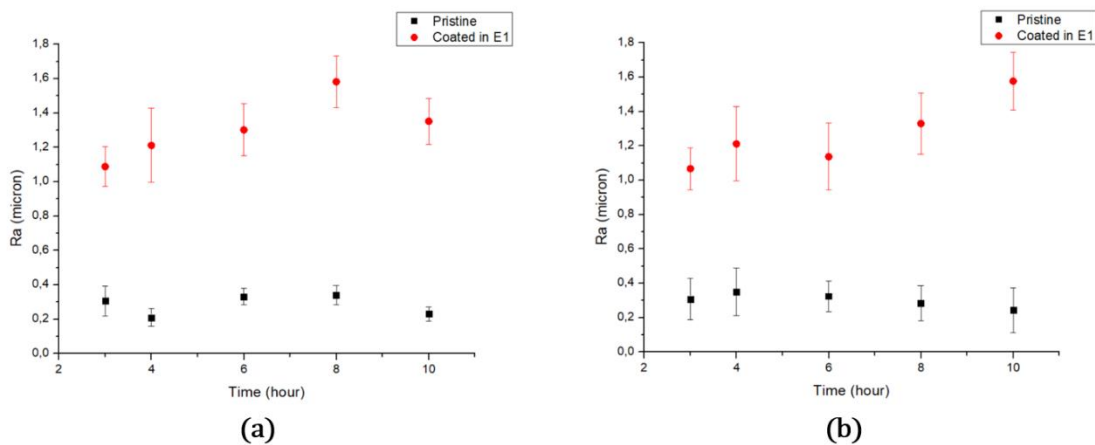
Figure 22 The change of average surface roughness of pure molybdenum samples that coated in E1 at 800°C (a) and at 900°C (b).

4.2 TZM Alloy Studies

4.2.1 Identification of Silicide Layer

TZM alloy samples were siliconized at 700, 800 and 900°C for the time varying between 1 and 6 hours using the molten salt method. Firstly, coated layers were examined using X-ray diffraction method to identify the formed silicide phase on TZM Alloy surface. Figure 23 shows that X-Ray Diffraction pattern of sample coated at 800°C for 3 hours was consistent with $MoSi_2$ phase.
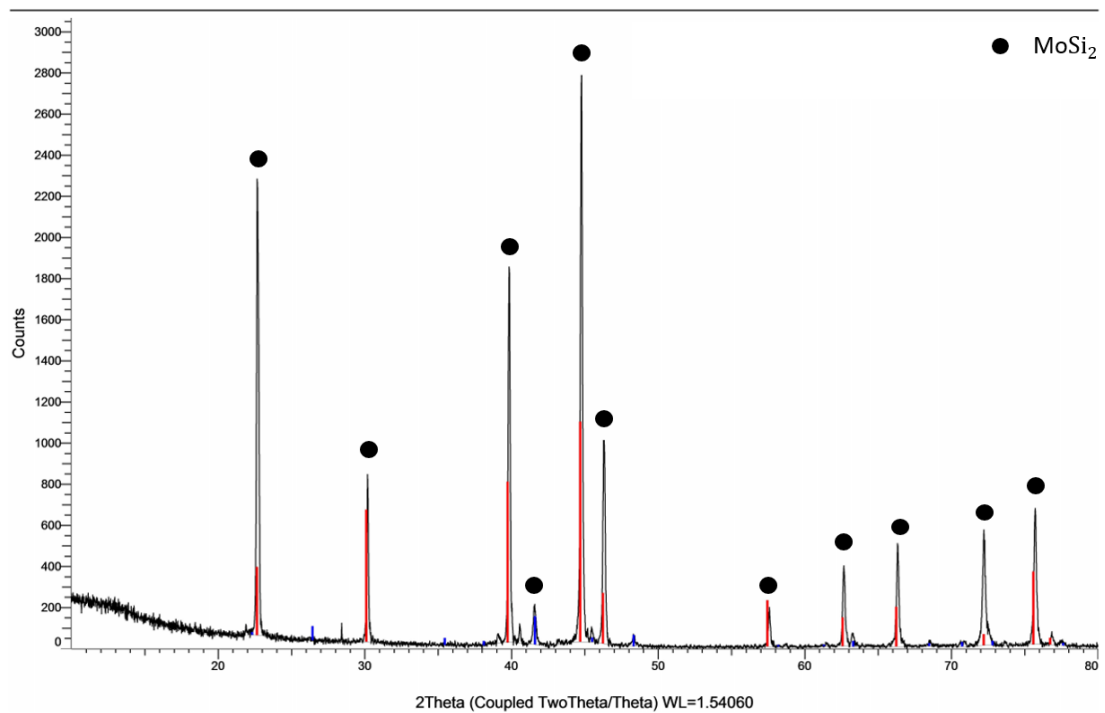
Figure 23 X-Ray Diffraction result of TZM Alloy sample coated at 800°C for 3 hours.

Also, cross-section of the sample was examined under scanning electron microscope and EDS analysis was performed to check out the phases formed on TZM Alloys substrate. As proved previously in X-ray diffraction, EDS analysis also showed that formed phase on surface was $MoSi_2$. Figure 24 shows EDS analysis of TZM Alloy sample coated at 800°C for 3 hours and quantitative analysis results is consistent with atomic ratio of $MoSi_2$ phase.
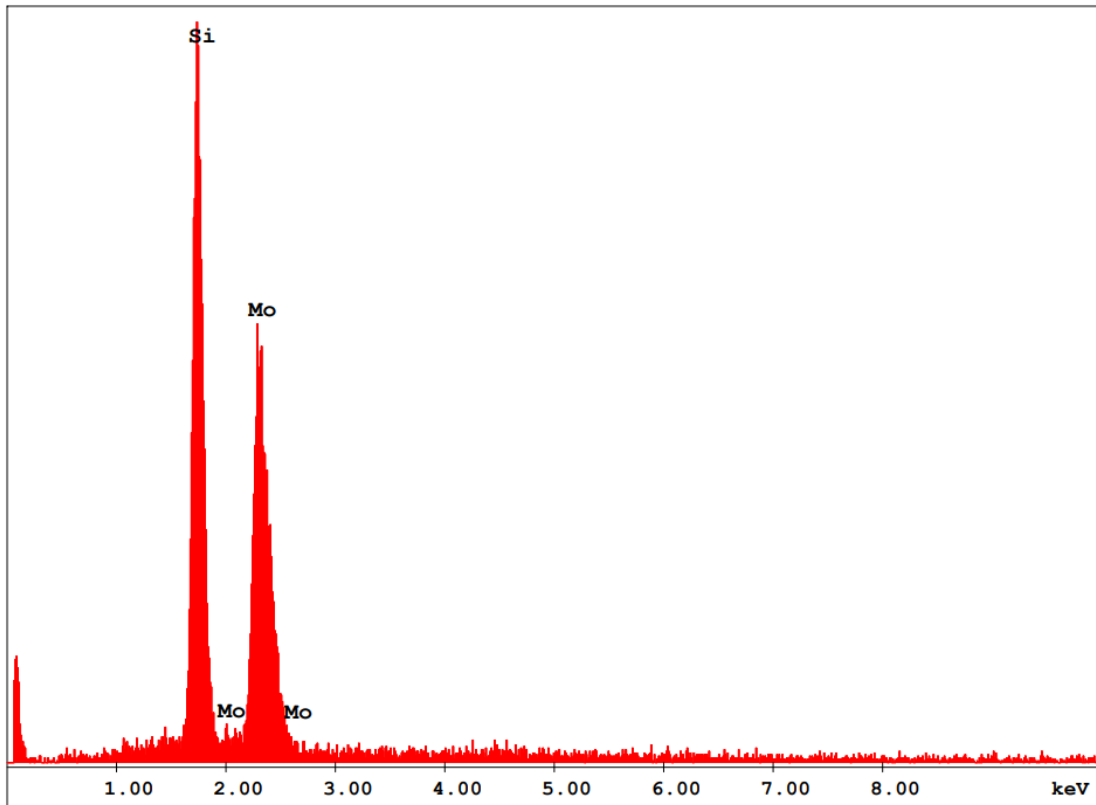
```
EDAX ZAF Quantification (Standardless)
Element Normalized
SEC Table : Default

Element   Wt %    At %      Z        A        F
   SiK   35.43   65.21   1.1175   0.7428   1.0150
   MoL   64.57   34.79   0.9083   0.8057   1.0000
 Total  100.00  100.00
```

Figure 24 EDS analysis of silicide layer of TZM Alloys sample that coated at 800°C for 3 hours.

Furthermore, molybdenum and silicon atoms were traced throughout the line that lies from molybdenum di-silicide to TZM Alloy substrate by using EDS line analysis as shown in Figure 25. The result of the EDS analysis given along the line with the red arrow in Figure 25 is shown Figure 26. As seen in Figure 26, it was determined that the distribution of silicon and molybdenum atoms was homogeneous in the coating section. Also, the composition was constant in the scanning from the coating surface to the base, which means there is only one phase, $MoSi_2$.
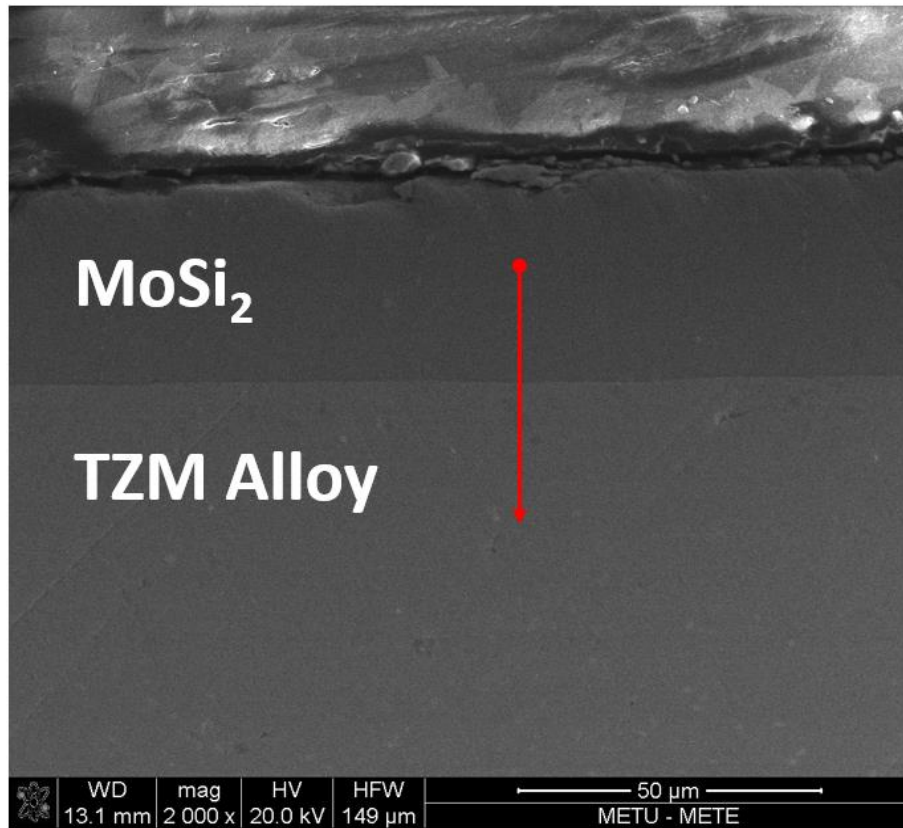
Figure 25 SEM image of the section of silicide coated TZM Alloy sample at 800°C for 3 hours and line on which EDS line analysis was done.
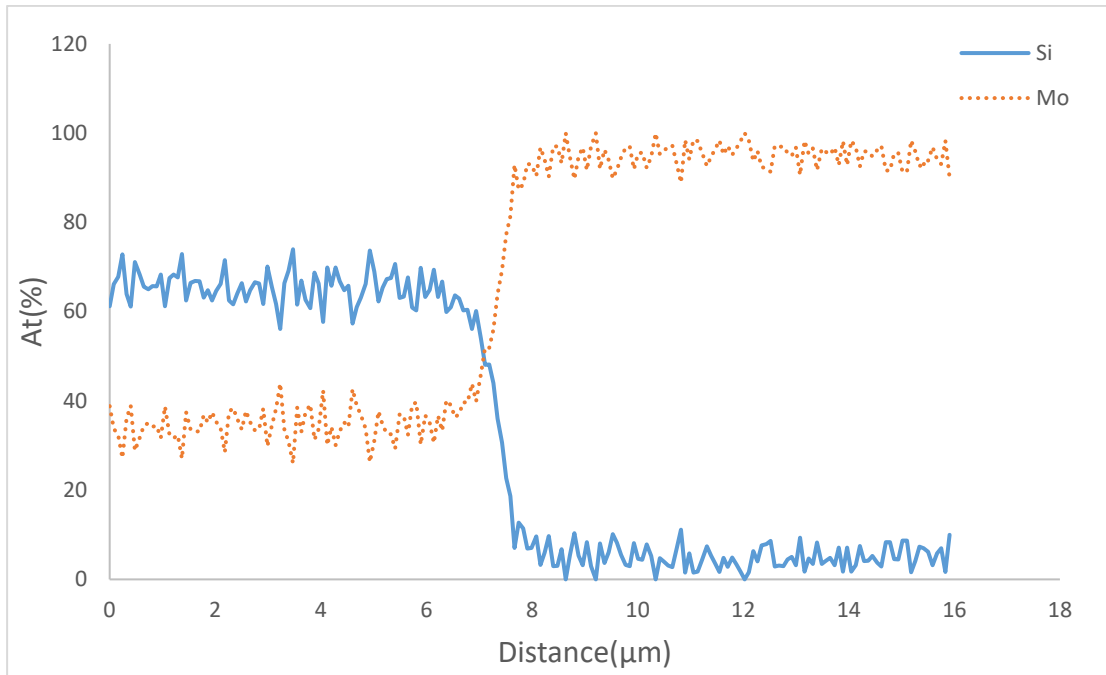
Figure 26 Silicon and molybdenum dispersion results obtained by line analysis in scanning electron microscope.

4.2.2 Coating Thickness

Silicide layers on TZM Alloys substrate were confirmed by X-ray diffraction and EDS examinations that the coating was $MoSi_2$ and no secondary phase was encountered. As with pure molybdenum samples, average thickness values were determined by thickness measurements made from different regions using scanning electron microscopy for TZM samples. Thicknesses of these di-silicide layers were examined under scanning electron microscope to investigate the effect of parameters on coating thickness. First of all, as a result of the regional scanning made on the edges of the section of the sample with scanning electron microscopy, obvious crack or pinholes were not observed on coating layer, and there is no adhesion problem. As shown in Figure 27, silicide layer is compatible with substrate, and coating layer obtained is homogeneously distributed on TZM Alloy.
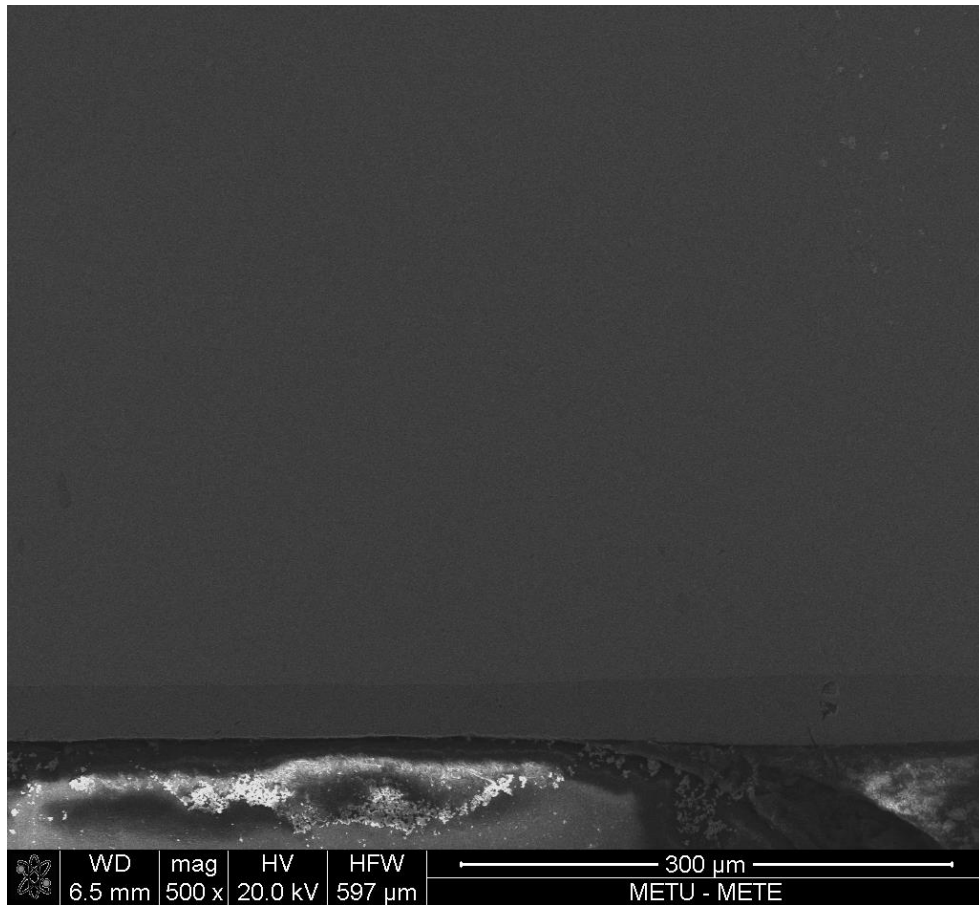
Figure 27 SEM image of the section of silicide coated TZM Alloy sample at 800°C for 4 hours.

In studies with TZM Alloy, parameters were designed by considering results obtained from pure molybdenum. As mentioned in pure molybdenum studies part, desired results were not obtained for longer processing times at both 800 and 900°C. Therefore, in TZM Alloy studies, operating time has been restricted by 6 hours at most. Figure 28 shows the change of coating thickness at 800 and 900°C for 3, 4 and 6 hours of processing time. Contrary to results obtained from pure molybdenum studies, thicker di-silicide layer was obtained at lower temperature, i.e. increase in temperature affected coating thickness negatively. As shown in Figure 28, processing time did not affect coating thickness at 900°C. However, in the studies carried out at 800°C, significant increase in coating thickness was encountered as the time increased. After 4 hours of processing time, the coating thickness reached approximately 40 microns. With increasing the treatment time to 6 hours, no increase in thickness was observed.

57

Most of the research efforts were directed to work at 800 and 900°C for both pure molybdenum and TZM Alloys samples. In literature survey, there are several researches that worked at 700°C for molybdenum and niobium samples [34], [37], but results were not satisfactory and was in the direction that increasing temperature increases coating thickness. However, in TZM studies, there was a decrease in thickness when process temperature increased to 900°C. Therefore, it was studied at 700°C for 3 hours of processing time. Since obtained thickness was thinner than obtained at 900°C, lower temperature studies were not performed anymore.
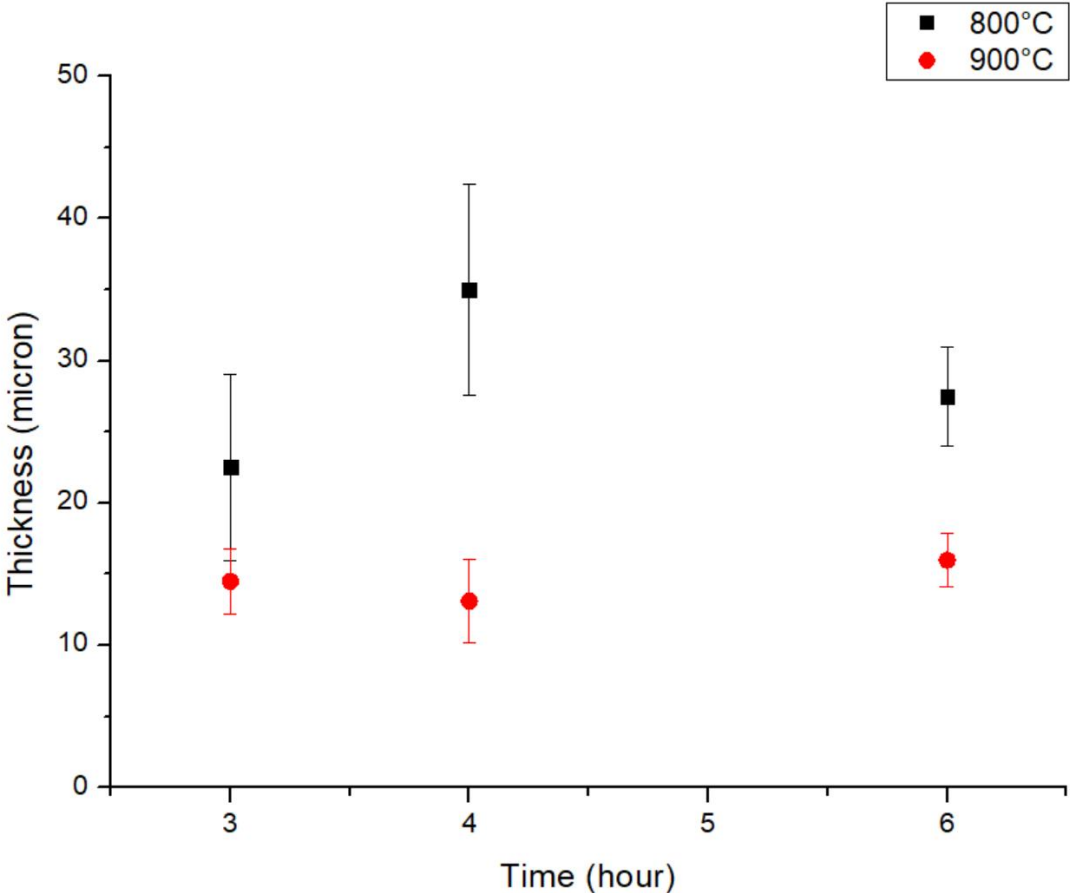
Figure 28 Time-dependent thickness changes of coatings on TZM Alloy substrates at 800°C and 900° C.

To increase coating thickness, the amount of silicon in system was increased by using E2 mixture. The results obtained from E2 mixture are shown in Figure 29 and Figure 30. For the studies performed at 800°C, the change in coating thickness with time was the same as that obtained using E1, in other words, response to processing time was

58

the same as obtained before. However, the effect of E2 mixture was evident, in particular, thickness reached approximately 60 microns after 4 hours of processing time. As experienced using E1 mixture, increasing the treatment time to 6 hours had no effect on coating thickness using E2 either. On the other hand, effect of E2 on coating thickness was also observed studies performed at 900°C. As shown in Figure 30, trend is almost same as using E1, however; thickness was increased evidently until 4 hours of processing time. As experienced in 800°C studies, desired thicknesses were not obtained for 6 hours of processing. Furthermore, it was observed that long hours of processing time, 6 hours, was not effective for enhancing coating thickness for all studies performed using TZM alloy samples.
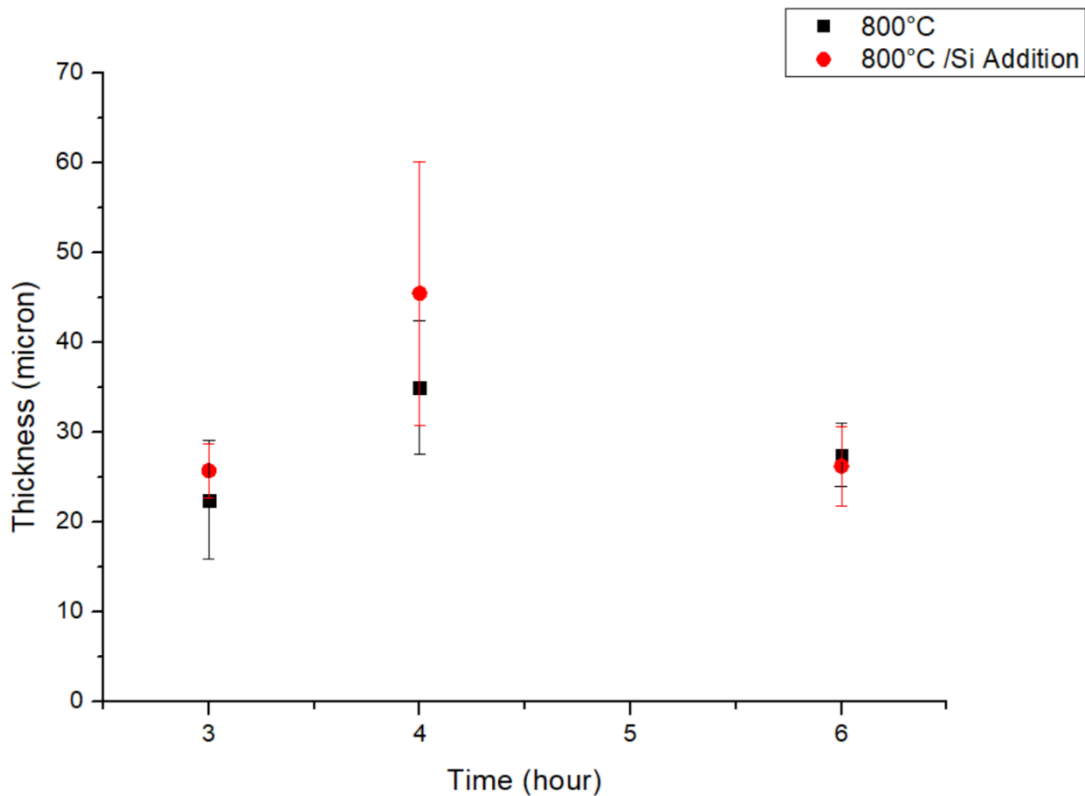
Figure 29 Time-dependent thickness changes of coatings using E1 and E2 mixtures on TZM alloy substrates at 800°C.
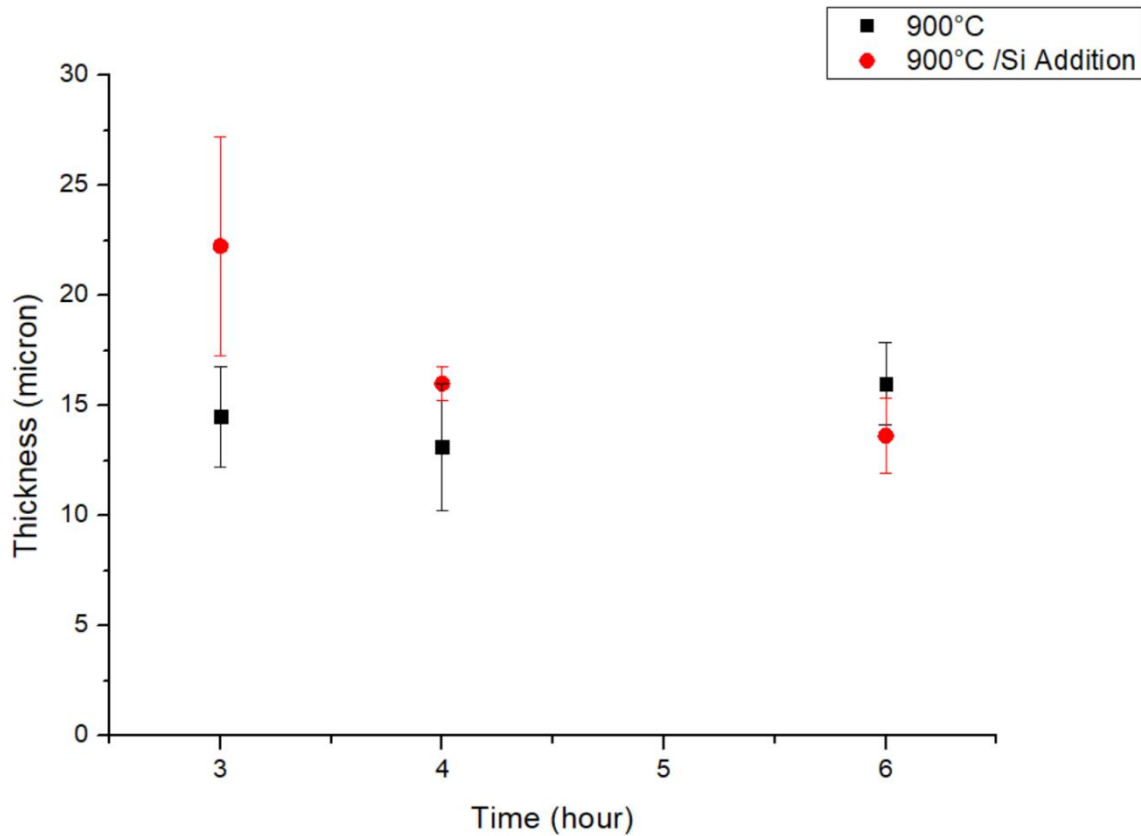
Figure 30 Time-dependent thickness changes of coatings using E1 and E2 mixtures on TZM Alloy substrates at 900°C.

To investigate the decrease in thickness for longer operating times, Inductively Coupled Plasma – Mass Spectrometer (ICP-MS) measurements were performed. for the samples taken from salt mixtures E1 and E2 after 6 hours of coating to observe whether di-silicide layer dissolved in salt mixture or not. In addition to molybdenum, other constituent of TZM alloy titanium and zirconium, and tungsten that might be present due to wire used were traced in this analysis. The ICP-MS results are given in Table 8. Obtained results showed that both samples includes molybdenum and alloy constituents in terms of titanium and zirconium as well. This results supported the idea of dissolution of di-silicide layer that initially formed and lost after longer processing time. Also, sample taken from E2 mixture had higher molybdenum content than E1 mixture. The reason for this difference was related to formed, and dissolved di-silicide layer. As experienced in studies earlier, thicker coating layer was obtained using E2 mixture, and therefore, more $MoSi_2$ formed and dissolved.

Table 8 Results of Inductively Coupled Plasma Mass Spectrometry analysis of samples taken from salt mixtures of samples studied in E1 and E2 mixtures at 800°C for 6 hours.

Element Sample	Mo (mg/kg)	Ti (mg/kg)	Zr (mg/kg)	W (mg/kg)
800°C/6 hours/E1	6.6±0.5	71±5	5.4±0.5	40±2
800°C/6 hours/E2	26±1	86±8	9.5±0.6	182±4

In addition to change in temperature and composition, short processing time, i.e. 1 hour, was studied at 800°C. The reason was to observe the proportionality of the thickness with time and estimate the deposition rate at the very beginning of the process. However, coating was very thin, around 6 microns in average, which proved that initially coated layer acts as catalyzer to develop further coating. Also, as mentioned in Pure Molybdenum Studies part, E3 mixture was used to enhance coating thickness by changing the amount of silicon in the system, but significant effect was not observed in thickness. Thus, E3 mixture was not used in TZM Alloy studies. Finally, it was summarized that TZM Alloy samples gave better coating thickness than pure molybdenum samples. The thicker coatings were obtained at 800°C and better results were obtained using E2 mixture for both temperatures.

4.2.3 Mass Change

Mass changes of TZM Alloy samples with coating thickness after siliciding are shown in Figure 31. The increase in coating thickness that was observed when the temperature decreased from 900°C to 800°C was also evident on weight change data as well. Therefore, thicker coating resulted in more mass gain as expected. The change in mass

of siliconized samples at 800°C was higher than that at 900°C, and there was a correlation between weight change and thickness for all TZM Alloy samples.
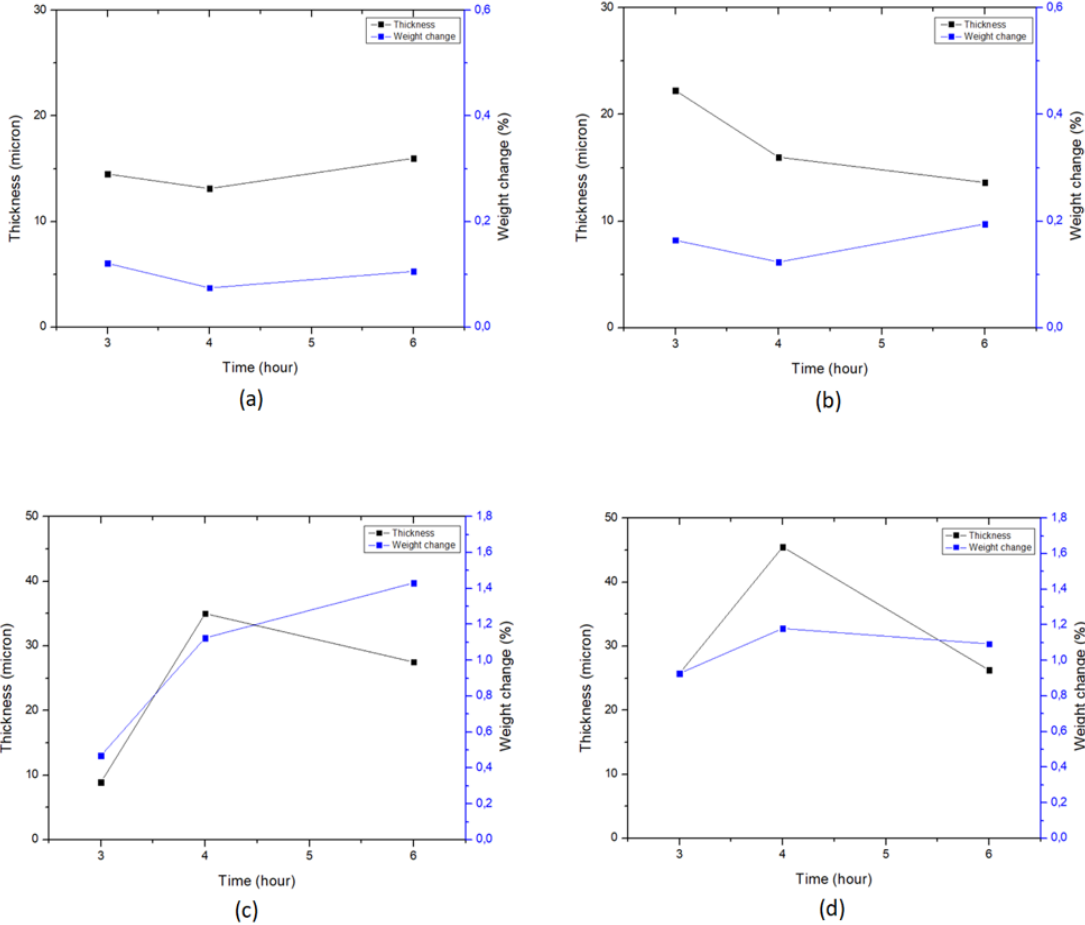
Figure 31 The relationship between mass change and coating thickness over time for the coated TZM Alloy samples: (a) at 900°C, (b) E2 mixture at 900°C, (c) at 800°C and (d) E2 mixture at 800°C.

The effect of using additional silicon on weight change was not obvious even though its effect on thickness was appearent. Also, it was observed that weight gain increases while coating thickness decreases for long hours of processing time. This was associated with higher deposition at the edges of the samples. As experienced in pure molybdenum samples, it is possible to have inhomogeneous deposition at the edges even though other surfaces are smoothly covered. Therefore, an inverse correlation was observed between thickness and weight gain. Therefore, it can be conculuded that there is a correlation between thickness and weight gain which is lost for long hours of processing time.

4.2.4   Surface Roughness

Surface roughness was measured to observe changes of surface morphology after coating process. Surface roughness values were obtained by measuring 3 mm along 6 different lines from both sides of the samples. Figure 32 shows the change of surface roughness of coated sample using two different salt mixture, E1 and E2, at 800°C.

As seen in Figure 32, the rougher surfaces were obtained after coating process for both compositions. However, as given in the coating thickness part, thicker coatings were obtained for 3 and 4 hours of processing time, but there was a decrease in thickness for 6 hours. Furthermore, roughness of surfaces for 3 and 4 hours was higher than 6 hours of processing time. There may be two possible ways to explain the correlation between thickness and roughness. Firstly, with the resulting increase in coating thickness, there may be an increase in residue on surface that cannot be got rid of soft cleaning process. Another possibility is etching effect of fluoride. It is known that F^- ions makes an etching effect on metal surface, which leads to have a rougher surface. Also, in this system, F^- ions leave the system as SiF_4, so that concentration of F^- ions will decrease as the processing time increase. Therefore, etching effect will be lower for 6 hours of processing time and surface roughness may decrease.
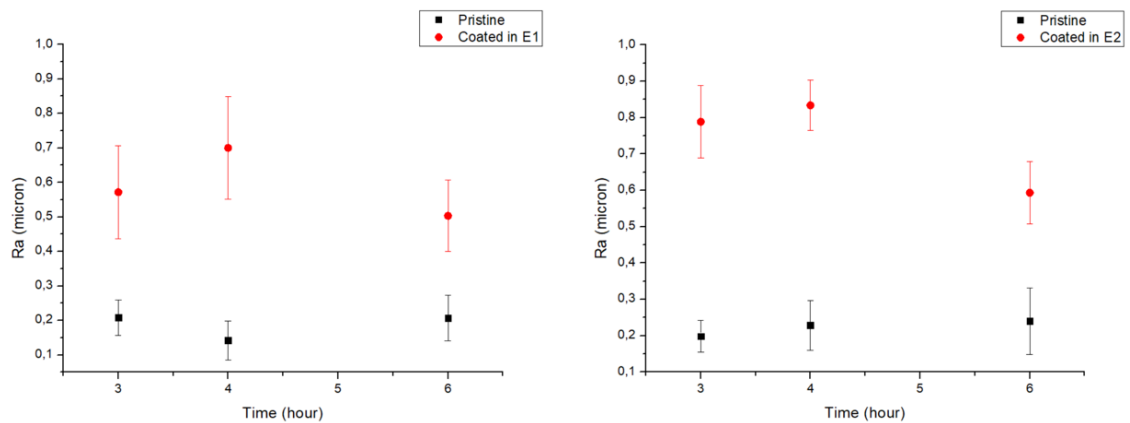

Figure 32 The change of average surface roughness of TZM Alloy samples that coated in E1 and E2 mixture at 800°C.

Figure 33 shows the change of surface roughness of coated sample after coating process in two different salt mixture, E1 and E2, at 900°C. Firstly, the surface of samples that coated at 900°C is rougher than those coated at 800°C. Thus, it was noted that the etching effect of SiF_4 may increase as the temperature is increased. Also, as observed at 800 °C, there was a decrease in average surface roughness over the longer processing time, which can also be associated to the decrease in the composition of F^- ions as a result of the evaporation of SiF_4. However, the final surface was rougher than initial for both temperatures and composition. Therefore, a post surface finishing process might be required to decrease surface roughness after coating process if a smooth surface is desired.
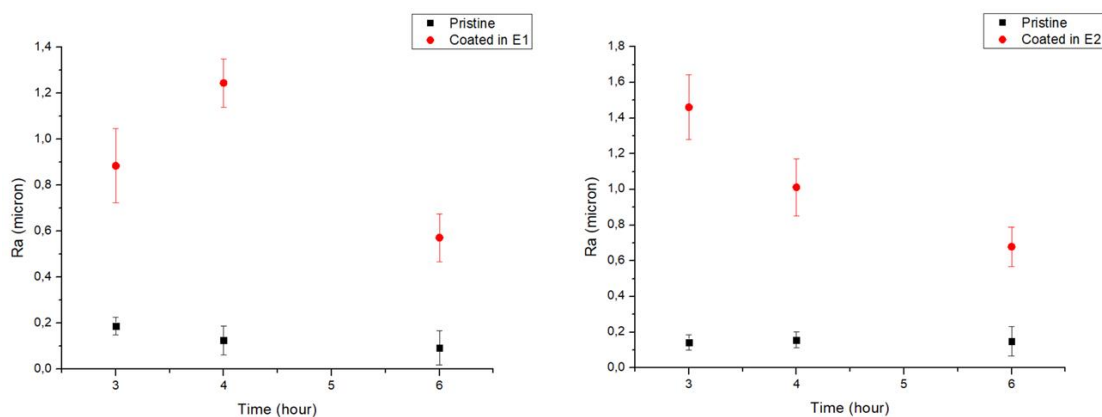
Figure 33 The change of average surface roughness of TZM Alloy samples that coated in E1 and E2 mixture at 900°C.

4.3 Oxidation Tests

4.3.1 Oxidation Test for Pure Molybdenum Samples

Pure molybdenum sample coated at 900°C for 6 hours was preferred because it had higher di-silicide layer thickness among the pure molybdenum studies. First of all, uncoated sample was tested at 800°C for 6 hours under the oxygen atmosphere in order to observe oxidation behavior of pure molybdenum and weight loss of the sample. During the test, dry air was supplied to the system at a rate of 5 lt/min. Uncoated molybdenum sample was oxidized and evaporated completely.

The coated pure molybdenum sample was subjected to oxidation test at 800°C for 6 hours under the same conditions. SEM image of the section of tested sample is shown

in Figure 34. The weight loss of the tested sample was less than 10%. This shows that molybdenum di-silicide formed on pure molybdenum sample, as shown in Figure 35, was protective against oxygen at 800°C for 6 hours.
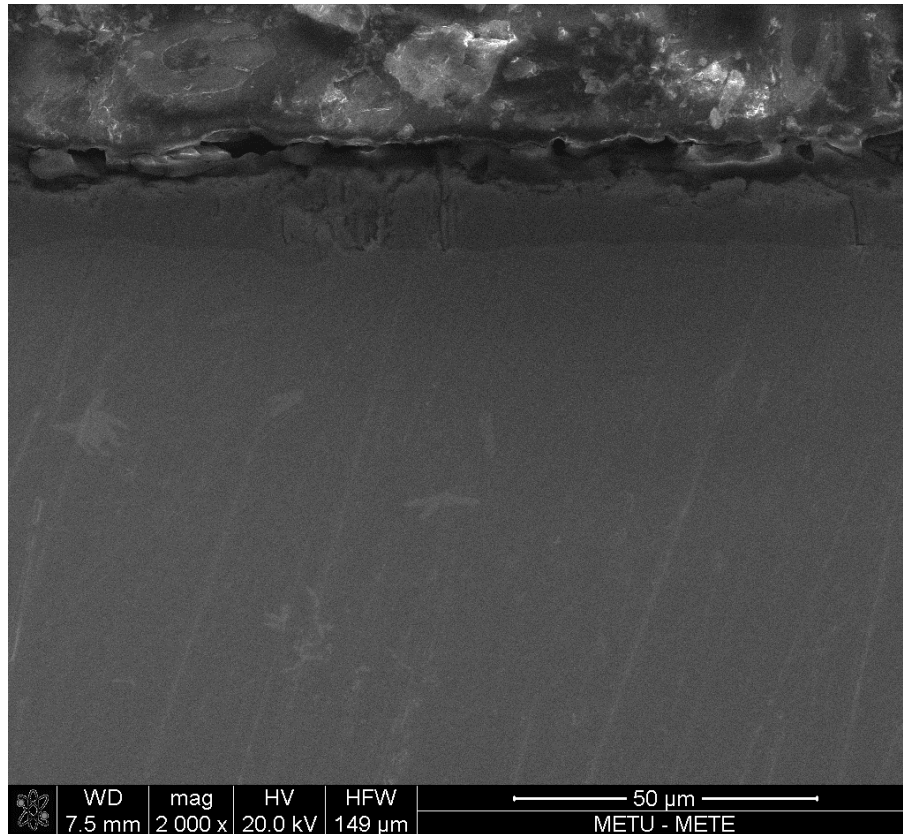
Figure 34 SEM image of the section of oxidized pure molybdenum sample at 800°C for 6 hours.

| Element	Wt %	At %	K-Ratio	Z	A	F
SiK	34.28	64.05	0.2791	1.1202	0.7161	1.0150
MoL	65.72	35.95	0.4757	0.9109	0.7946	1.0000
Total	100.00	100.00				
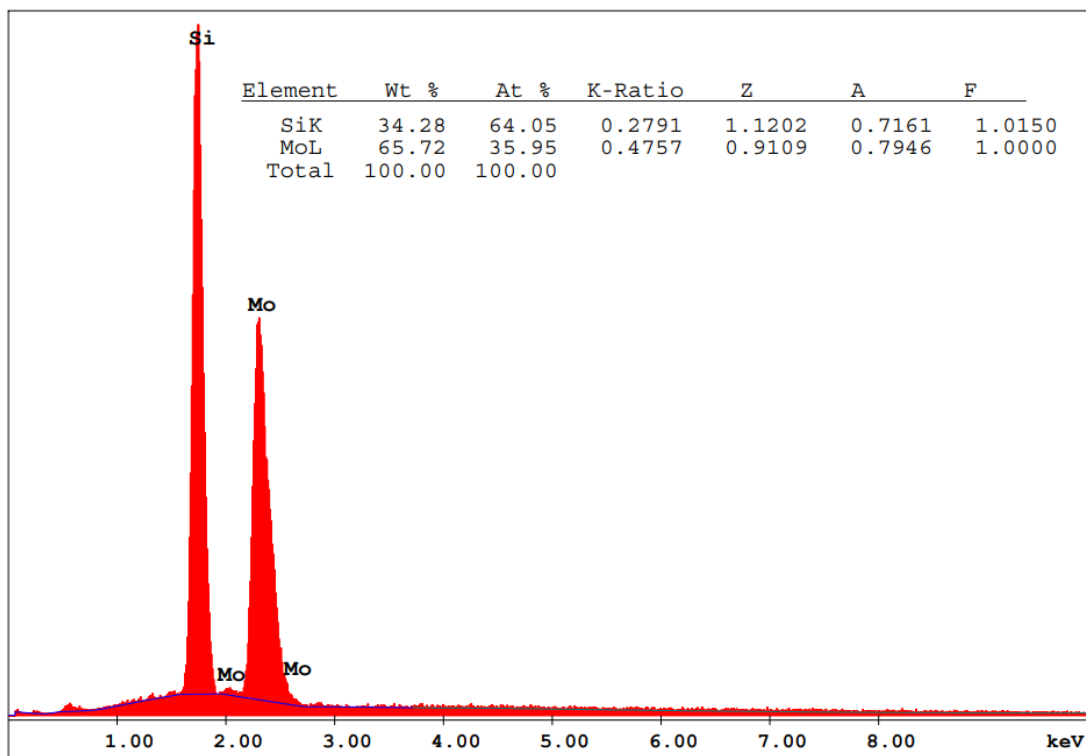
Figure 35 EDS analysis of oxidized coated pure molybdenum sample at 800°C for 6 hours.

4.3.2 Oxidation Test for TZM Alloy Samples

Selected samples were tested in high-temperature oxygen atmosphere to investigate the oxidation behavior after silicide coating. For the test, TZM Alloy sample coated at 800°C for 4 hours was preferred since it has the thickest silicide layer reached among the results obtained from TZM Alloy studies. Oxidation studies were conducted at 800 and 1200°C for 1, 3 and 6 hours.

Firstly, uncoated TZM Alloy sample was tested under oxygen atmosphere at 800°C for 6 hours to see the weight loss and formed phases, and also to compare the results with the oxidized coated sample. Dry air was supplied to the system at a rate of 5lt/min. The weight loss of the uncoated sample was approximately 60%, which shows how molybdenum is susceptible and weak against oxygen at high temperature environment. Also, molybdenum oxide phase formed on the surface as shown in Figure 36.

66
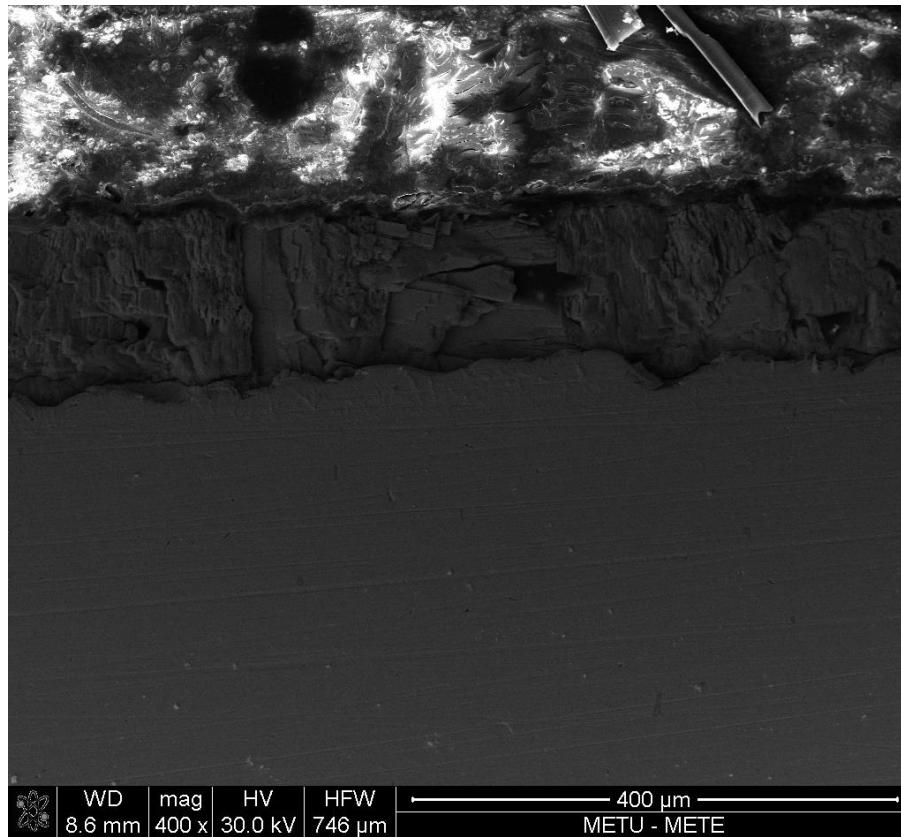
Figure 36 SEM image of the section of oxidized pure TZM Alloy sample at 800°C for 6 hours.

The coated sample was oxidized at 800°C for 6 hours. SEM image of the section of tested sample is shown in Figure 37. Firstly, the weight loss of sample was 12%, which indicates that coating was protective against oxygen at high temperature environment. The coated layer was detected as $MoSi_2$ using both EDX and X-ray diffraction analyses, whose silicon and molybdenum concentrations 66 and 33 at% after oxidation test, and consistent with molybdenum di-silicide. Also, a lighter colored layer was observed above the di-silicide layer as shown in Figure 37. High silicon and very low molybdenum concentrations were detected by EDX analysis performed at this region. Therefore, it was thought that this layer was silica which formed as a result of oxidation. Also, X-ray diffraction analysis was performed to confirm the formation of silica, and result is shown in Figure 38. It is proved that formed phase on di-silicide layer is oxidation protective silica and this silicide layer is protective against oxygen at 800°C.
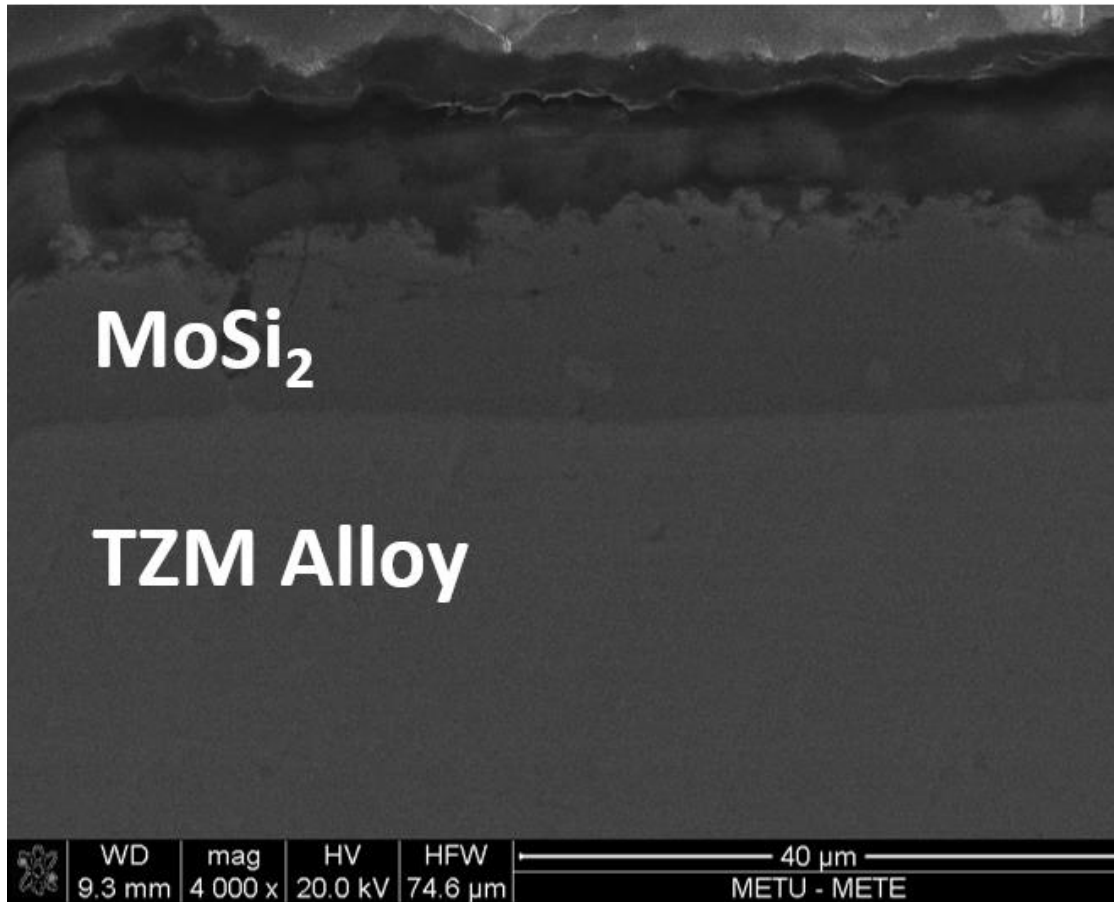
Figure 37 SEM image of the section of coated TZM Alloy sample after oxidation test at 800°C for 6 hours.
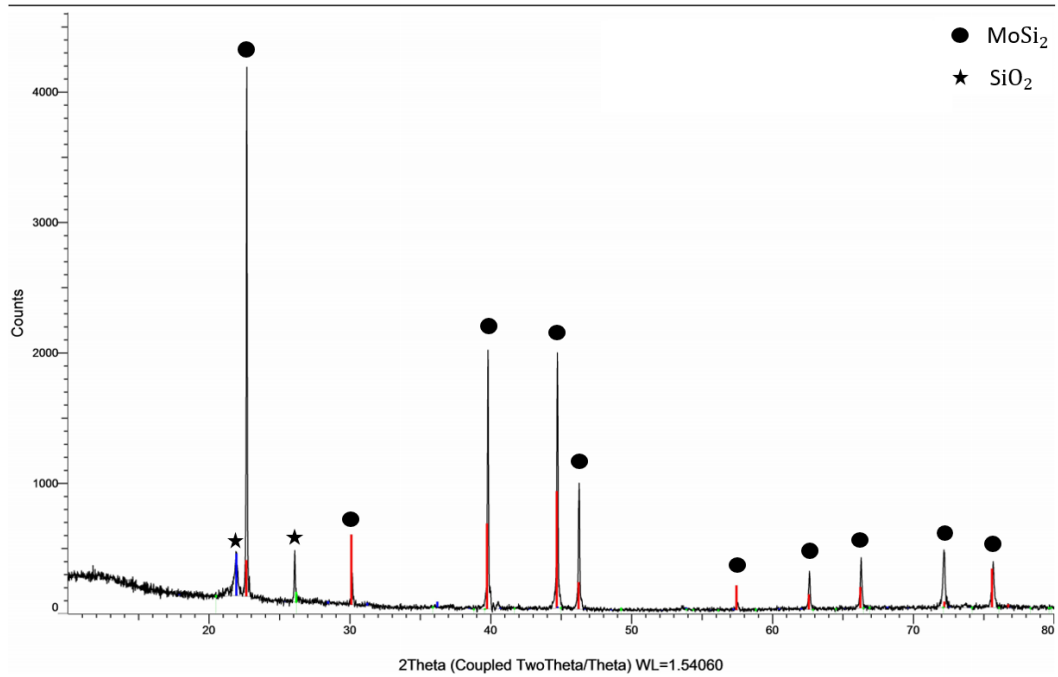
Figure 38 X-Ray Diffraction result of coated TZM Alloy sample after oxidation test at 800°C for 6 hours.

It was expected that molybdenum rich phase (Mo_5Si_3) forms between substrate and molybdenum di-silicide by mutual diffusion [87]. However, it was not encountered by the scans made with SEM. Also, Mo_5Si_3 was not detected in X-ray diffraction analysis as seen in Figure 38. In order to make sure whether Mo_5Si_3 formed or not, EDS line analysis and EDS mapping were performed through a line that lies from molybdenum di-silicide to the substrate. However, concentration profile did not change as shown in Figure 39. Furthermore, EDS mapping was performed on substrate and coating region, and Mo_5Si_3 phase was not encountered, and accumulation of silicon and molybdenum atoms were homogeneous as shown in Figure 40. Therefore, there was no evidence to prove formation of Mo_5Si_3. The reason might be lower operation temperature (800°C), which could be insufficient to form this phase by mutual diffusion.
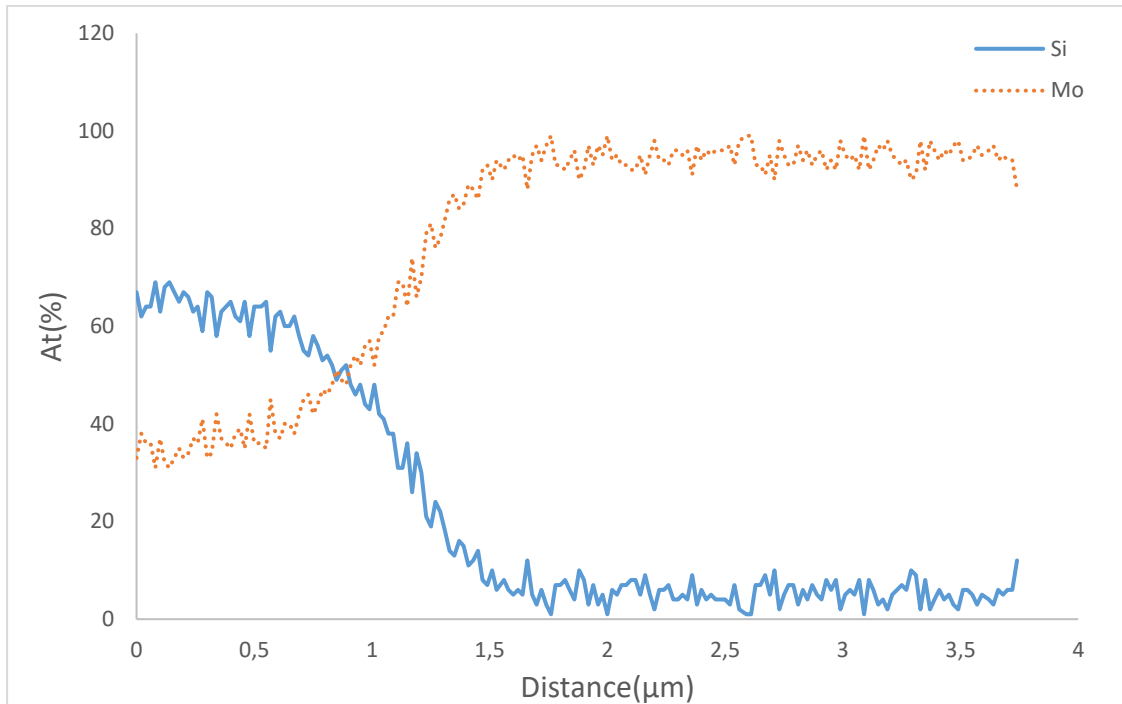
Figure 39 Silicon and molybdenum dispersion results obtained by line analysis in scanning electron microscope.
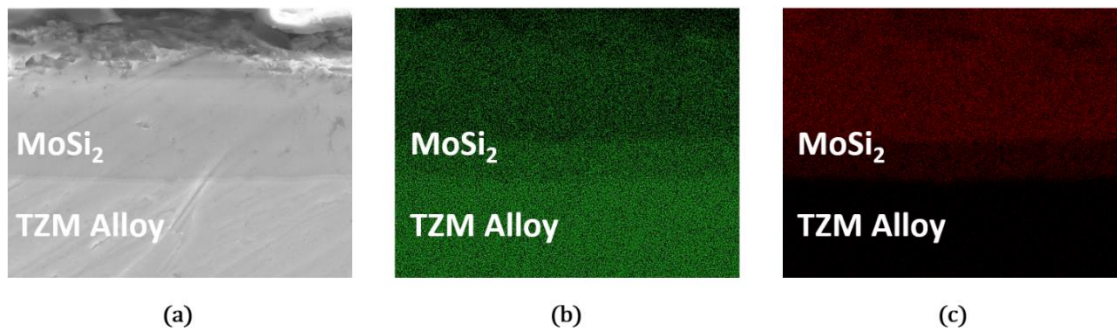
Figure 40 The EDS mapping results: (a) SEM image of the region EDS mapping performed; (b) distribution of molybdenum atoms and (c) distribution of silicon atoms.

Another oxidation study was performed at 1200°C for 1 hour. SEM image of the section of the oxidized sample for 1 hour is shown in Figure 41. As shown in SEM image, there was a contrast difference between substrate and molybdenum di-silicide. EDS analysis showed that Mo_5Si_3 phase formed as expected, and upper layer was $MoSi_2$ as shown in Figure 42. It was proved that transition layer is Mo_5Si_3 whose

silicon and molybdenum concentrations are 60 and 40 at%, which is consistent with Mo_5Si_3.
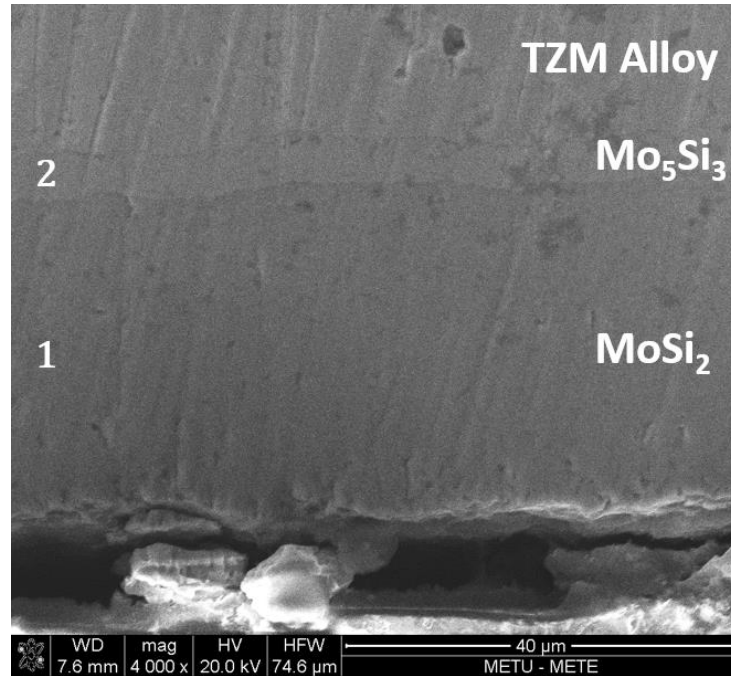
Figure 41 SEM image of the section of oxidized coated TZM Alloy sample at 1200°C for 1 hour.
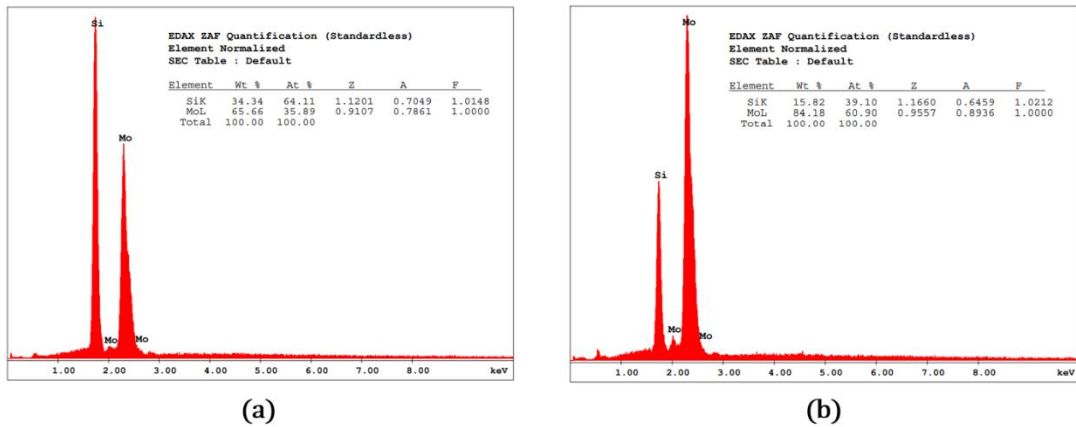
Figure 42 EDS analysis of silicide layers: (a) taken from region 1 in Figure 39 and (b) taken from region 2 Figure 39.

Also, EDS line analysis and EDS mapping were performed. As shown in Figure 43, transition region, Mo_5Si_3, is obvious, and molybdenum atomic concentration decreases gradually. First, concentrations stabilizes at molybdenum rich region, Mo_5Si_3, than stabilizes at silicon rich region, $MoSi_2$. Then, atomic % of molybdenum decreases and silicon increases. Finally, $MoSi_2$ phase exists whose molybdenum and silicon concentrations are 66 and 33 at% respectively.

Furthermore, existence of molybdenum rich phase is more evident in EDS mapping results. As shown in Figure 44 b, molybdenum atom concentration decreases from substrate to the surface. Likewise, silicon atom concentration increases from substrate to the surface as shown in Figure 44 c. The reason for existence of molybdenum rich phase is that the increase in oxidation-test temperature increases the mutual diffusion between molybdenum substrate and $MoSi_2$, and Mo_5Si_3 forms.
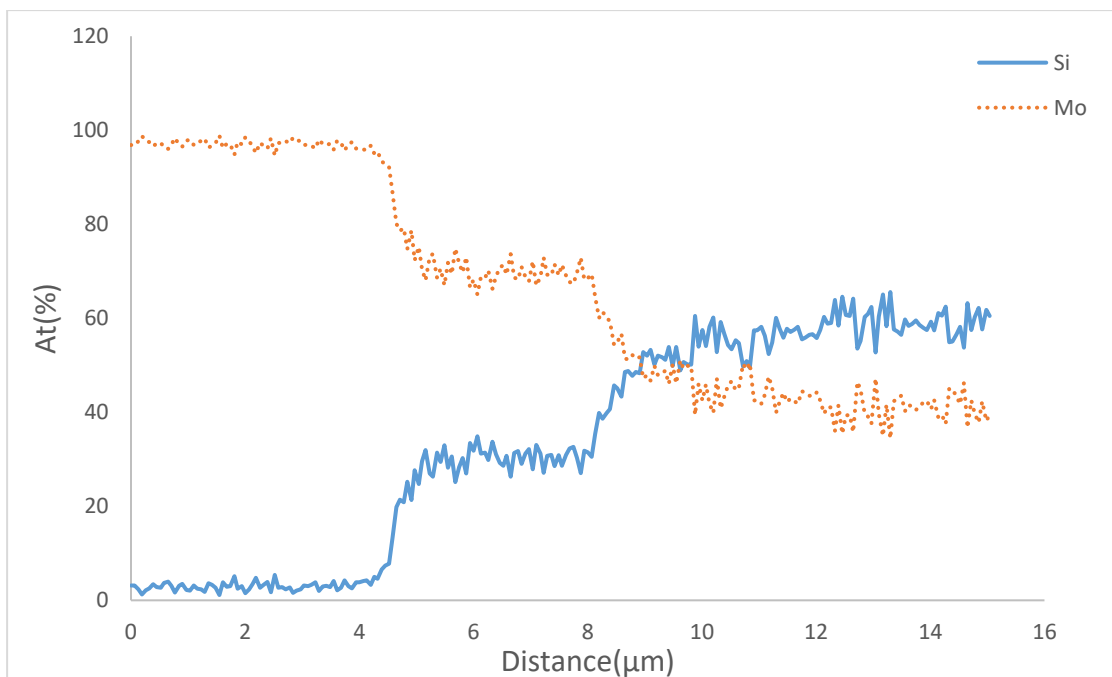

Figure 43 Silicon and molybdenum dispersion results obtained by line analysis in scanning electron microscope.
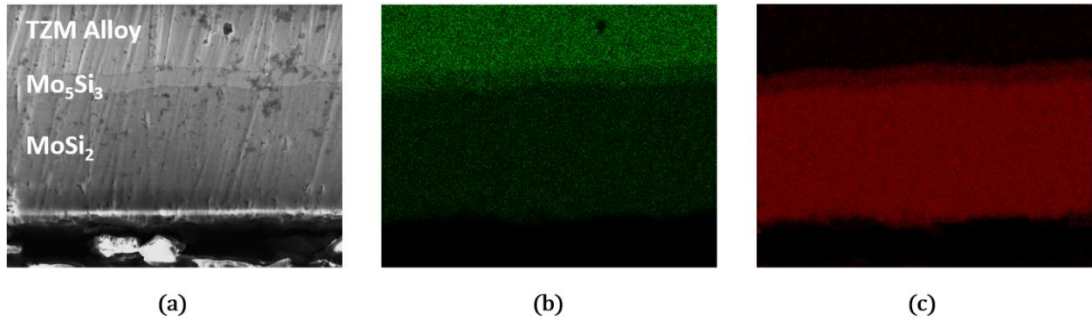
Figure 44 The EDS mapping results: (a) SEM image of the region EDS mapping performed; (b) distribution of molybdenum atoms and (c) distribution of silicon atoms.

Formation of glassy silica on molybdenum di-silicide as a result of oxidation could not be detected by EDS analysis even though high silicon concentration was obtained, and a light colored layer was seen as shown in Figure 44 (a). Therefore, X-ray diffraction analysis was performed to prove silica formation. As given in Figure 45, formation of silica layer was observed in addition to $MoSi_2$ and Mo_5Si_3.
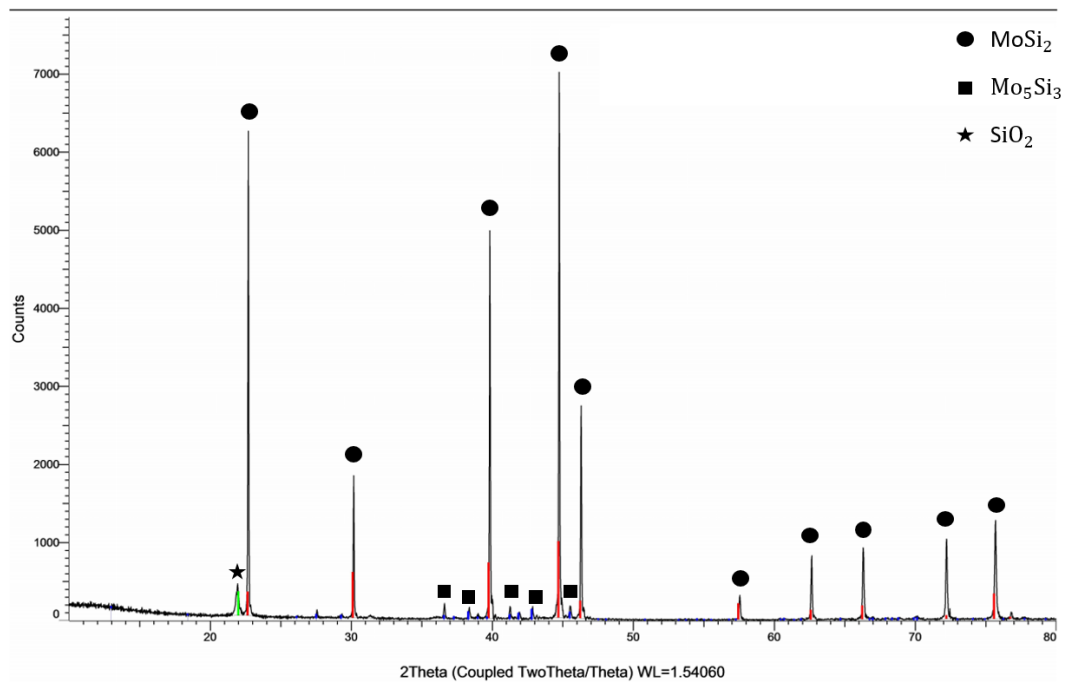
Figure 45 X-Ray Diffraction result of oxidized coated TZM Alloy sample at 1200°C for 1 hours.

The last oxidation study was performed at 1200°C for 3 hours. SEM image of oxidized sample is shown in Figure 46. Formation of $MoSi_2$ and Mo_5Si_3 phases are proved using EDS analysis as shown in Figure 47. Also, a light colored layer was detected at outer surface during the scans around the sample. As a result of X-ray diffraction analysis of sample, SiO_2 formation was confirmed in addition to $MoSi_2$ and Mo_5Si_3, which is shown in Figure 48.
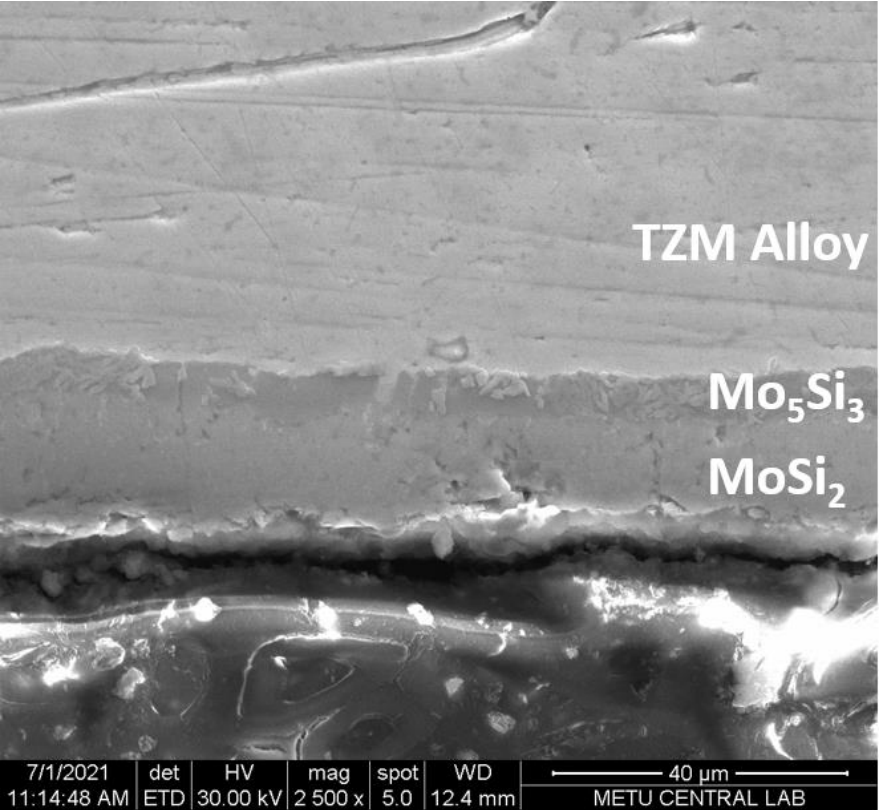
Figure 46 SEM image of the section of oxidized coated TZM Alloy sample at 1200°C for 3 hours.
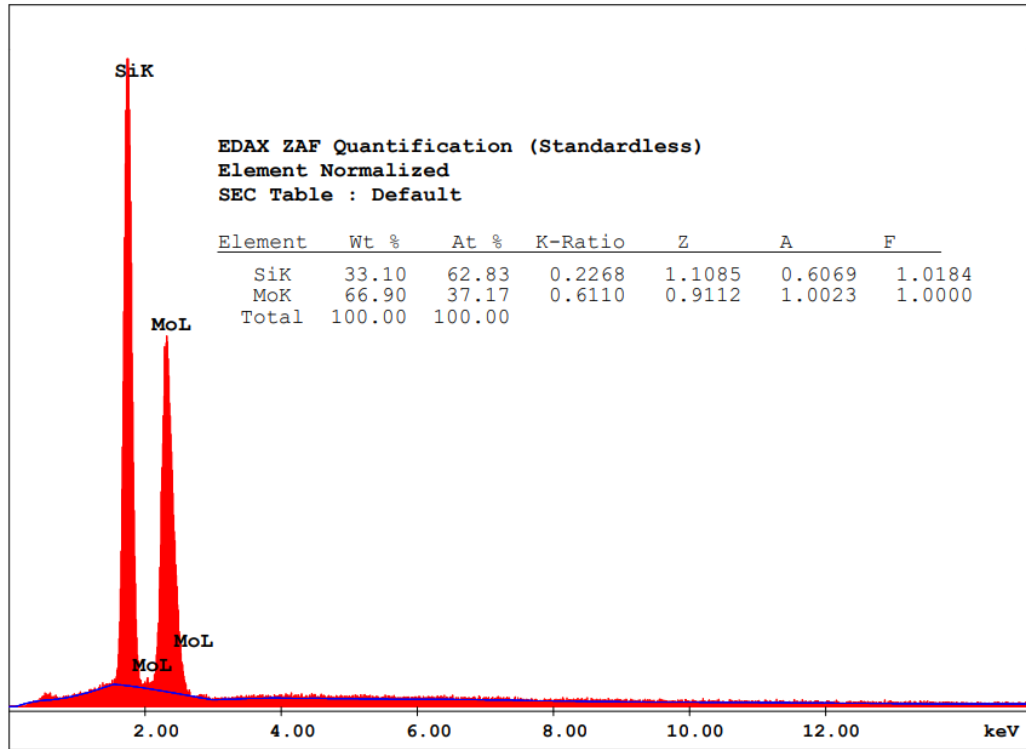
Figure 47 EDS analysis of oxidized coated TZM Alloy sample at 1200°C for 3 hours.
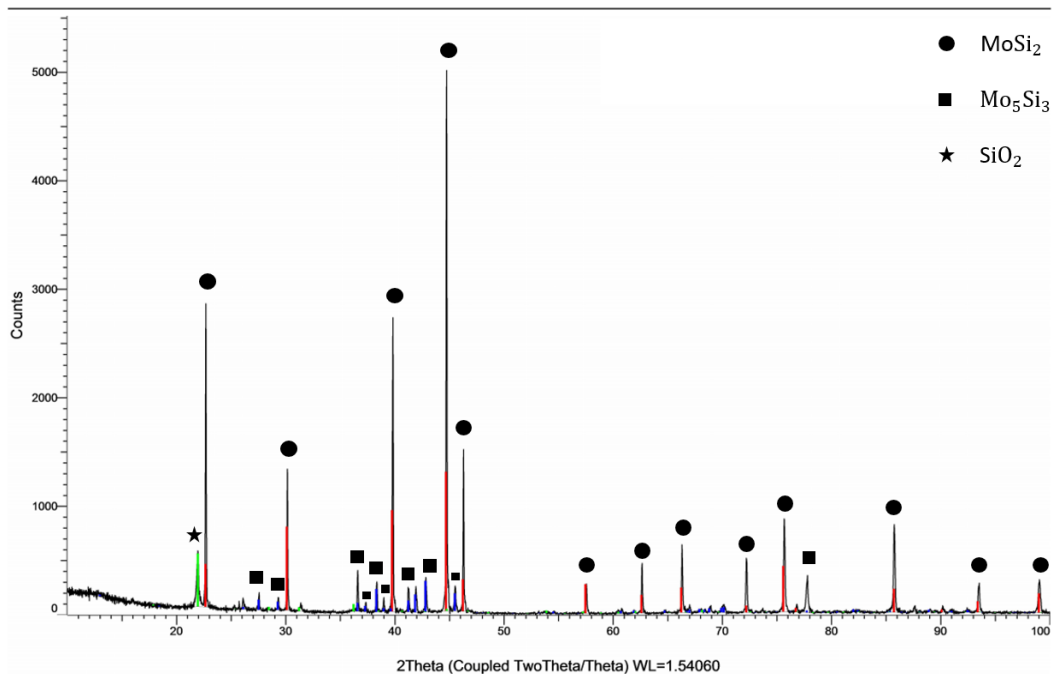
Figure 48 X-Ray Diffraction result of oxidized coated TZM Alloy sample at 1200°C for 3 hours.

The weight losses of the samples oxidized at 1200°C for 1 and 3 hours were very close to each other, which are 14% and 12%. Firstly, the weight loss was almost same level as the test which was done at 800°C. Increasing test temperature is thought to be the reason why weight loss is the same since protective silica formation increases on the surface. Although increasing temperature accelerates oxidation of molybdenum, silica layer grows up on the surface instantly, and volatilization of molybdenum stops. Also, test at 1200°C, the weight loss in 1 hour study was slightly more than 3 hours. It was thought that MoO_3 volatilizes initially, and then silica layer covers the surface. Therefore, silica layer grows, and volatilization does not occur anymore.

CHAPTER 5

CONCLUSION

Molybdenum di-silicide was successfully coated on pure molybdenum and molybdenum alloy (TZM) using molten salt method.

In pure molybdenum studies, coating thickness varied between 10 and 25 microns. The effect of temperature on coating thickness was not observed for shorter processing time, however; it was apparent that increasing temperature and processing time increased coating thickness. The weight gain of coated samples showed correspondence with coating thickness. A considerable effect of salt composition on coating thickness and quality, using E2 and E3 mixtures, was not observed. The change in silicon amount in salt mixture using E2 to supply more silicon through the system was not at desired level, and it did not have an impact on coating thickness. Another attempt was made to increase coating thickness by using E3 mixture in order to stabilize F^- ion and silicon amount in molten salt, and it did not increase coating thickness positively. Therefore, it was concluded that amount of silicon and fluoride in the system was sufficient and efficient to develop silicide coating.

In molybdenum alloy (TZM) studies, coating thickness reached out nearly 60 microns. It was evident that increasing temperature does not increase the coating thickness. Moreover, the coating thickness increased up to a certain point when processing time was increased for both temperatures, and then there was a decrease in thickness of silicide layer. The reason for this decrease was dissolution of silicide layer in molten salt since molybdenum was detected in the residue salt mixture that was taken from a longer processing time. As in pure molybdenum samples, weight gain of coated samples showed agreement with thickness, however; surface roughness of coated samples was higher than initial for both pure molybdenum and TZM alloy samples. Therefore, surface finishing process could be needed after process.

The silicide coated TZM alloy samples were picked up for oxidation tests at high-temperature oxygen environment to observe the oxidation behavior of molybdenum di-silicide. Silica layer covered whole surface as a result of oxidation test performed at 800°C, and there was no phase formation other than silica. However, Mo_5Si_3 phase formed between substrate and $MoSi_2$ in addition to silica as a result of test performed at 1200°C since increasing temperature increased mutual diffusion. Also, non-coated sample was oxidized to compare, and its weight loss nearly reached out 60% at 800°C. Even though there was a weight loss in coated samples after oxidation test, it remained at about 12% level. Furthermore, the weight losses of the samples which were oxidized at 1200°C for 1 and 3 hours remained at 14% and 12%, respectively.

Suggestions for Future Work

The di-silicide layer on molybdenum and TZM surface can be developed further in terms of coating thickness.

The final surface after deposition process was rougher than initial for both temperatures and compositions. Therefore, it's suggested that a post surface finishing process should be required to decrease surface roughness after coating process if a smooth surface is desired.

The electrolytic deposition could be tested for alternative silicon sources and to increase coating thickness.

REFERENCES

[1]   S. N. Hasan, M. Xu, and E. Asselin, "Electrodeposition of metallic molybdenum and its alloys–a review," *Canadian Metallurgical Quarterly*, vol. 58, no. 1, pp. 1–18, 2019, doi: 10.1080/00084433.2018.1511252.

[2]   Q. Wang, L. Zhang, L. L. Zhai, J. D. Li, and J. W. Zhang, "In-situ synthesis of silicide coatings on molybdenum substrates by electrodeposition in chloride-fluoride molten salts," *International Journal of Refractory Metals and Hard Materials*, vol. 82, no. February, pp. 340–348, 2019, doi: 10.1016/j.ijrmhm.2019.05.011.

[3]   T. Mrotzek, A. Hoffmann, and U. Martin, "Hardening mechanisms and recrystallization behaviour of several molybdenum alloys," *International Journal of Refractory Metals and Hard Materials*, vol. 24, no. 4, pp. 298–305, 2006, doi: 10.1016/j.ijrmhm.2005.10.003.

[4]   J. H. Perepezko, "The hotter the engine, the better," *Science*, 326(5956):1068-9 2009, doi: 10.1126/science.1179327.

[5]   B. v. Cockeram, E. K. Ohriner, T. S. Byun, M. K. Miller, and L. L. Snead, "Weldable ductile molybdenum alloy development," *Journal of Nuclear Materials*, vol. 382, no. 2–3, pp. 229–241, 2008, doi: 10.1016/j.jnucmat.2008.08.021.

[6]   Z. Alam, B. Venkataraman, B. Sarma, and D. K. Das, "$MoSi_2$ coating on Mo substrate for short-term oxidation protection in air," vol. 487, pp. 335–340, 2009, doi: 10.1016/j.jallcom.2009.07.141.

[7]   Y. Zhang, J. Zhao, J. Li, J. Lei, and X. Cheng, "E ff ect of hot-dip siliconizing time on phase composition and microstructure of Mo – MoSi 2 high temperature structural materials," vol. 45, no. November 2018, pp. 5588–5593, 2019, doi: 10.1016/j.ceramint.2018.12.018.

[8] Y. Wang, J. Yan, and D. Wang, "International Journal of Refractory Metals High temperature oxidation and microstructure of MoSi 2 / MoB composite coating for Mo substrate," vol. 68, no. May, pp. 60–64, 2017.

[9] S. Govindarajan, B. Mishra, D. L. Olson, J. J. Moore, and J. Disam, "Synthesis of molybdenum disilicide on molybdenum substrates," *Surface and Coatings Technology*, vol. 76–77, pp. 7–13, 1995, doi: 10.1016/0257-8972(95)02524-3.

[10] S. P. Chakraborty, S. Banerjee, I. G. Sharma, and A. K. Suri, "Development of silicide coating over molybdenum based refractory alloy and its characterization," *Journal of Nuclear Materials*, 2010, doi: 10.1016/j.jnucmat.2010.06.014.

[11] N. R. Council, *High-Temperature Oxidation-Resistant Coatings: Coatings for Protection From Oxidation of Superalloys, Refractory Metals, and Graphite*. Washington, DC, 1970.

[12] C. A. Krier, *Coatings for the Protection of Refractory Metals from Oxidation*, DMIC Report. 1961.

[13] V. M. Voyevodin, V. I. Zmii, and S. G. Rudenkyi, "High-Temperature Heat-Resistant Coatings for Protection of Refractory Metals and Their Alloys (Overview)," *Powder Metallurgy and Metal Ceramics*, vol. 56, no. 3–4, pp. 198–209, 2017, doi: 10.1007/s11106-017-9887-3.

[14] H. J. Lunk and H. Hartl, "Discovery, properties and applications of molybdenum and its compounds," *ChemTexts*, vol. 3, no. 3, pp. 1–23, 2017, doi: 10.1007/s40828-017-0048-6.

[15] K. Natesan and S. C. Deevi, "Oxidation behavior of molybdenum silicides and their composites," *Intermetallics*, vol. 8, no. 9–11, pp. 1147–1158, 2000, doi: 10.1016/S0966-9795(00)00060-1.

[16] D. Y. Oh, H. C. Kim, J. K. Yoon, and I. J. Shon, "One step synthesis of dense MoSi2-SiC composite by high-frequency induction heated combustion and its mechanical properties," *Journal of Alloys and Compounds*, vol. 395, no. 1–2, pp. 174–180, 2005, doi: 10.1016/j.jallcom.2004.10.072.

[17] J. J. Petrovic, "Mechanical behavior of MoSi$_2$, and MoSi$_2$ composites," *Materials Science and Engineering*, vol. 193, pp. 31–37, 1995.

[18] A. K. Vasudévan and J. J. Petrovic, "A comparative overview of molybdenum disilicide composites," *Materials Science and Engineering A*, vol. 155, no. 1–2, pp. 1–17, 1992, doi: 10.1016/0921-5093(92)90308-N.

[19] M. L. Heilig, "United States Patent Office," *ACM SIGGRAPH Computer Graphics*, vol. 28, no. 2, pp. 131–134, 1994, doi: 10.1145/178951.178972.

[20] Y. L. Jeng and E. J. Lavernia, "Processing of molybdenum disilicide," *Journal of Materials Science*, vol. 29, no. 10, pp. 2557–2571, 1994, doi: 10.1007/BF00356804.

[21] J. Sun, Q. G. Fu, L. P. Guo, Y. Liu, C. X. Huo, and H. J. Li, "Effect of filler on the oxidation protective ability of MoSi2 coating for Mo substrate by halide activated pack cementation," *Materials and Design*, vol. 92, pp. 602–609, 2016, doi: 10.1016/j.matdes.2015.12.079.

[22] S. Majumdar, I. Sharma, I. Samajdar, and P. Bhargava, "Relationship Between Pack Chemistry and Growth of Silicide Coatings on Mo–TZM Alloy," *Journal of The Electrochemical Society*, 2008, doi: 10.1149/1.2987954.

[23] X. D. Tian, X. P. Guo, Z. P. Sun, J. L. Qu, and L. J. Wang, "Oxidation resistance comparison of MoSi2 and B-modified MoSi2 coatings on pure Mo prepared through pack cementation," *Materials and Corrosion*, vol. 66, no. 7, pp. 681–687, 2015, doi: 10.1002/maco.201407631.

[24] C. Republic and E. Faculty, "Structural Characterization of Molybdenum Silicides Deposited on Molybdenum By Pack Method," pp. 15–18, 2013.

[25] S. Knittel, S. Mathieu, L. Portebois, S. Drawin, and M. Vilasi, "Development of silicide coatings to ensure the protection of Nb and silicide composites against high temperature oxidation," *Surface and Coatings Technology*, vol. 235, pp. 401–406, 2013, doi: 10.1016/j.surfcoat.2013.07.053.

[26] G. A. West, K. W. B. J. E. Soc, G. A. West, and K. W. Beeson, "Chemical Vapor Deposition of Molybdenum Silicide C h e m i c a l V a p o r Deposition of M o l y b d e n u m," 1988.

[27] J. K. Yoon, J. K. Lee, J. Y. Byun, G. H. Kim, Y. H. Paik, and J. S. Kim, "Effect of ammonia nitridation on the microstructure of MoSi2 coatings formed by chemical vapor deposition of Si on Mo substrates," *Surface and Coatings Technology*, vol. 160, no. 1, pp. 29–37, 2002, doi: 10.1016/S0257-8972(02)00379-1.

[28] M. Erfanmanesh and S. R. Bakhshi, "Oxidation behavior of nanostructured and conventional MoSi2 plasma-sprayed coatings," *Ceramics International*, vol. 44, no. 13, pp. 15839–15844, 2018, doi: 10.1016/j.ceramint.2018.05.263.

[29] S. Madhukar *et al.*, "Pulsed laser-ablation deposition of thin films of molybdenum suicide and its properties as a conducting barrier for ferroelectric random-access memory technology," *Journal of Materials Research*, vol. 14, no. 3, pp. 940–947, 1999, doi: 10.1557/jmr.1999.0125.

[30] R. Chow and D. Nichols, "Properties of MoSi2 Films Deposited from Composite Target," *Thin Solid Films*, vol. 8, no. 2, pp. 139–147, 1984.

[31] X. Fei, Y. Niu, H. Ji, L. Huang, and X. Zheng, "A comparative study of MoSi2 coatings manufactured by atmospheric and vacuum plasma spray processes," *Ceramics International*, vol. 37, no. 3, pp. 813–817, 2011, doi: 10.1016/j.ceramint.2010.10.018.

[32] K. Tatemoto, Y. Ono, and R. O. Suzuki, "Silicide coating on refractory metals in molten salt," *Journal of Physics and Chemistry of Solids*, vol. 66, no. 2–4, pp. 526–529, 2005, doi: 10.1016/j.jpcs.2004.06.043.

[33] L. Dai *et al.*, "In-situ synthesis of MoSi2 coating on molybdenum substrate by electro-deoxidation of a SiO2 layer in molten salt," *Ceramics International*, vol. 41, no. 10, pp. 13663–13670, 2015, doi: 10.1016/j.ceramint.2015.07.164.

[34] R. O. Suzuki, M. Ishikawa, and K. Ono, "MoSi2 coating on molybdenum using molten salt," *Journal of Alloys and Compounds*, vol. 306, no. 1–2, pp. 285–291, 2000, doi: 10.1016/S0925-8388(00)00792-1.

[35] R. O. Suzuki, T. Nishibata, K. I. Nakanishi, M. Ishikawa, and K. Ono, "Electroless coating of Fe3Si on steel in the molten salt," *Steel Research*, vol. 71, no. 4, pp. 130–137, 2000, doi: 10.1002/srin.200005702.

[36] E. S. S. A, A. J. Gay, and J. Quakernaat, "A Study of Electroless Siliconizing of Nickel," vol. 40, pp. 21–28, 1975.

[37] R. O. Suzuki, M. Ishikawa, and K. Ono, "NbSi2 coating on niobium using molten salt," *Journal of Alloys and Compounds*, vol. 336, no. 1–2, pp. 280–285, 2002, doi: 10.1016/S0925-8388(01)01879-5.

[38] T. A. Adler, D. Aylor, and A. Bray, "Effects of Metallurgical Variables on the Corrosion of Stainless Steels[1]," in *Corrosion in the Petrochemical Industry*, 2nd ed., Victoria Burt, Ed. 2015, pp. 62–69.

[39] C. Xu and W. Gao, "Pilling-bedworth ratio for oxidation of alloys," *Materials Research Innovations*, vol. 3, no. 4, pp. 231–235, 2000, doi: 10.1007/s100190050008.

[40] N. Birks, G. H. Meier, and F. S. Pettit, *Introduction to the High Temperature Oxidation of Metals*, 2nd ed. Cambridge: Cambridge University Press, 2006.

[41] A. S. Sultan, "Effect of Chromium on the Oxidation of Steels Used in the Construction of Petroleum Refinery Heaters," 2013.

[42] W. J. Quadakkers, D. Naumenko, E. Wessel, V. Kochubey, and L. Singheiser, "Growth rates of alumina scales on Fe-Cr-Al alloys," *Oxidation of Metals*, vol. 61, no. 1–2, pp. 17–37, 2004, doi: 10.1023/b:oxid.0000016274.78642.ae.

[43] S. Chevalier, "Mechanisms and kinetics of oxidation," *Shreir's Corrosion*, pp. 132–152, 2010, doi: 10.1016/B978-044452787-5.00010-X.

[44] G. R. Smolik, D. A. Petti, and S. T. Schuetz, "Oxidation and volatilization of TZM alloy in air," *Journal of Nuclear Materials*, vol. 283–287, no. PART II, pp. 1458–1462, 2000, doi: 10.1016/S0022-3115(00)00303-2.

[45] A. T. Nelson, E. S. Sooby, Y. J. Kim, B. Cheng, and S. A. Maloy, "High temperature oxidation of molybdenum in water vapor environments," *Journal of Nuclear Materials*, vol. 448, no. 1–3, pp. 441–447, 2014, doi: 10.1016/j.jnucmat.2013.10.043.

[46] E. A. Gulbransen, K. F. Andrew, and F. A. Brassart, "Vapor Pressure of Molybdenum Trioxide," *Journal of The Electrochemical Society*, vol. 110, no. 242, pp. 242–243, 1963.

[47] E. A. Gulbransen, K. F. Andrew, and F. A. Brassart, "Oxidation of Molybdenum 550° to 1700°C," *Journal of The Electrochemical Society*, vol. 110, no. 9, p. 952, 1963, doi: 10.1149/1.2425918.

[48] Jones E. S. , Mosher J. F., Speiser R. and Spretnak, J. W. "The Oxidation of Molybdenum," *Corrosion*, vol. 14, no. 1, pp. 20–26, 1958, doi: https://doi.org/10.5006/0010-9312-14.1.20.

[49] R. W. Bartlett, "Molybdenum Oxidation Kinetics at High Temperatures," *Journal of The Electrochemical Society*, vol. 112, no. 7, p. 744, 1965, doi: 10.1149/1.2423679.

[50] M. Noguchi and H. Yakuwa, "Lecture on Fundamental Aspects of High Temperature Corrosion and Corrosion Protection Part 2: Corrosion Protection and Coatings," *Ebara Engineering Review*, vol. 10, no. 252, pp. 1–11, 2016.

[51] C. A. Krier and W. A. Baginski, *Coated Refractory Metals*, vol. 5. ACADEMIC PRESS INC., 1965.

[52] SM Sabol, BT Randall, JD Edington, CJ Larkin, and BJ Close, "Barrier Coatings for Refractory Metals and Superalloys," 2006.

[53] A. P. Epik, "Boride Coatings," in *Boron and Refractory Borides*, 1977, pp. 597–612.

[54] C. E. Ramberg, P. Beatrice, Kurokawa. K., and W. L. Worrell, "High Temperature Oxidation Behavior of Structural Silicides," *Materials Research Society Symposium Proceedings*, vol. 322, pp. 243–253, 1994.

[55] L. N. Lie, W. A. Tiller, and K. C. Saraswat, "Thermal oxidation of silicides," *Journal of Applied Physics*, vol. 56, no. 7, pp. 2127–2132, 1984, doi: 10.1063/1.334212.

[56] C. D. WIRKUS and D. R. WILDER, "High-Temperature Oxidation of Molybdenum Disilicide," *Journal of the American Ceramic Society*, vol. 49, no. 4, pp. 173–177, 1966, doi: 10.1111/j.1151-2916.1966.tb13227.x.

[57] C. E. Birchenall, *Kinetics of High-Temperature Processes*. Technology Press of Massachusetts Institute of Technology, Cambridge, and John Wiley & Sons, New York, 1959.

[58] A. W. Searcy, "Predicting the Thermodynamic Stabilities and Oxidation Resistances of Silicide Cermets," *Journal of the American Ceramic Society*, vol. 40, no. 12, pp. 431–435, 1957, doi: 10.1111/j.1151-2916.1957.tb12567.x.

[59] G. B. Cherniack and A. G. Elliot, "High-Temperature Behavior of MoSi2 and Mo5Si3," *Journal of the American Ceramic Society*, vol. 47, no. 3, pp. 136–141, 1964.

[60] H. W. Lavendel and A. G. Elliot, "Evaluation of silicide coatings on columbium and tantalum and a means for improving their Oxidation resistance," *Trans. AIME*, no. 239, pp. 143–148, 1967.

[61] A. Brenner, "Electroless plating comes of age," *Metal Finishing*, vol. 52, no. 11, p. 68, 1954.

[62] A. Da and M. Bestetti, "Electroless and Electrochemical Deposition of Metallic Coatings on Magnesium Alloys Critical Literature Review," *Magnesium Alloys - Corrosion and Surface Treatments*, 2011, doi: 10.5772/13975.

[63] A. Brenner and G. E. Riddell, "Electroless plating comes of age," *Metal Fishing*, vol. 52, pp. 68–76, 1954.

[64] A. Brenner and G. E. Riddell, "Deposition of nickel and cobalt by chemical reduction," *Journal of Research of the National Bureau of Standards*, vol. 39, pp. 385–395, 1947.

[65] G. O. Mallory and J. B. Hajdu, "Electroless plating : fundamentals and applications," *American Electroplaters and Surface Finishers Society*, 1990.

[66] G.G. Gawrilov, "Chemical (Electroless) Nickel Plating," *Portcullis Press Limited*, 1979.

[67] Stojan S. Djokić, "Electroless Deposition of Metals and Alloys," *Modern Aspects of Electrochemistry*, vol. 35, pp. 51–133, 2002, doi: https://doi.org/10.1007/0-306-47604-5_2.

[68] S. S. Djokićc and P. L. Cavallott, "Electroless Deposition: Theoryand Applications," *Modern Aspects of Electrochemistry*, vol. 48, pp. 251–289, 2010.

[69] K. Matiašovsky, P. Fellner, and M. C. Ž. Lubyová, "Electrolytic metal coating in molten salts," vol. 41, no. iv, 1987.

[70] B. Mishra and D. L. Olson, "Molten salt applications in materials processing," *Journal of Physics and Chemistry of Solids*, vol. 66, no. 2–4, pp. 396–401, 2005, doi: 10.1016/j.jpcs.2004.06.049.

[71] S. v. Volkov, "Chemical reactions in molten salts and their classification," *Chemical Society Reviews*, vol. 19, no. 1, pp. 21–28, 1990, doi: 10.1039/CS9901900021.

[72] S. A. Kuznetsov, S. v. Kuznetsova, E. v. Rebrov, M. J. M. Mies, M. H. J. M. de Croon, and J. C. Schouten, "Synthesis of molybdenum borides and molybdenum silicides in molten salts and their oxidation behavior in an air-water mixture," *Surface and Coatings Technology*, 2005, doi: 10.1016/j.surfcoat.2004.05.021.

[73] V. v. Malysheva *et al.*, "Review of the electrodeposition of molybdenum carbide on the surfaces of disperse dielectric and semiconductor materials,"

Acta Chimica Slovaca, vol. 5, no. 2, pp. 139–144, 2018, doi: 10.2478/v10188-012-0021-3.

[74]   T. Ueda, T. Goto, and Y. Ito, "The implantation of Si and formation of silicide by molten salt electrochemical process," *Hyomen Gijutsu/Journal of the Surface Finishing Society of Japan*, vol. 46, no. 12, pp. 1173–1179, 1995.

[75]   H. Bloom, A. Doroszkowski, and S. B. Tricklebank, "Molten salt mixtures. IX. The thermal conductivities of molten nitrate systems," *Australian Journal of Chemistry*, vol. 18, no. 8, pp. 1171–1176, 1965.

[76]   P. Saltarella, L. Ott, and G. Yonder, "Physical properties and correlations for the molten salt FLIBE and their implementation in the RELAP5/ATHENA thermal-hydraulics code," *Oakville National Laboratory Report, Nuclear Science and Technology Division*, 2004.

[77]   D. Nagle and D. Zhang, "Carbide Coatings for Nickel Alloys, Graphite and Carbon/Carbon Composites to be used in Fluoride Salt Valves," no. 10, 2015.

[78]   G. W. Mellors and S. Senderoff, "ELECTRODEPOSITION OF REFRACTORY METALS," Patent No:688546, 1964.

[79]   K. H. Stern, "Electrodeposition of refractory carbide coatings from fluoride melts," *Journal of Applied Electrochemistry*, vol. 22, no. 8, pp. 717–721, 1992, doi: 10.1007/BF01027499.

[80]   Y. Wang, X. Li, N. Li, C. Ling, Z. Tang, and Z. Li, "Thermal transport and storage performances of NaCl–KCl–NaF eutectic salt for high temperatures latent heat," *Solar Energy Materials and Solar Cells*, vol. 218, no. July, pp. 2–7, 2020, doi: 10.1016/j.solmat.2020.110756.

[81]   Z. Cai, Y. Li, X. He, and J. Liang, "Electrochemical behavior of silicon in the (NaCl-KCl-NaF-SiO2) molten salt," *Metallurgical and Materials Transactions B: Process Metallurgy and Materials Processing Science*, vol. 41, no. 5, pp. 1033–1037, 2010, doi: 10.1007/s11663-010-9393-1.

[82] K. Hasokawa, "Surface Layer Formed on Iron and Steel Impregnated Simultaneously with Carbon and Silicon," *Journal of the Japan Institute of Metals and Materials*, vol. 39, pp. 345–351, 1975.

[83] T. Oki and J. Tanikawa, "Formation of Graphite-dispersed Fe-Si Films on Steel by Reaction with Fused Salts," *Journal of the Metal Finishing Society of Japan*, vol. 31, no. 10, pp. 561–566, 1980, doi: https://doi.org/10.4139/sfj1950.31.561.

[84] M. Tyagi, B. Vishwanadh, K. Bhattacharyya, S. K. Ghosh, and R. Tewari, "A study on reaction kinetics and development of silicide coatings on Nb-1Zr-0.1C alloy by molten salt technique," *RSC Advances*, vol. 6, no. 101, pp. 99331–99338, 2016, doi: 10.1039/c6ra08280g.

[85] A. Paul, "Systematic Variation of Diffusion Rates of Components in Silicides Depending on Atomic Number of Refractory Metal Component," *arXiv*, 2018.

[86] P. C. Tortorici and M. A. Dayananda, "Growth of silicides and interdiffusion in the Mo-Si system," *Metallurgical and Materials Transactions A*, vol. 30, no. 3, pp. 545–550, 1999, doi: 10.1007/s11661-999-0046-4.

[87] S. Prasad and A. Paul, "Growth mechanism of phases by interdiffusion and atomic mechanism of diffusion in the molybdenum-silicon system," *Intermetallics*, vol. 19, no. 8, pp. 1191–1200, 2011, doi: 10.1016/j.intermet.2011.03.027.

[88] M. Tyagi, S. K. Ghosh, and R. Tewari, "High temperature behaviour of NbSi2 coating on the Nb-1Zr-0.1C alloy," *Surface Engineering*, vol. 36, no. 2, pp. 158–166, 2020, doi: 10.1080/02670844.2019.1622204.

[89] H. Okamoto, "Mo-Si (Molybdenum-Silicon)," *Journal of Phase Equilibria and Diffusion*, vol. 32, no. 2, p. 176, 2011, doi: 10.1007/s11669-010-9843-0.

[90] P. Jang, H. Li, W. Kim, Z. Wang, and F. Liu, "Preparation of Al-La master alloy by thermite reaction in NaF-NaCl-KCl molten salt," *Jom*, vol. 67, no. 5, pp. 1130–1136, 2015, doi: 10.1007/s11837-015-1392-x.
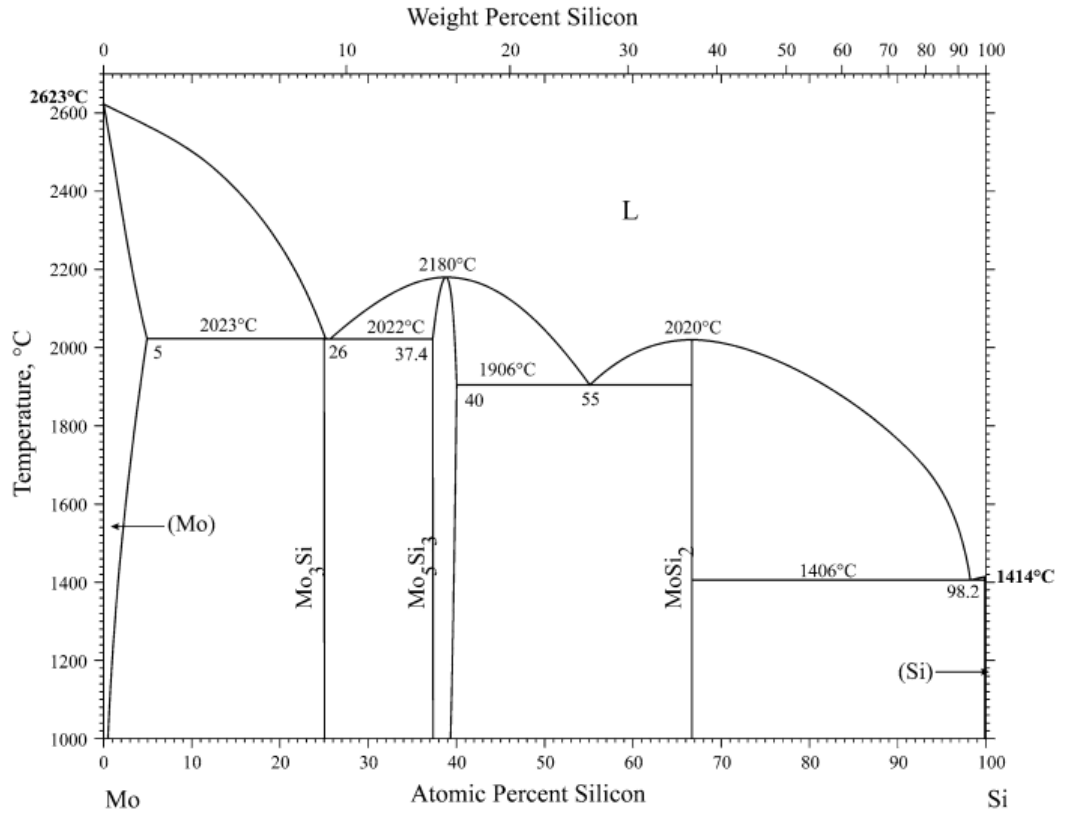
Figure 49.1 Mo-Si phase diagram [89].
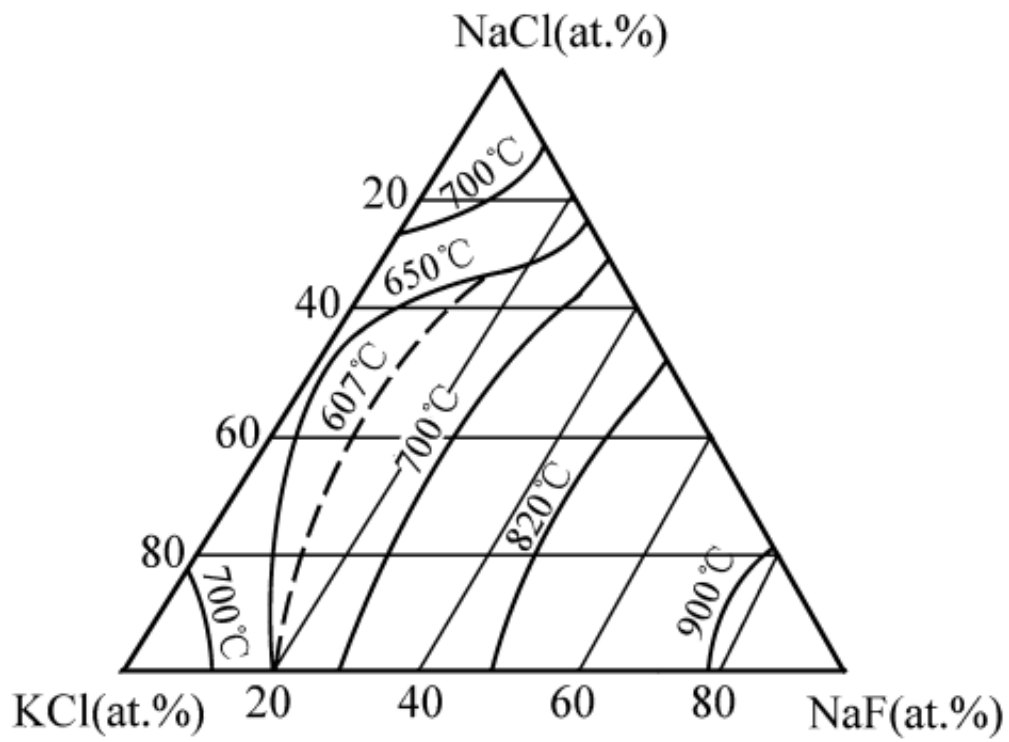
Figure A.2 NaCl-KCl-NaF ternary phase diagram [90].